

# Supplementary Material for

## DeepGEM-EGF: A Bayesian strategy for joint estimates of source time functions and empirical Green's functions

**Théa Ragon<sup>1,2,\*</sup>, Angela Gao<sup>3</sup>, Zachary Ross<sup>1</sup>**

<sup>1</sup>Seismological Laboratory, California Institute of Technology, Pasadena, CA, USA, <sup>2</sup>now at CNRS, Univ. Grenoble Alpes, IRD, ISTERre, Grenoble, France, <sup>3</sup>Computing and Mathematical Sciences Department, California Institute of Technology, Pasadena, CA, USA, \*Corresponding author: thea.ragon@univ-grenoble-alpes.fr

### Contents

<b>S1</b>	<b>Description of DeepGEM-egf arguments</b>	<b>2</b>
<b>S2</b>	<b>Toy models with synthetic waveforms</b>	<b>4</b>
S2.1	Description of the forward model	4
S2.2	Prior assumptions for DeepGEM	4
S2.3	Prior assumptions for the Multitaper Spectrum Analysis	4
S2.4	Results	5
<b>S3</b>	<b>Toy models with recorded waveforms: the 2016 Borrego Springs sequence, CA</b>	<b>27</b>
S3.1	Data	27
S3.2	Description of the forward model	27
	Prior assumptions for DeepGEM	27
	Prior assumptions for the Landweber approach	27
S3.3	Results	27
<b>S4</b>	<b>Case study: the 2019 Cahuilla swarm, CA</b>	<b>31</b>
S4.1	Data	31
S4.2	Toy models with recorded waveforms	31
	Description of the forward model	31
	Prior assumptions for DeepGEM	31
	Results	33
S4.3	Description of the forward model	48
	Prior assumptions for the Landweber approach	48
S4.4	Results	48

## S1 Description of DeepGEM-egf arguments

**Table S1** List of arguments for DeepGEM (continued on Table S2).

Parameter	Description	type	Default value
<b>User parameters</b>			
<code>dir</code>	Output directory	string	<code>'./results'</code>
<code>trc0</code>	Path or name of trace file	string. File must be npy array or obspy stream	<code>''</code>
<code>egf0</code>	Path or name of EGF file	string. File must be npy array or obspy stream	<code>''</code>
<code>stf0</code>	Path or name of prior STF file	numpy array	<code>''</code>
<code>synthetics</code>	True if we know the target	bool	<b>False</b>
<code>gf_true</code>	Path or name of target EGF file	string. File must be npy array or obspy stream	<code>''</code>
<code>stf_true</code>	Path or name of target STF file	string. File must be npy array or obspy stream	<code>''</code>
<code>stf_size</code>	Number of samples in STF (optional if <code>stf_dur</code> specified)	int	100
<code>stf_dur</code>	Duration of STF in seconds	float	<b>None</b>
<code>samp_rate</code>	Sampling rate (Hz)	float	<b>None</b>
<code>num_egf</code>	Number of EGFs	int	1
<code>M0</code>	Seismic moment of main event	float	<b>None</b>
<code>M0_egf</code>	Seismic moment of EGF event	float or list if several EGFs	<b>None</b>
<b>Network parameters</b>			
<code>btsize</code>	Batch size	int	1024
<code>num_epochs</code>	Number of epochs	int	150
<code>num_subepochsE</code>	Number of sub-epochs for E step	int	350
<code>num_subepochsM</code>	Number of sub-epochs for M step	int	50
<code>EMFull</code>	True: E to convergence, M to convergence False: alternate E, M every epoch	bool	<b>False</b>
<code>x_rand</code>	random x or from a certain sample	bool	<b>True</b>
<code>seqfrac</code>		6	
<code>num_layers</code>	number of layers for GF generator	int	7
<code>Elr</code>	Learning rate on E step	float	1e-3
<code>Mlr</code>	Learning rate on M step	float	1e-5

**Table S2** List of arguments for DeepGEM (continued).

Parameter	Description	type	Default value
<b>Weights</b>			
data_sigma	Data sigma, weight for MSE loss	float	1e-6
stf0_sigma	E step - sigma on prior STF	float	2e-1
stf0_weight	E step - weight for distance to prior STF	float	<b>None</b> = function of data_sigma
stf_weight	E step - list of weights for priors on STF [boundaries, total variation, L1]	list	<b>None</b> = function of data_sigma
logdet_weight	E step - weight on $q_\theta$ , controls entropy	float	<b>None</b> = function of data_sigma
egf_norm_weight	M step - weight for L1 norm on EGF	float	<b>None</b> = function of data_sigma
prior_phi_weight	M step - list of weights for the priors on the EGFs [L1, L2, total variation]	list	<b>None</b> = function of data_sigma
egf_multi_weight	M step - if multiple EGFs, weight to closeness of EGFs to best EGF (the one that minimizes the fit to the data)	float	<b>None</b> = function of data_sigma
egf_qual_weight	Mstep - if multiple EGFs, weights the Mstep MSE loss of each EGFs	float	<b>None</b> = 1 for each
<b>Misc.</b>			
save_every	Save output every sub-epoch	int	50
print_every	Print output every sub-epoch	int	500
dv	which GPU to use, or cpu by default	string	'cpu'
multidv	use multiple gpus, use -1 for all	string	<b>None</b>
output	Plot figures, store output	bool	<b>True</b>
seed	random seed	int	1
reverse	permute parameter, if False, random, if True, reverse	bool	<b>False</b>

## S2 Toy models with synthetic waveforms

### S2.1 Description of the forward model

Waveforms for seismic events of reference are calculated from multiple variable and randomized parameters. The absolute source location is fixed. The source is defined by variable parameters (see Tables S3, S4, S5) that include moment magnitude ( $M_w$ ), source depth, strike, dip and rake, and a source time function (STF). The STF is a stack of  $N_{STF}$  (ranging from 3 to 10) Gaussian STFs, each of the Gaussian STFs being characterized by a random risetime, a random amplitude, and a random padding, while the total duration  $D_{STF}$  of the stack of Gaussian STFs cannot be larger than a pre-defined duration (STF duration).

Green's functions are calculated with Fomosto with the QSEIS backend (Heimann et al., 2017), using one of three synthetic 1D crustal velocity models (see Tables S6, S7 and S8) for a randomly located receiver at distance  $D$  from the absolute source location of the event of reference. Sample rate is of 10 Hz.

EGFs are calculated for a double-couple source whose parameters are defined relatively to the ones of the event of reference. The EGF source is randomly located at a pre-defined  $\delta$  distance (0 to 100 m) and  $\delta$  depth (0 to 5 km) from the absolute location of the event of reference. The  $M_w$  varies from 1 to 3.5. Each parameter of the focal mechanism (strike, dip, rake) is equal to the one of the event of reference, to which is added a random variation whose value is between  $\delta/2$  and  $\delta$ ,  $\delta$  ranging from 0 to 30°. A random variation is applied to all parameters (therefore if  $\delta = 10^\circ$ , all 3 of strike, dip and rake will vary of more than 5°). Equivalent Kagan angles between moment tensors of the main event and assumed EGFs are similar to the assumed  $\delta$ , but can reach up to 40° for  $\delta = 30^\circ$ .

Some white noise can be added, with a peak signal to noise (PSNR) ratio ranging from 0 to 10% of the peak EGF amplitude.

As varying the  $\delta$  depth or  $\delta$  distance between the location of the source of reference and the location of the EGF have a similar effect on the EGF waveforms, we mostly investigate the effect of varying the  $\delta$  depth.

### S2.2 Prior assumptions for DeepGEM

We used the following non-default parameters for DeepGEM for tests a to s:

```
num_epochs = 150
EMFull = False
seqfrac = 6
stf_dur = 9
samp_rate = 10
Elr = 1e-3
Mlr = 5e-5
data_sigma = 1e-6
```

And the following for the other tests:

```
num_epochs = 10
num_subepochsE = 100
num_subepochsM = 100
EMFull = True
seqfrac = 6
samp_rate = 10
Elr = 1e-3
Mlr = 5e-5
data_sigma = 1e-6
```

### S2.3 Prior assumptions for the Multitaper Spectrum Analysis

For some tests, we compare DeepGEM inference with frequency-domain deconvolution with the Multitaper Spectrum Analysis. We use a time-bandwidth product of 4 and 6 tapers. We first calculate individual spectral estimates for each channel of every time serie, calculate the cross-spectrum and finally the deconvolution, in the time domain, of the EGF to the waveform of reference. The deconvolved signal is filtered with a Butterworth bandpass between 0.2 and 3.0 Hz. When only one EGF is used, the inferred (and shown for comparison in following figures) STF is the mean of the deconvolved signals for each channel. When multiple EGFs are used, one STF is shown for each EGF.



## S2.4 Results

### List of figures:

First serie, tests a to s (in Fig. 1):

- Fig. [S1](#)
- Fig. [S2](#)
- Fig. [S3](#)
- Fig. [S4](#)

Second serie, tests a0 to g4:

- Fig. [S5](#)
- Fig. [S6](#)
- Fig. [S7](#)
- Fig. [S8](#)
- Fig. [S9](#)
- Fig. [S10](#)

The average run time for these toy models is of 1 s per iteration in a `EMFull = False` setting on one CPU, and 30 s per iteration in a `EMFull = True` setting. On average, run time is therefore of less than 1.5 minute for tests a to i, but can be of up to 5 minutes for the other tests. The additional runtime is not needed and those tests could have been run with the `EMFull = False` setting.

**Table S3** Parameters used for the calculation of waveforms for synthetic tests **a** to **s**.  $D_{STF}$  = 5 to 9 s.

test	Mw	D (km)	Depth (km)	Strike (°)	Dip (°)	Rake (°)	Vel. model	STF ( $N_{STF}$ )	STF duration ( $s, D_{STF}$ )	EGF dist. to source (km)	EGF $\delta$ depth (km)	EGF Mw	EGF $\delta$ FM (°)	EGF vel. model	noise PSNR (%)
a	4.0	25	10.	25	83.	30	c1	8	5	1	1.5	2.5	5	c1	3
b	4.0	25	10.	35	65	160	c1	8	5	1	1.5	2.5	5	c1	3
c	4.0	25	10.	40	78	90	c1	10	10	1	1.5	2.5	5	c1	3
d	4.0	30	10.	55.	83.	30	c1	8	5	1	1.5	2.5	5	c1	3
e	4.0	30	10.	25	105	120	c1	10	5	1	1.5	2.5	5	c1	3
f	4.0	40	10.	35	78	78	c1	15	10	1	1.5	2.5	5	c1	3
g	4.0	40	10.	40	83.	30	c1	8	5	1	1.5	2.5	5	c1	3
h	4.0	50	10.	55.	78	90	c1	15	10	1	1.5	2.5	5	c1	3
i	4.0	50	10.	25	65	160	c1	8	5	1	1.5	2.5	5	c1	3
j	4.0	25	10.	25	83.	30	c1	8	5	1	1.5	2.5	15	c1	3
k	4.0	25	10.	35	65	160	c1	8	5	1	1.5	2.5	15	c1	3
l	4.0	25	10.	40	78	90	c1	10	10	1	1.5	2.5	15	c1	3
m	4.0	30	10.	55.	83.	30	c1	8	5	1	1.5	2.5	15	c1	3
n	4.0	30	10.	25	105	120	c1	10	5	1	1.5	2.5	15	c1	3
o	4.0	25	10.	25	83.	30	c1	8	5	1	1.5	2.5	30	c1	3
p	4.0	25	10.	35	65	160	c1	8	5	1	1.5	2.5	30	c1	3
q	4.0	25	10.	40	78	90	c1	10	10	1	1.5	2.5	30	c1	3
r	4.0	30	10.	55.	83.	30	c1	8	5	1	1.5	2.5	30	c1	3
s	4.0	30	10.	25	105	120	c1	10	5	1	1.5	2.5	30	c1	3

**Table S4** Parameters used for the calculation of waveforms for synthetic tests **a0** to **g4**.  $D_{STF}=3$  s.

test	Mw	D (km)	Depth (km)	Strike (°)	Dip (°)	Rake (°)	Vel. model	STF ( $N_{STF}$ )	EGF dist. to source (km)	EGF $\delta$ depth (km)	EGF Mw	EGF $\delta$ FM (°)	EGF vel. model	noise PSNR (%)
a0	4.0	5.	10.	5.	83.	180.	c1	3	0	0	2.5	0	c1	0
a1	4.0	5.	10.	5.	83.	180.	c1	3	0	0.1	2.5	0	c1	0
a2	4.0	5.	10.	5.	83.	180.	c1	3	0	0.2	2.5	0	c1	0
a3	4.0	5.	10.	5.	83.	180.	c1	3	0	0.5	2.5	0	c1	0
a4	4.0	5.	10.	5.	83.	180.	c1	3	0	1	2.5	0	c1	0
a5	4.0	5.	10.	5.	83.	180.	c1	3	0	2	2.5	0	c1	0
a6	4.0	5.	10.	5.	83.	180.	c1	3	0	5	2.5	0	c1	0
b1	4.0	5.	10.	5.	83.	180.	c1	3	0	0	2.5	2	c1	0
b2	4.0	5.	10.	5.	83.	180.	c1	3	0	0	2.5	4	c1	0
b3	4.0	5.	10.	5.	83.	180.	c1	3	0	0	2.5	6	c1	0
b4	4.0	5.	10.	5.	83.	180.	c1	3	0	0	2.5	8	c1	0
b5	4.0	5.	10.	5.	83.	180.	c1	3	0	0	2.5	10	c1	0
c2	4.0	5.	10.	5.	83.	180.	c1	3	0	0	2.5	0	c2	0
c3	4.0	5.	10.	5.	83.	180.	c1	3	0	0	2.5	0	c3	0
d1	4.0	5.	10.	5.	83.	180.	c1	3	0	0	2.5	0	c1	2
d2	4.0	5.	10.	5.	83.	180.	c1	3	0	0	2.5	0	c1	5
d3	4.0	5.	10.	5.	83.	180.	c1	3	0	0	2.5	0	c1	10
e1	4.0	5.	10.	5.	83.	180.	c1	2	0	0	2.5	0	c1	0
e2	4.0	5.	10.	5.	83.	180.	c1	4	0	0	2.5	0	c1	0
e3	4.0	5.	10.	5.	83.	180.	c1	5	0	0	2.5	0	c1	0
e4	4.0	5.	10.	5.	83.	180.	c1	6	0	0	2.5	0	c1	0
f1	4.0	5.	10.	5.	83.	180.	c1	3	0	0	3.5	0	c1	0
f2	4.0	5.	10.	5.	83.	180.	c1	3	0	0	3.25	0	c1	0
f3	4.0	5.	10.	5.	83.	180.	c1	3	0	0	3	0	c1	0
f4	4.0	5.	10.	5.	83.	180.	c1	3	0	0	2.75	0	c1	0
f5	4.0	5.	10.	5.	83.	180.	c1	3	0	0	2.25	0	c1	0
f6	4.0	5.	10.	5.	83.	180.	c1	3	0	0	2	0	c1	0
f7	4.0	5.	10.	5.	83.	180.	c1	3	0	0	1.75	0	c1	0
f10	4.0	5.	10.	5.	83.	180.	c1	3	0	0	1	0	c1	0
g1	4.0	5.	10.	5.	83.	180.	c1	3	0.1	1	2.25	3	c2	2.
g2	4.0	5.	10.	5.	83.	180.	c1	3	0.1	1	2	5	c3	2.
g3	4.0	5.	10.	55.	63.	80.	c1	3	0.1	1	2.25	3	c2	2.
g4	4.0	5.	10.	55.	63.	80.	c1	3	0.1	1	2	5	c3	2.

**Table S5** Parameters used for the calculation of waveforms for synthetic tests **2a1** to **2b11**.  $D_{STF} = 10$  s.

test	Mw	D (km)	Depth (km)	Strike (°)	Dip (°)	Rake (°)	Vel. model	STF ( $N_{STF}$ )	EGF dist. to source (km)	EGF $\delta$ depth (km)	EGF Mw	EGF $\delta$ FM (°)	EGF vel. model	noise PSNR (%)
2a0	4.0	20.	10.	5.	83.	180.	c1	3	0	0	2.5	0	c1	0
2a1	4.0	20.	10.	5.	83.	180.	c1	3	0	0.1	2.5	0	c1	0
2a2	4.0	20.	10.	5.	83.	180.	c1	3	0	0.2	2.5	0	c1	0
2a3	4.0	20.	10.	5.	83.	180.	c1	3	0	0.5	2.5	0	c1	0
2a4	4.0	20.	10.	5.	83.	180.	c1	3	0	1	2.5	0	c1	0
2a5	4.0	20.	10.	5.	83.	180.	c1	3	0	2	2.5	0	c1	0
2a6	4.0	20.	10.	5.	83.	180.	c1	3	0	5	2.5	0	c1	0
2b1	4.0	20.	10.	5.	83.	180.	c1	3	0	0	2.5	2	c1	0
2b2	4.0	20.	10.	5.	83.	180.	c1	3	0	0	2.5	4	c1	0
2b3	4.0	20.	10.	5.	83.	180.	c1	3	0	0	2.5	6	c1	0
2b4	4.0	20.	10.	5.	83.	180.	c1	3	0	0	2.5	8	c1	0
2b5	4.0	20.	10.	5.	83.	180.	c1	3	0	0	2.5	10	c1	0
2b6	4.0	20.	10.	55.	63.	80.	c1	3	0	0	2.5	10	c1	0
2c2	4.0	20.	10.	5.	83.	180.	c1	3	0	0	2.5	0	c2	0
2e1	4.0	20.	10.	5.	83.	180.	c1	2	0	0	2.5	0	c1	0
2e2	4.0	20.	10.	5.	83.	180.	c1	4	0	0	2.5	0	c1	0
2e3	4.0	20.	10.	5.	83.	180.	c1	5	0	0	2.5	0	c1	0
2e4	4.0	20.	10.	5.	83.	180.	c1	6	0	0	2.5	0	c1	0
2f1	4.0	20.	10.	5.	83.	180.	c1	3	0	0	3.5	0	c1	0
2f2	4.0	20.	10.	5.	83.	180.	c1	3	0	0	3.25	0	c1	0
2f3	4.0	20.	10.	5.	83.	180.	c1	3	0	0	3	0	c1	0
2f4	4.0	20.	10.	5.	83.	180.	c1	3	0	0	2.75	0	c1	0
2f5	4.0	20.	10.	5.	83.	180.	c1	3	0	0	2.25	0	c1	0
2f6	4.0	20.	10.	5.	83.	180.	c1	3	0	0	2	0	c1	0
2f7	4.0	20.	10.	5.	83.	180.	c1	3	0	0	1.75	0	c1	0
2f8	4.0	20.	10.	5.	83.	180.	c1	3	0	0	1.5	0	c1	0
2f9	4.0	20.	10.	5.	83.	180.	c1	3	0	0	1.25	0	c1	0
2f10	4.0	20.	10.	5.	83.	180.	c1	3	0	0	1	0	c1	0
2g1	4.0	20.	10.	5.	83.	180.	c1	3	0.1	1	2.25	3	c2	2.
2g2	4.0	20.	10.	5.	83.	180.	c1	3	0.1	1	2	5	c3	2.
2g3	4.0	20.	10.	55.	63.	80.	c1	3	0.1	1	2.25	3	c2	2.
2g4	4.0	20.	10.	55.	63.	80.	c1	3	0.1	1	2	5	c3	2.
2g5	4.0	20.	10.	5.	83.	180.	c1	3	0.1	1	2.25	3	c2	5
2g6	4.0	20.	10.	5.	83.	180.	c1	3	0.1	1	2	5	c3	5
2g7	4.0	20.	10.	55.	63.	80.	c1	3	0.1	1	2.25	3	c2	10
2g8	4.0	20.	10.	55.	63.	80.	c1	3	0.1	1	2	5	c3	10
2b10	4.0	20.	10.	56.	64.	81.	c1	3	0	0	2.5	20	c1	0
2b11	4.0	20.	10.	56.	64.	81.	c1	3	0	0	2.5	20	c1	0

**Table S6** Crustal velocity model **c1** used for calculation of the synthetic Green's functions.

Depth (km)	Vp (km/s)	Vs (km/s)	density (kg/cm <sup>3</sup> )	P-wave attenuation Qp	S-wave attenuation Qs
0.	2.5	1.2	2.1	50.	50.
1.	2.5	1.2	2.1	50.	50.
1.	4.	2.1	2.4	200.	200.
2.	4.	2.1	2.4	200.	200.
2.	6.2	3.6	2.8	600.	400.
14.	6.2	3.6	2.8	600.	400.
14.	6.6	3.7	2.9	1432.	600.
27.	6.6	3.7	2.9	1432.	600.
27.	7.3	4.	3.1	1499.	600.
36.	7.3	4.	3.1	1499.	600.

**Table S7** Crustal velocity model **c2** used for calculation of the synthetic Green's functions.

Depth (km)	Vp (km/s)	Vs (km/s)	density (kg/cm <sup>3</sup> )	P-wave attenuation Qp	S-wave attenuation Qs
0.	2.5	1.2	2.1	50.	50.
3.	2.5	1.2	2.1	50.	50.
3.	4.	2.1	2.4	200.	200.
4.	4.	2.1	2.4	200.	200.
4.	6.2	3.6	2.8	600.	400.
10.	6.2	3.6	2.8	600.	400.
10.	6.6	3.7	2.9	1432.	600.
12.	6.6	3.7	2.9	1432.	600.
12.	4.	2.1	2.4	200.	200.
18.	4.	2.1	2.4	200.	200.
18.	6.6	3.7	2.9	1432.	600.
24.	6.6	3.7	2.9	1432.	600.
24.	7.3	4.	3.1	1499.	600.
36.	7.3	4.	3.1	1499.	600.

**Table S8** Crustal velocity model **c3** used for calculation of the synthetic Green's functions.

Depth (km)	Vp (km/s)	Vs (km/s)	density (kg/cm <sup>3</sup> )	P-wave attenuation Qp	S-wave attenuation Qs
0.	2.5	1.2	2.1	50.	50.
2.	2.5	1.2	2.1	50.	50.
2.	4.	2.1	2.4	200.	200.
4.	4.	2.1	2.4	200.	200.
4.	2.5	1.2	2.1	50.	50.
8.	2.5	1.2	2.1	50.	50.
8.	6.2	3.6	2.8	600.	400.
10.	6.2	3.6	2.8	600.	400.
10.	6.6	3.7	2.9	1432.	600.
12.	6.6	3.7	2.9	1432.	600.
12.	4.	2.1	2.4	200.	200.
18.	4.	2.1	2.4	200.	200.
18.	8.037	4.485	3.598	966.6	401.3
19.	8.037	4.485	3.598	966.6	401.3
19.	6.6	3.7	2.9	1432.	600.
24.	6.6	3.7	2.9	1432.	600.
24.	7.3	4.	3.1	1499.	600.
36.	7.3	4.	3.1	1499.	600.

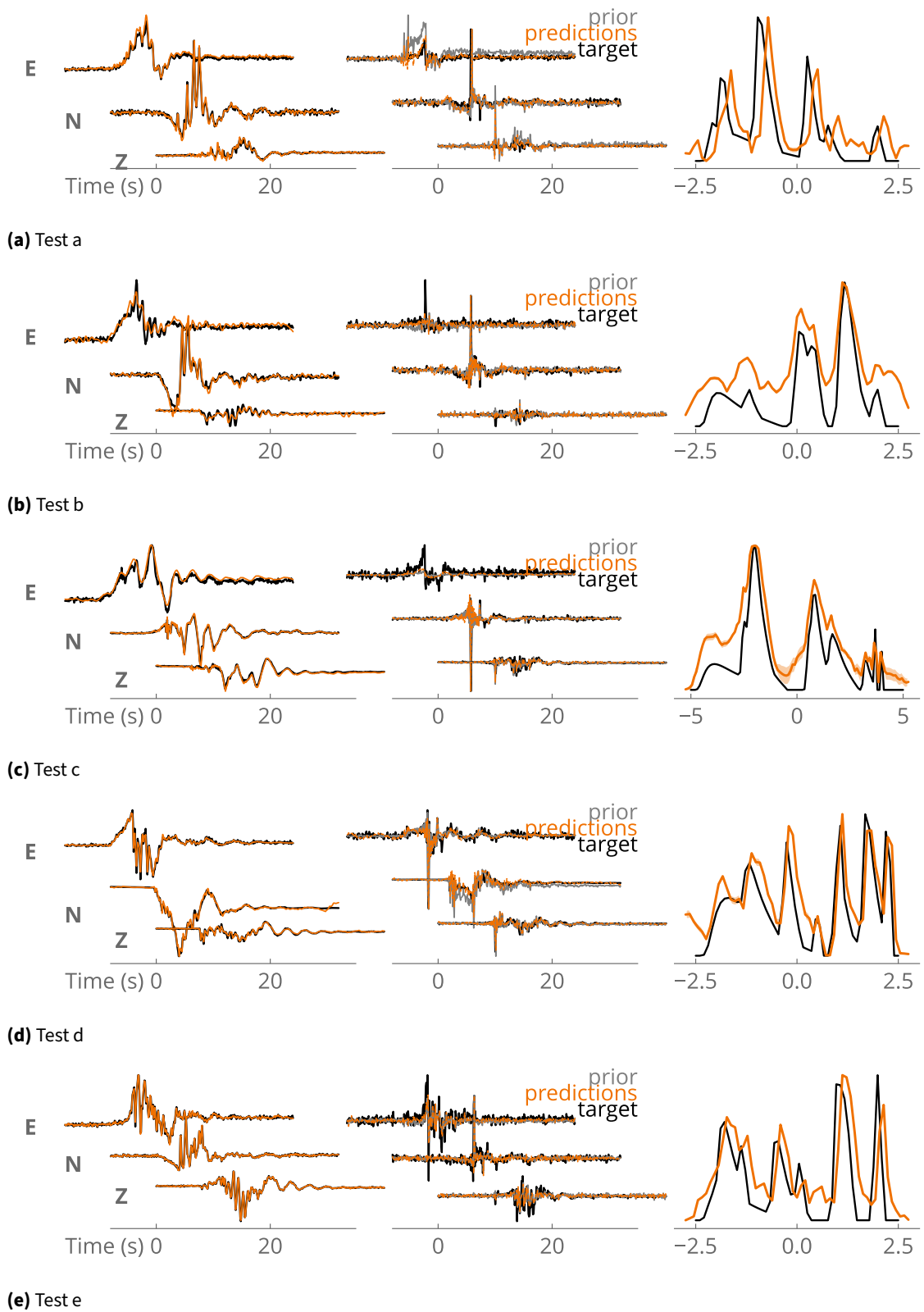


**Figure S1** Inferred (orange) and target (black) waveforms (left), EGF (middle) and STF (right) for synthetic tests **a** to **e**. Prior EGF is in gray.

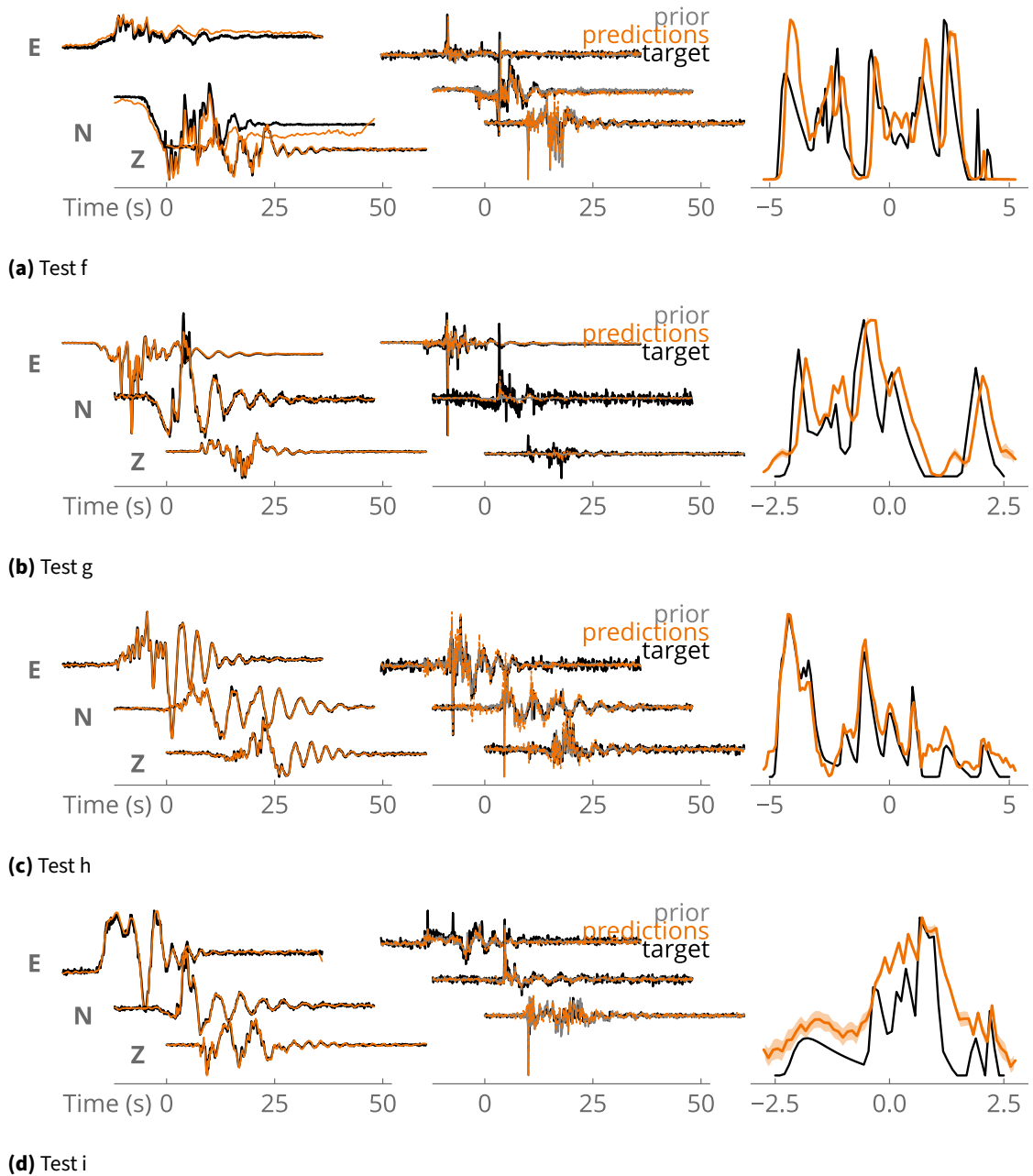


**Figure S2** Inferred (orange) and target (black) waveforms (left), EGF (middle) and STF (right) for synthetic tests **f** to **i**. Prior EGF is in gray.

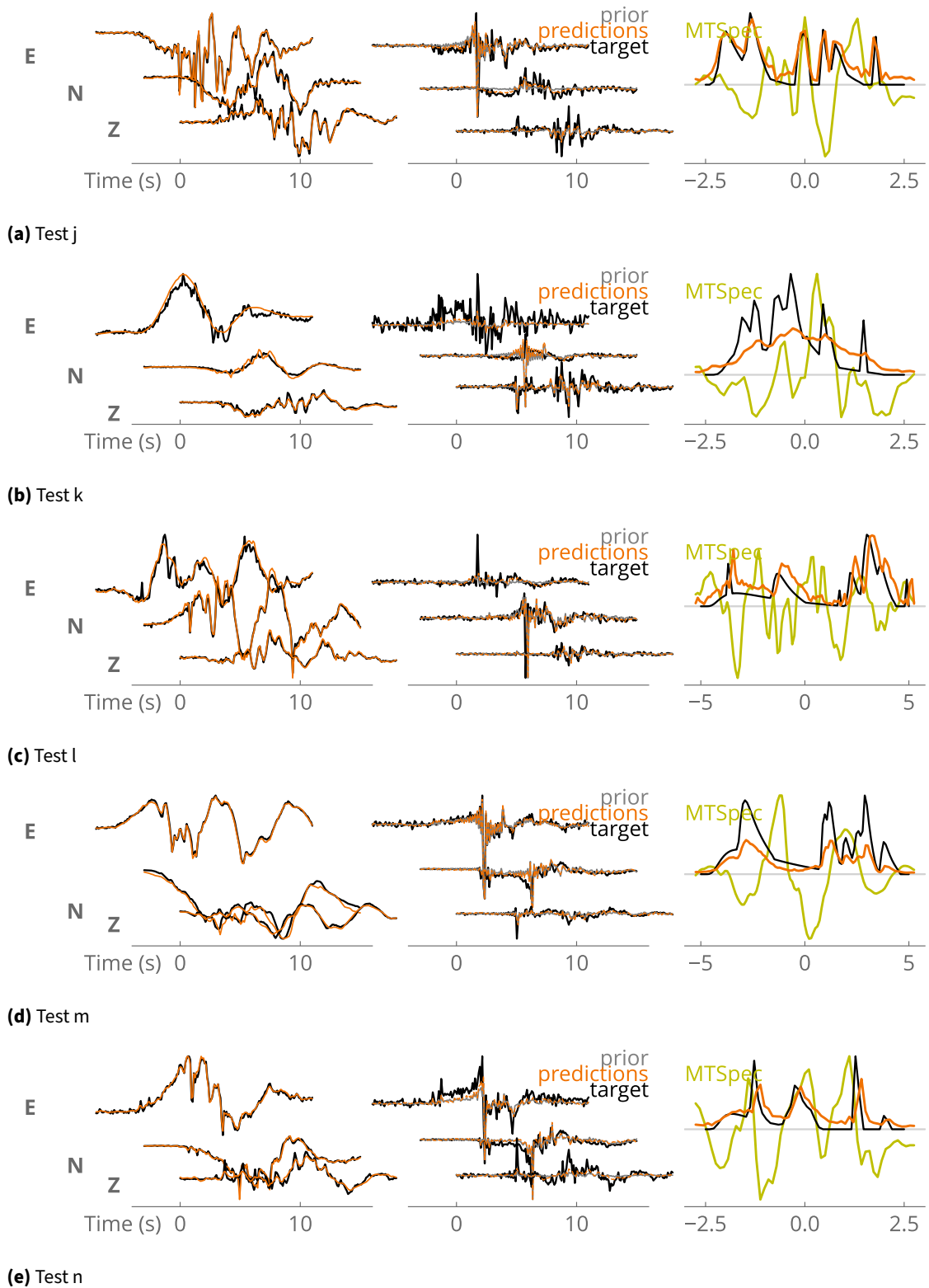


**Figure S3** Inferred (orange) and target (black) waveforms (left), EGF (middle) and STF (right) for synthetic tests **j** to **n**. Prior EGF is in gray.



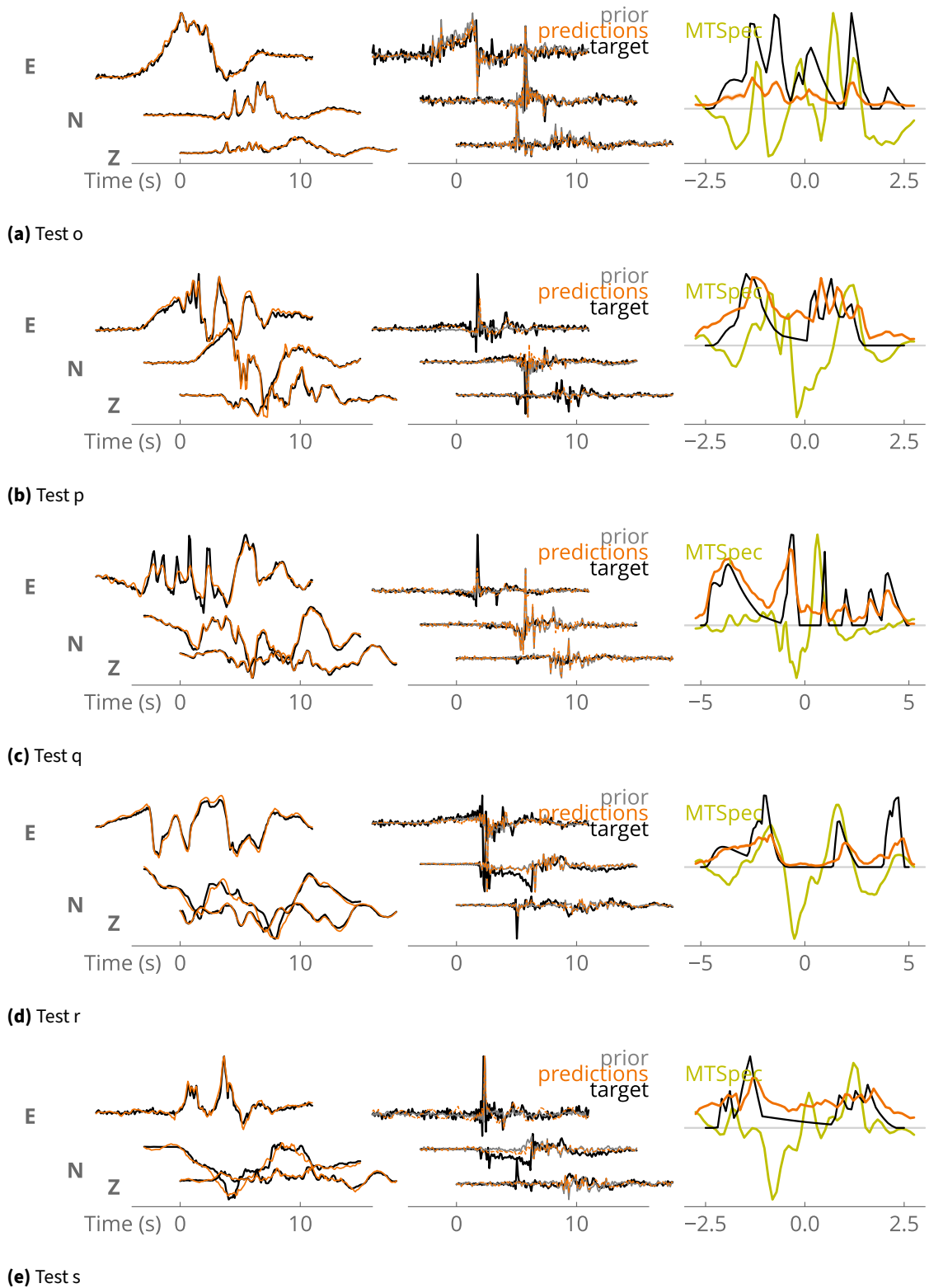


**Figure S4** Inferred (orange) and target (black) waveforms (left), EGF (middle) and STF (right) for synthetic tests o to s. Prior EGF is in gray.

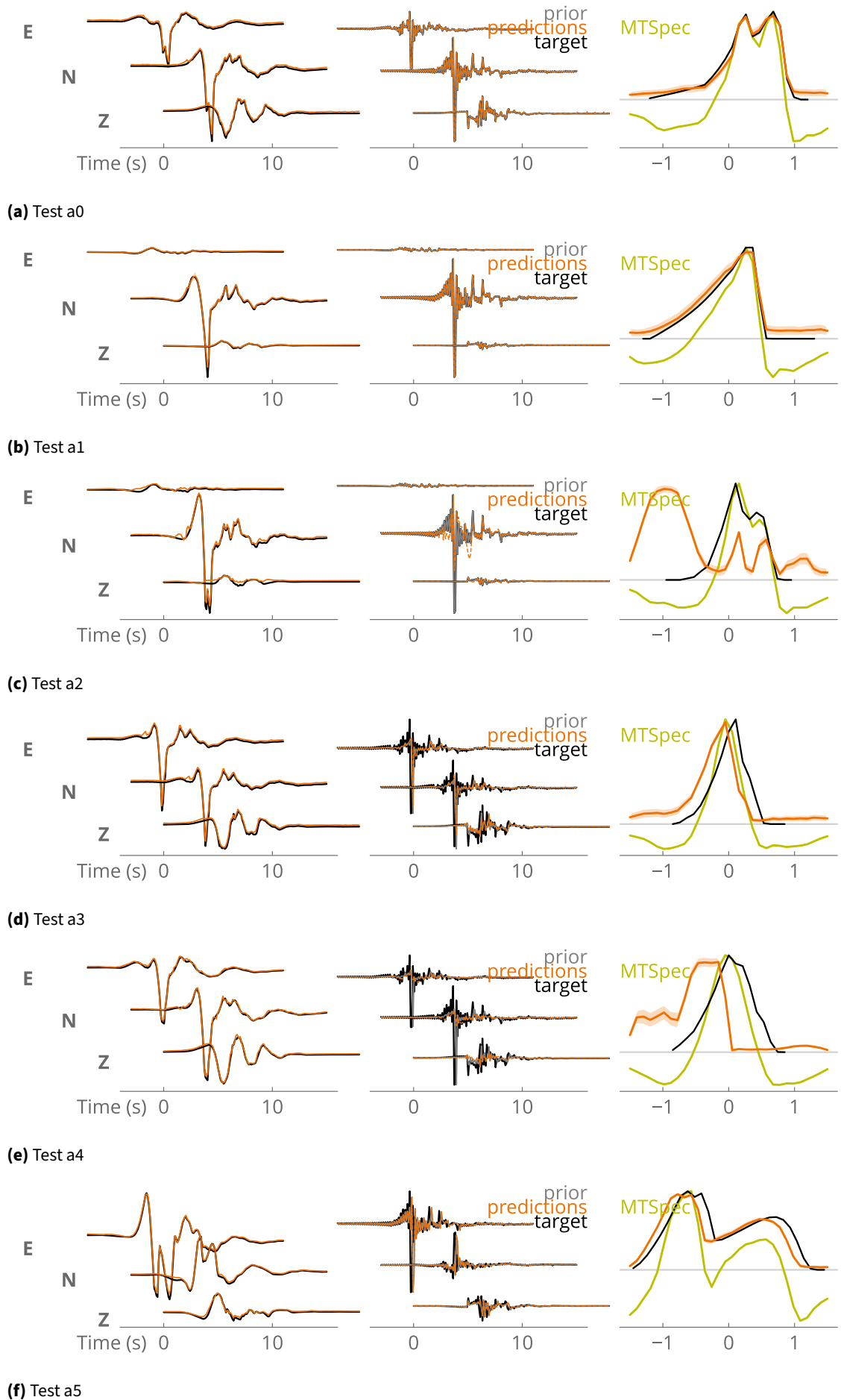


**Figure S5** Inferred (orange) and target (black) waveforms (left), EGF (middle) and STF (right) for synthetic tests **a0** to **a5**. Prior EGF is in gray, and the STF inferred with MTSpec in green.

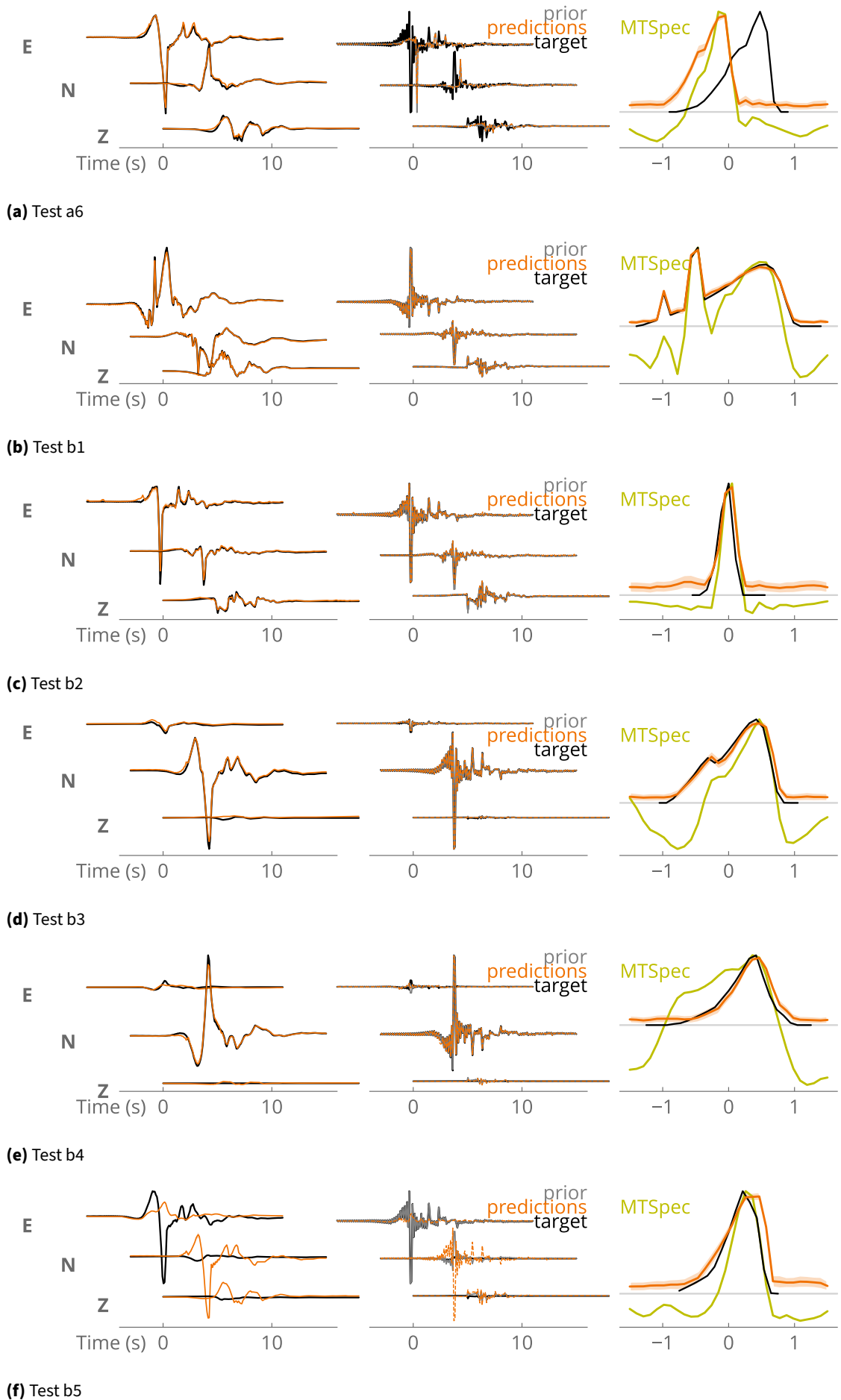


**Figure S6** Inferred (orange) and target (black) waveforms (left), EGF (middle) and STF (right) for synthetic tests **a6** to **b5**. Prior EGF is in gray, and the STF inferred with MTSpec in green.

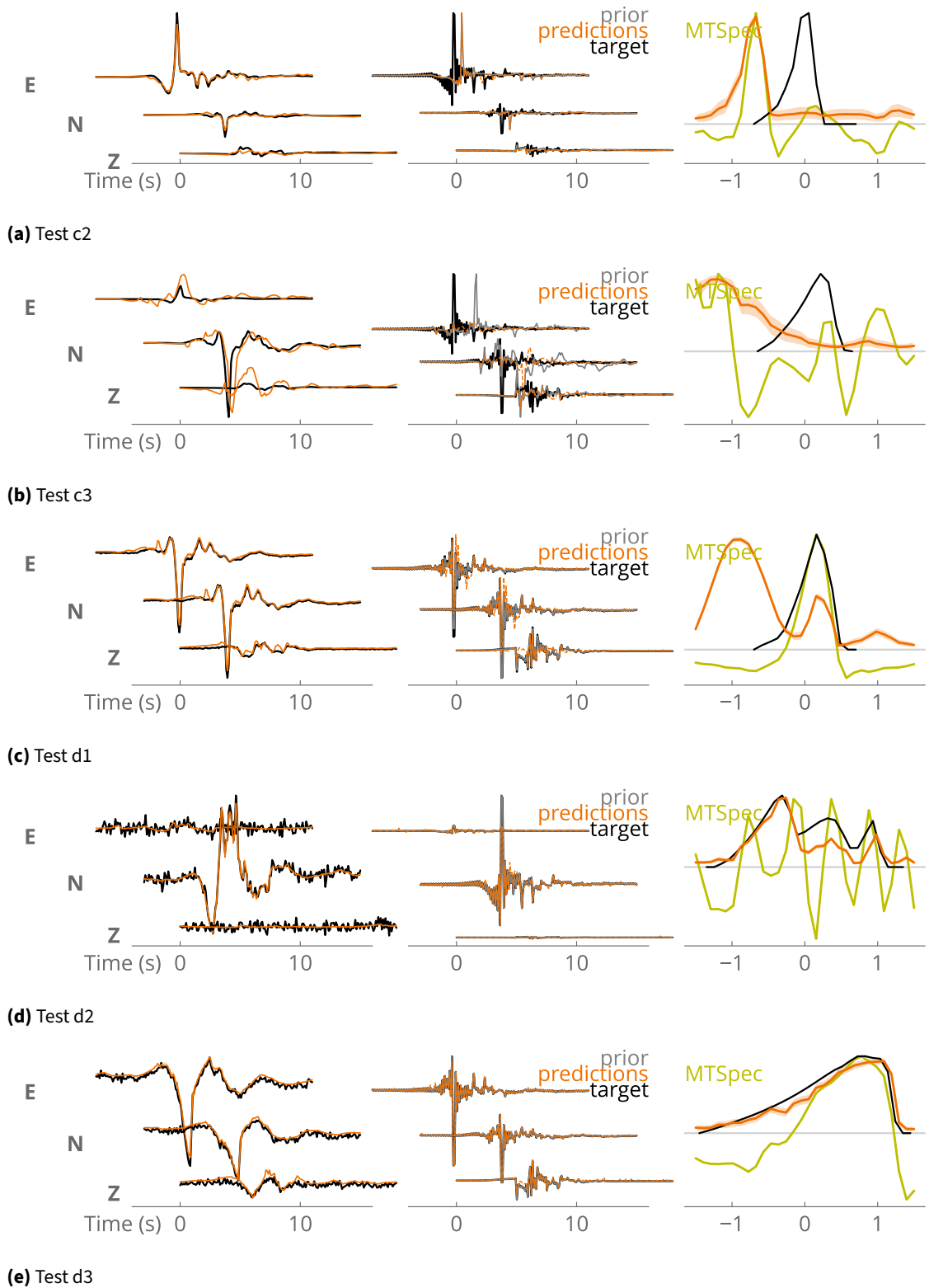


**Figure S7** Inferred (orange) and target (black) waveforms (left), EGF (middle) and STF (right) for synthetic tests **c2** to **d3**. Prior EGF is in gray.

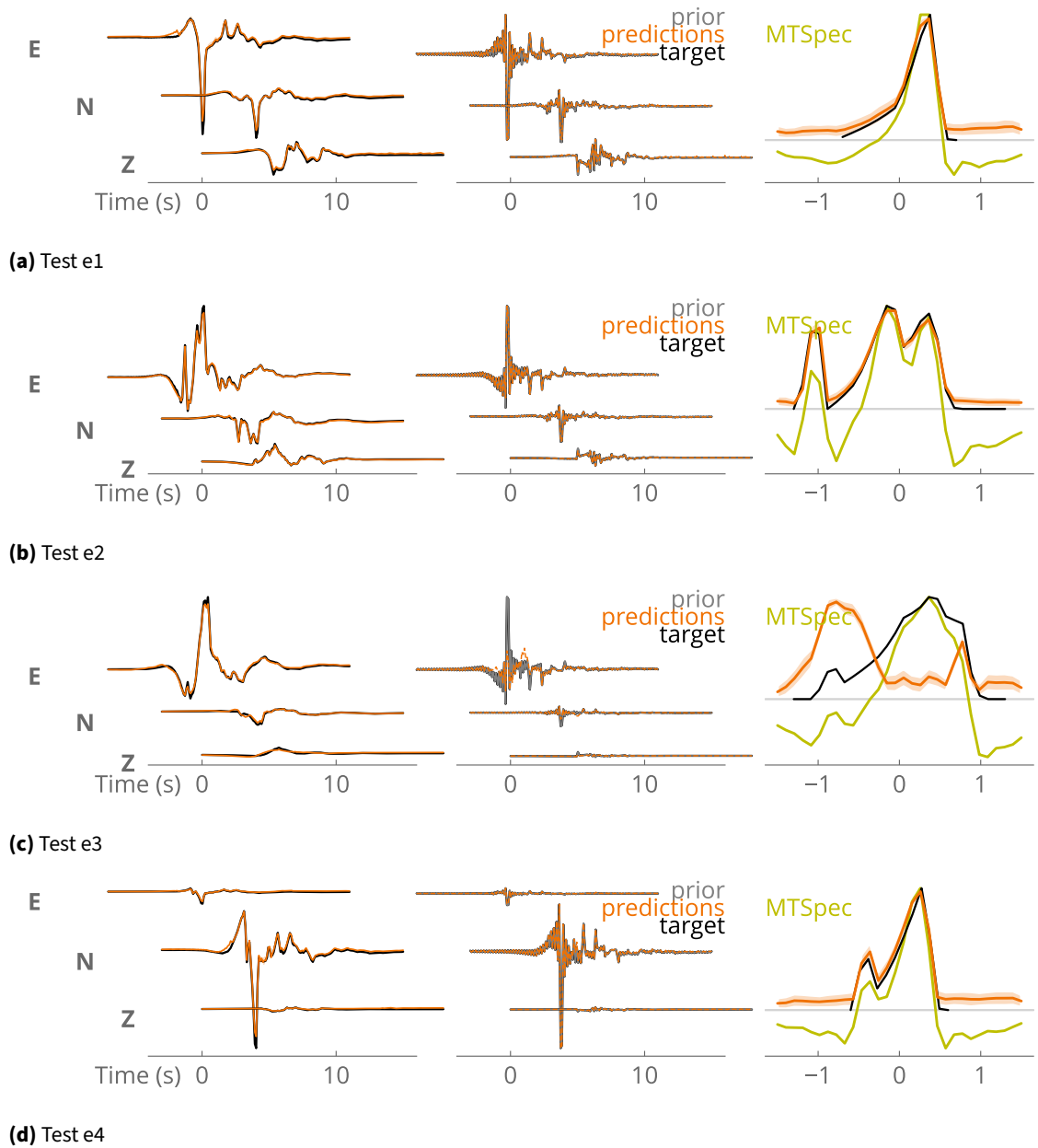


**Figure S8** Inferred (orange) and target (black) waveforms (left), EGF (middle) and STF (right) for synthetic tests **e1** to **e4**. Prior EGF is in gray.

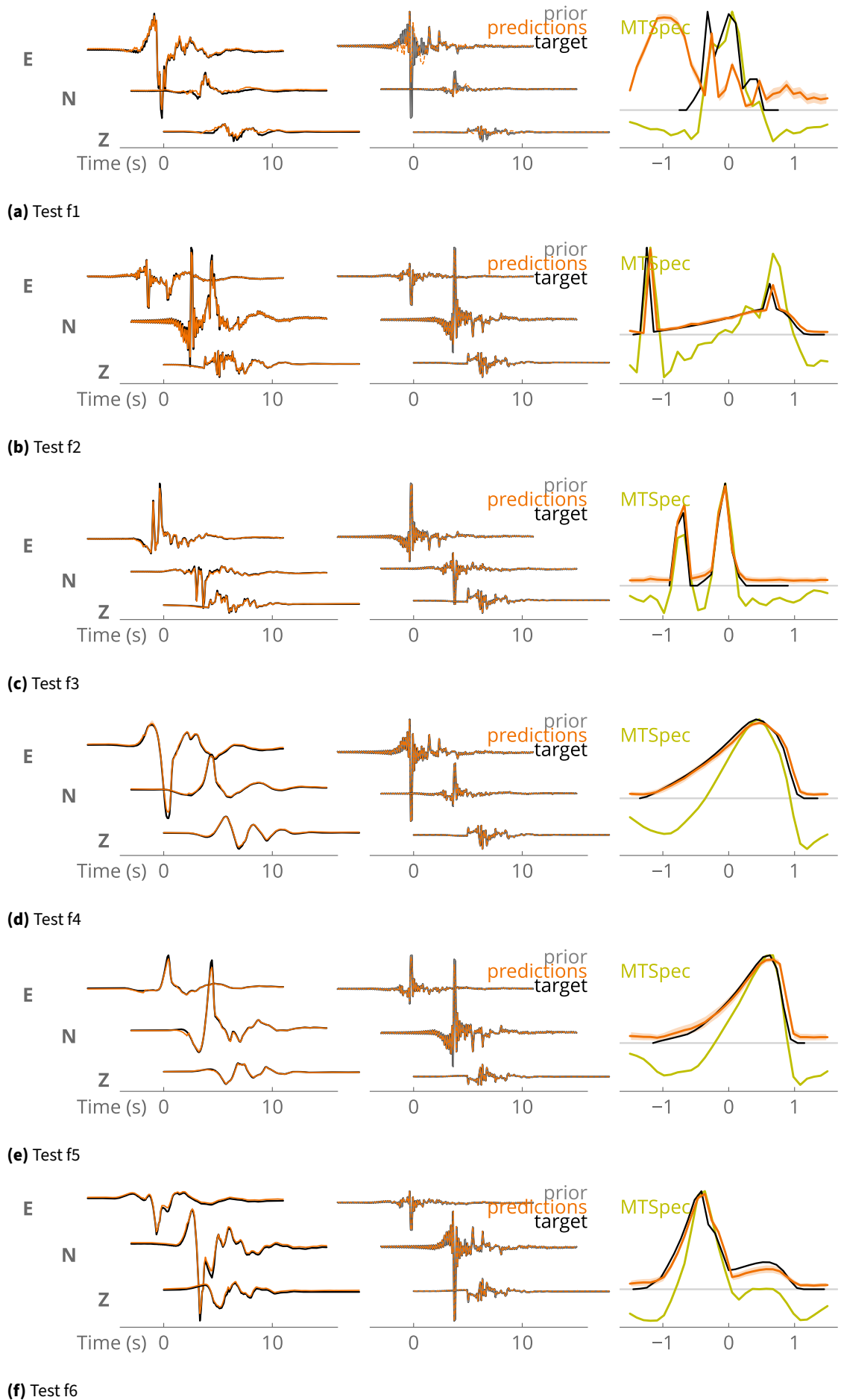


**Figure S9** Inferred (orange) and target (black) waveforms (left), EGF (middle) and STF (right) for synthetic tests **f1** to **f6**. Prior EGF is in gray, and the STF inferred with MTSpec in green.

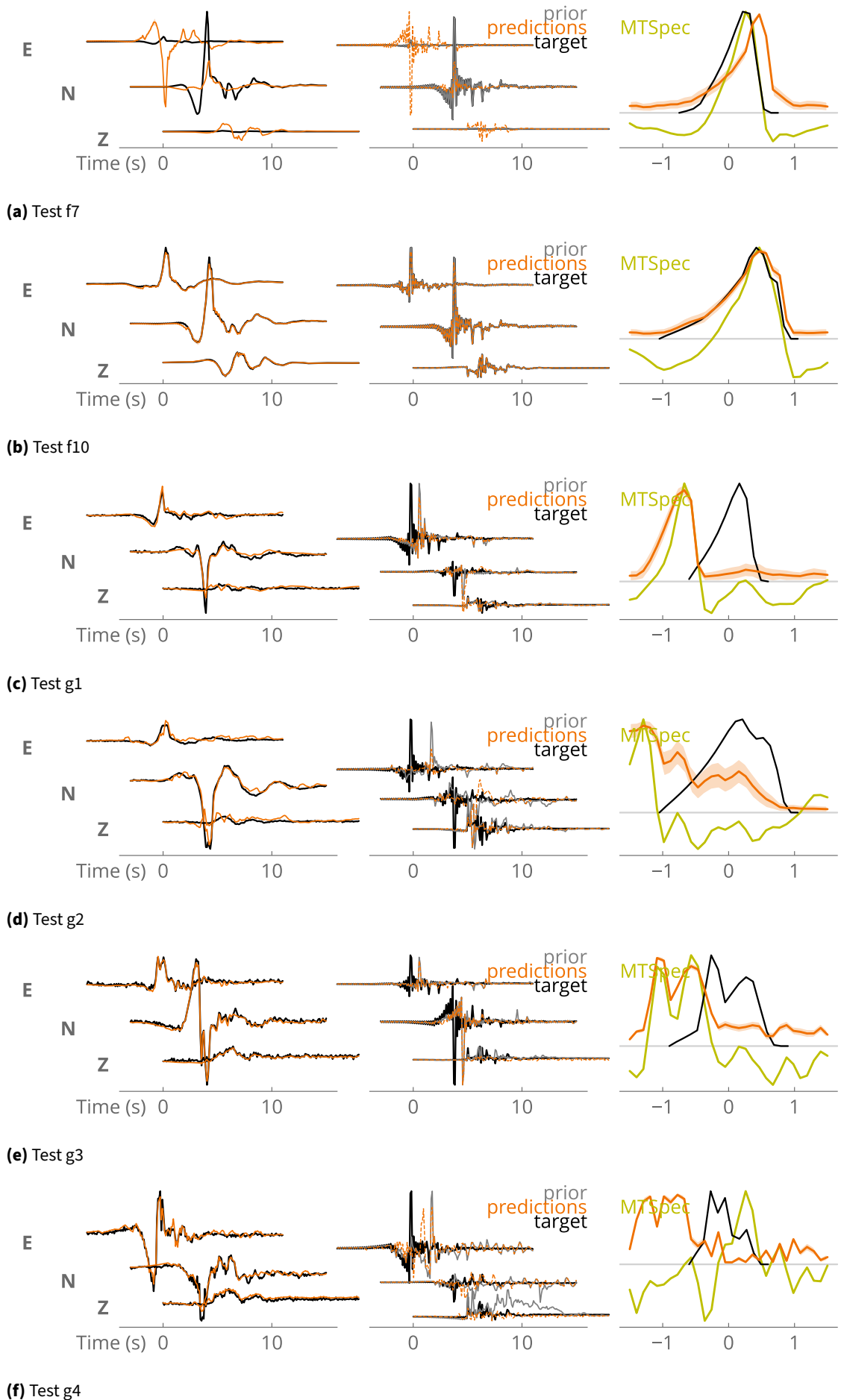


**Figure S10** Inferred (orange) and target (black) waveforms (left), EGF (middle) and STF (right) for synthetic tests **f7** to **g4**. Prior EGF is in gray, and the STF inferred with MTSpec in green.

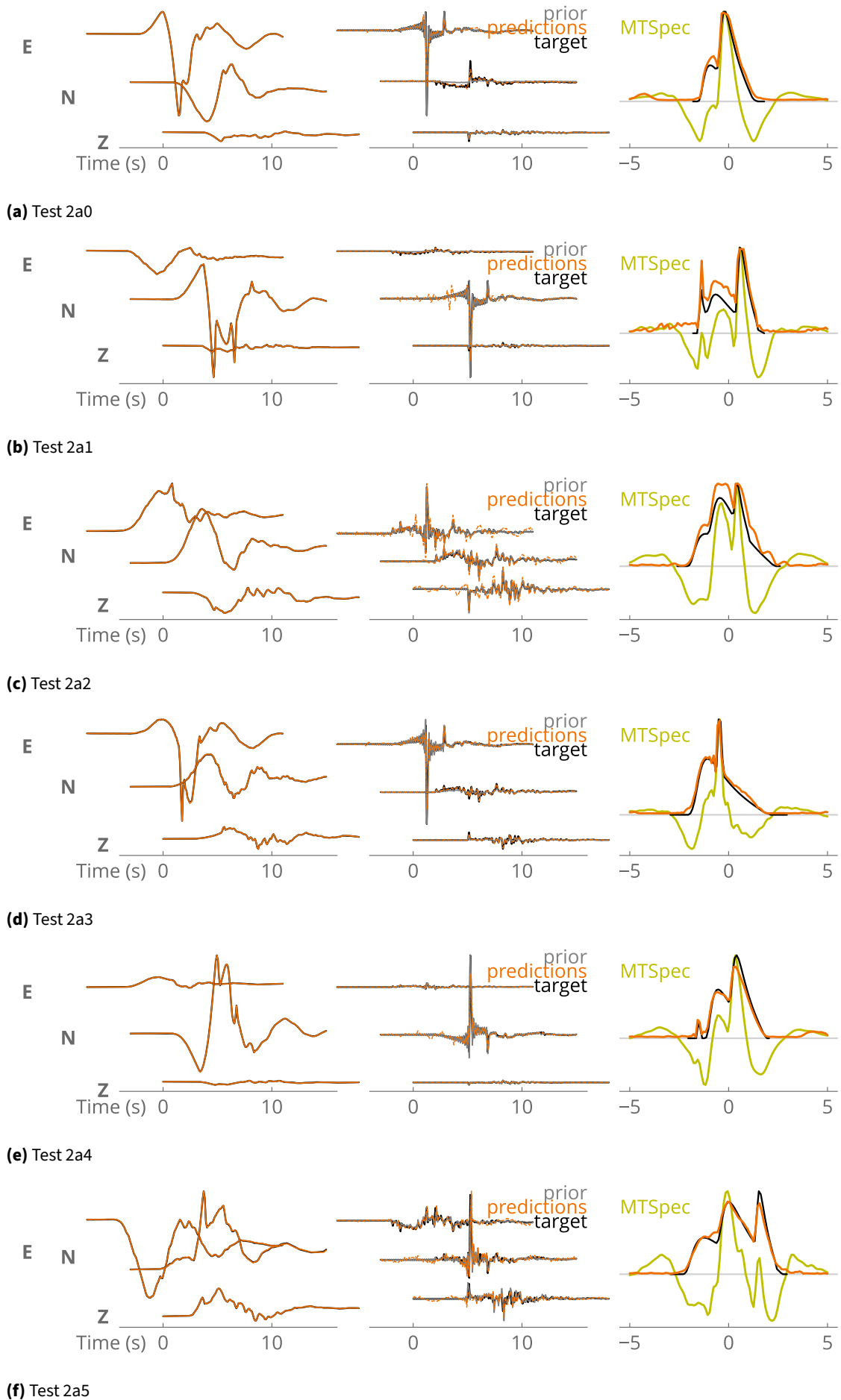


**Figure S11** Inferred (orange) and target (black) waveforms (left), EGF (middle) and STF (right) for synthetic tests **2a0** to **2a5**. Prior EGF is in gray, and the STF inferred with MTSpec in green.



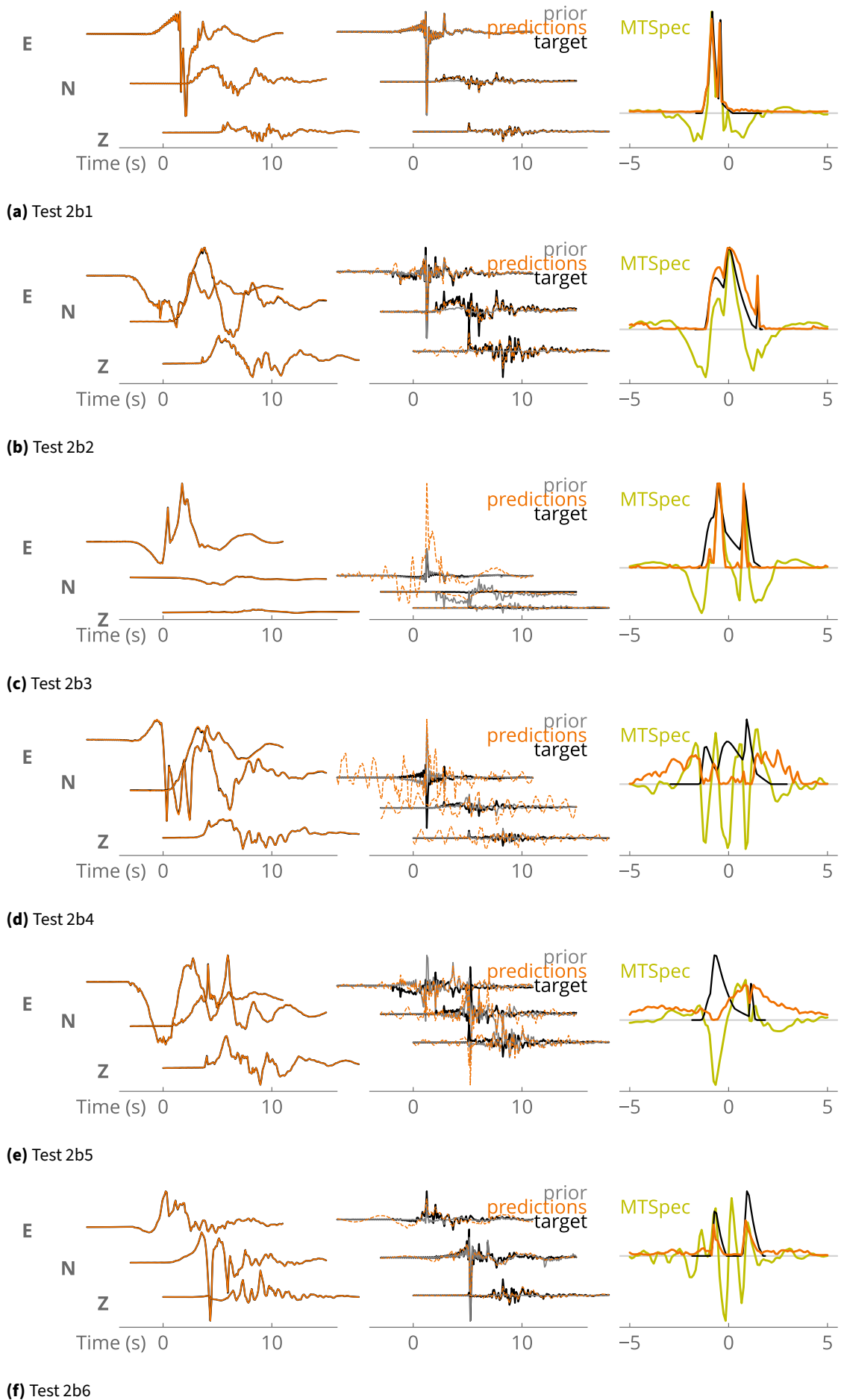


**Figure S12** Inferred (orange) and target (black) waveforms (left), EGF (middle) and STF (right) for synthetic tests **2b1** to **2b6**. Prior EGF is in gray, and the STF inferred with MTSpec in green.

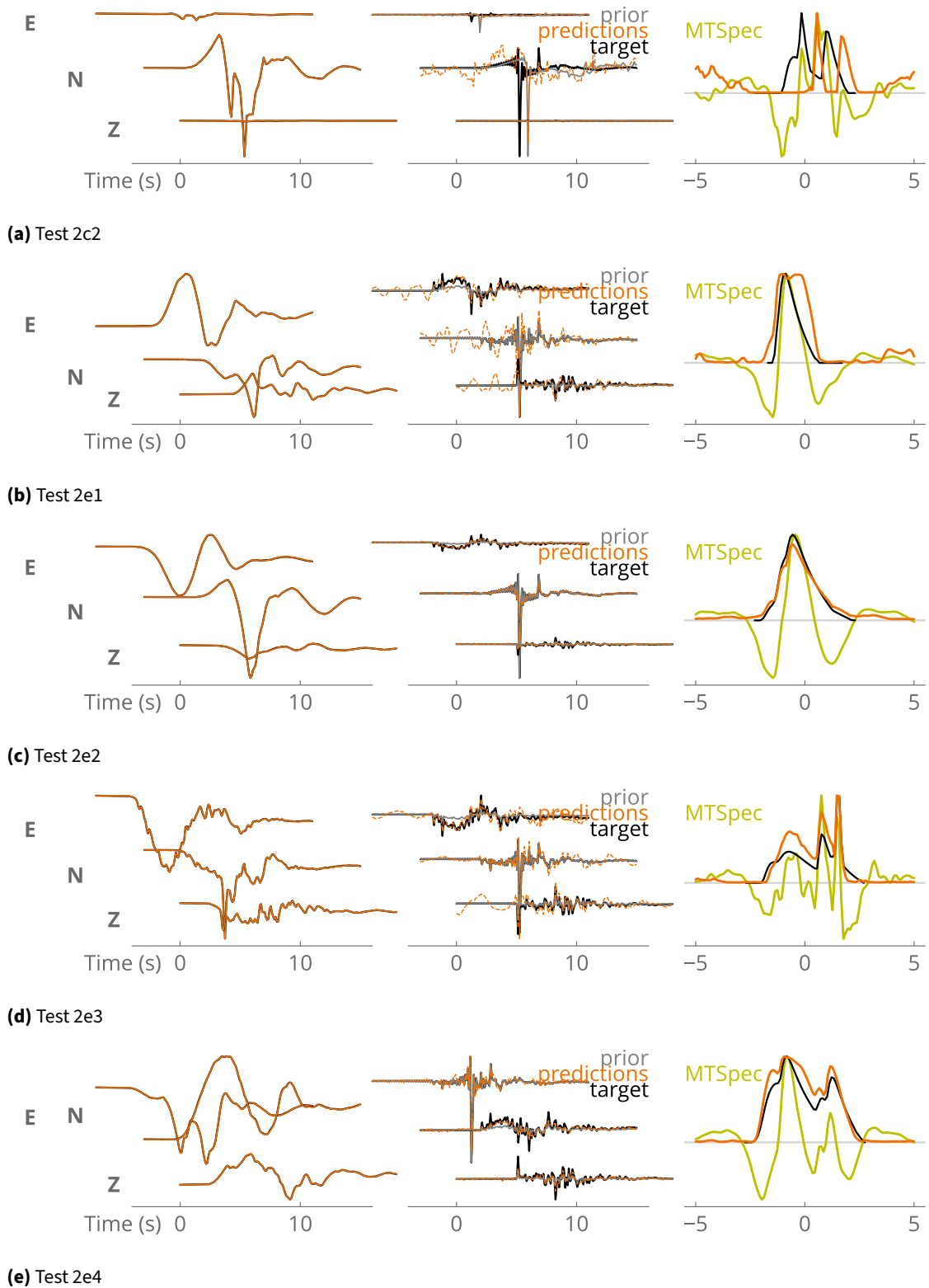


**Figure S13** Inferred (orange) and target (black) waveforms (left), EGF (middle) and STF (right) for synthetic tests **2c2** to **2e4**. Prior EGF is in gray.

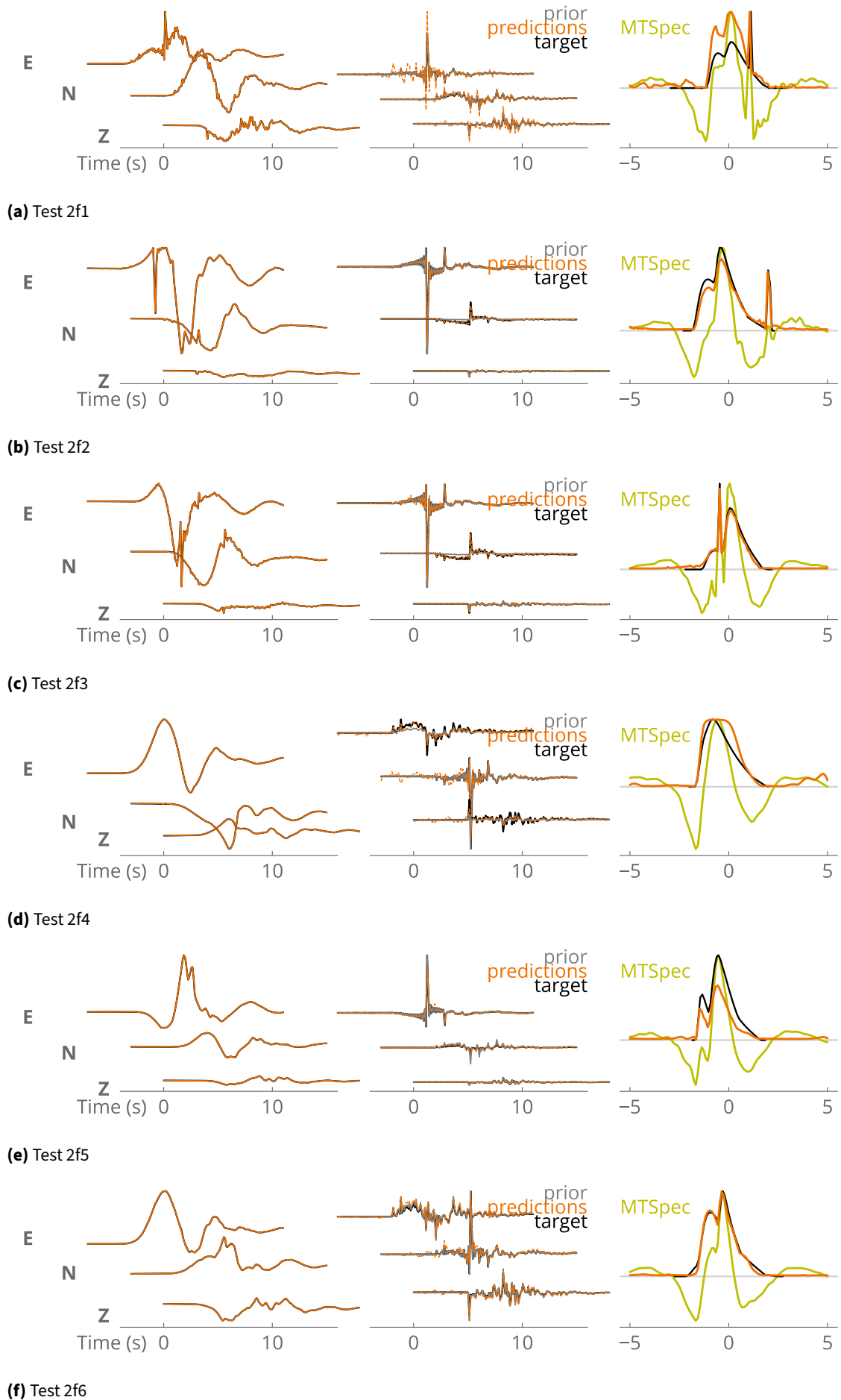


**Figure S14** Inferred (orange) and target (black) waveforms (left), EGF (middle) and STF (right) for synthetic tests 2f1 to 2f6. Prior EGF is in gray, and the STF inferred with MTSpec in green.

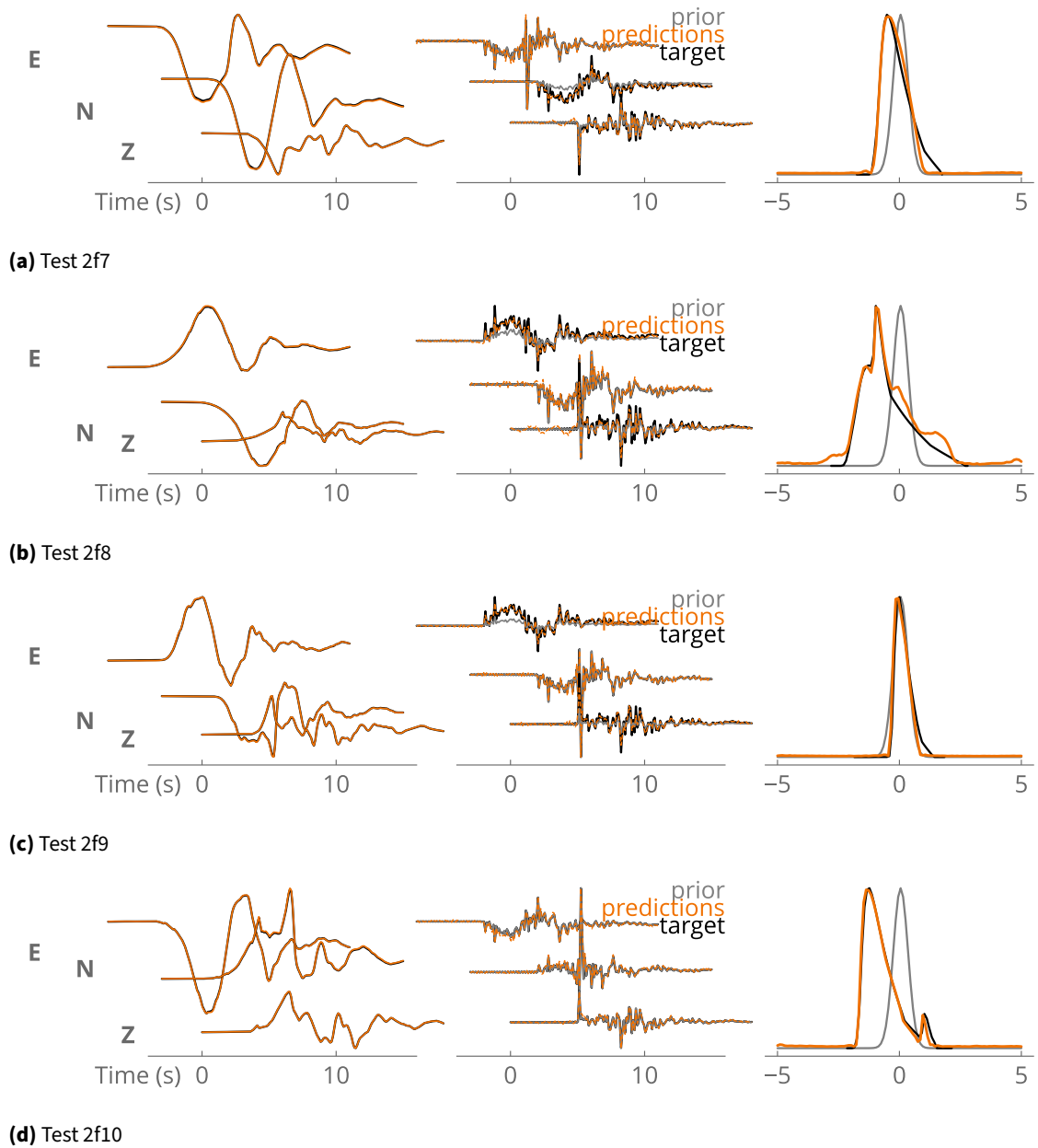


**Figure S15** Inferred (orange) and target (black) waveforms (left), EGF (middle) and STF (right) for synthetic tests **2f7** to **2f10**. Prior EGF is in gray.

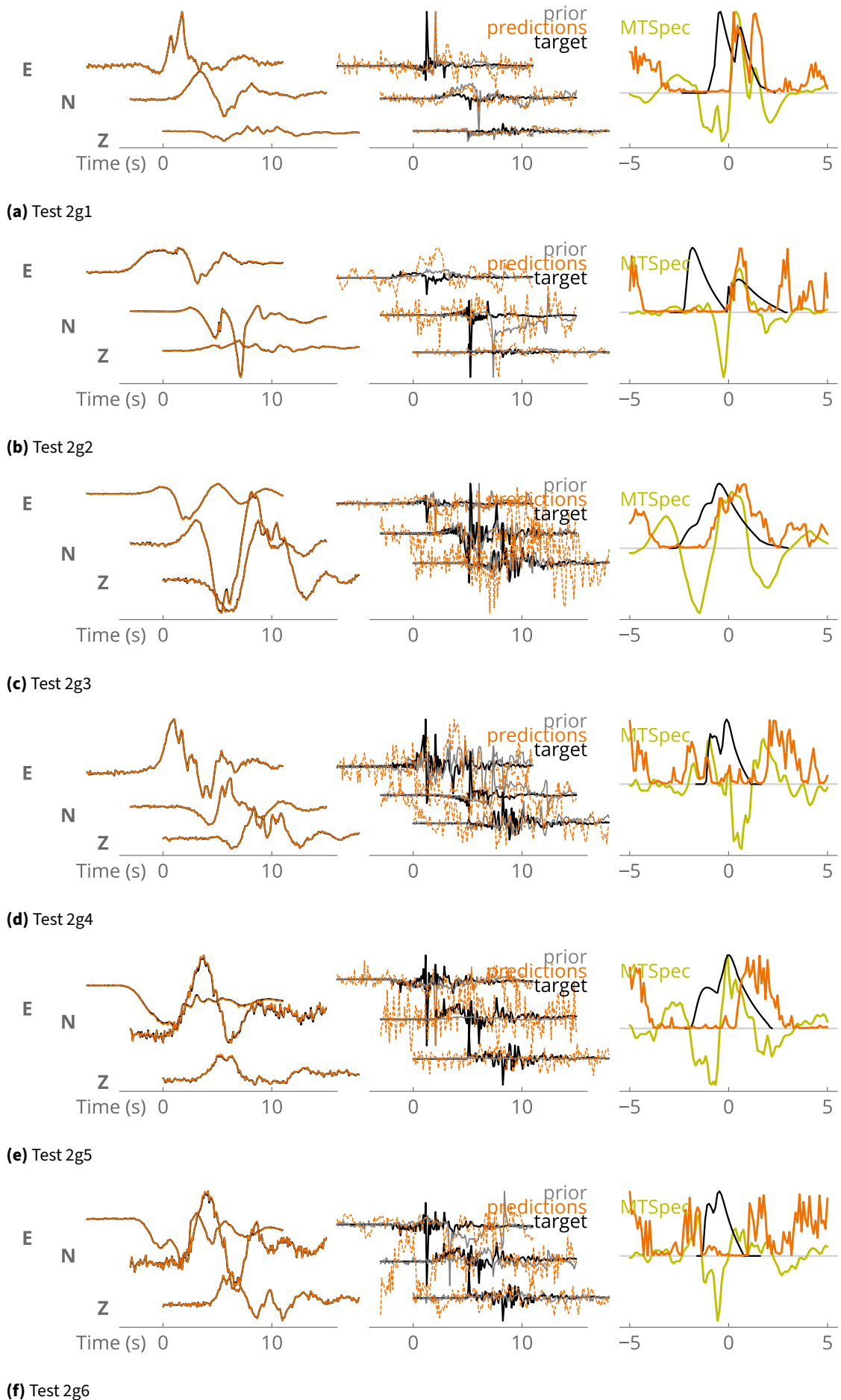


**Figure S16** Inferred (orange) and target (black) waveforms (left), EGF (middle) and STF (right) for synthetic tests **2g1** to **2g6**. Prior EGF is in gray, and the STF inferred with MTSpec in green.

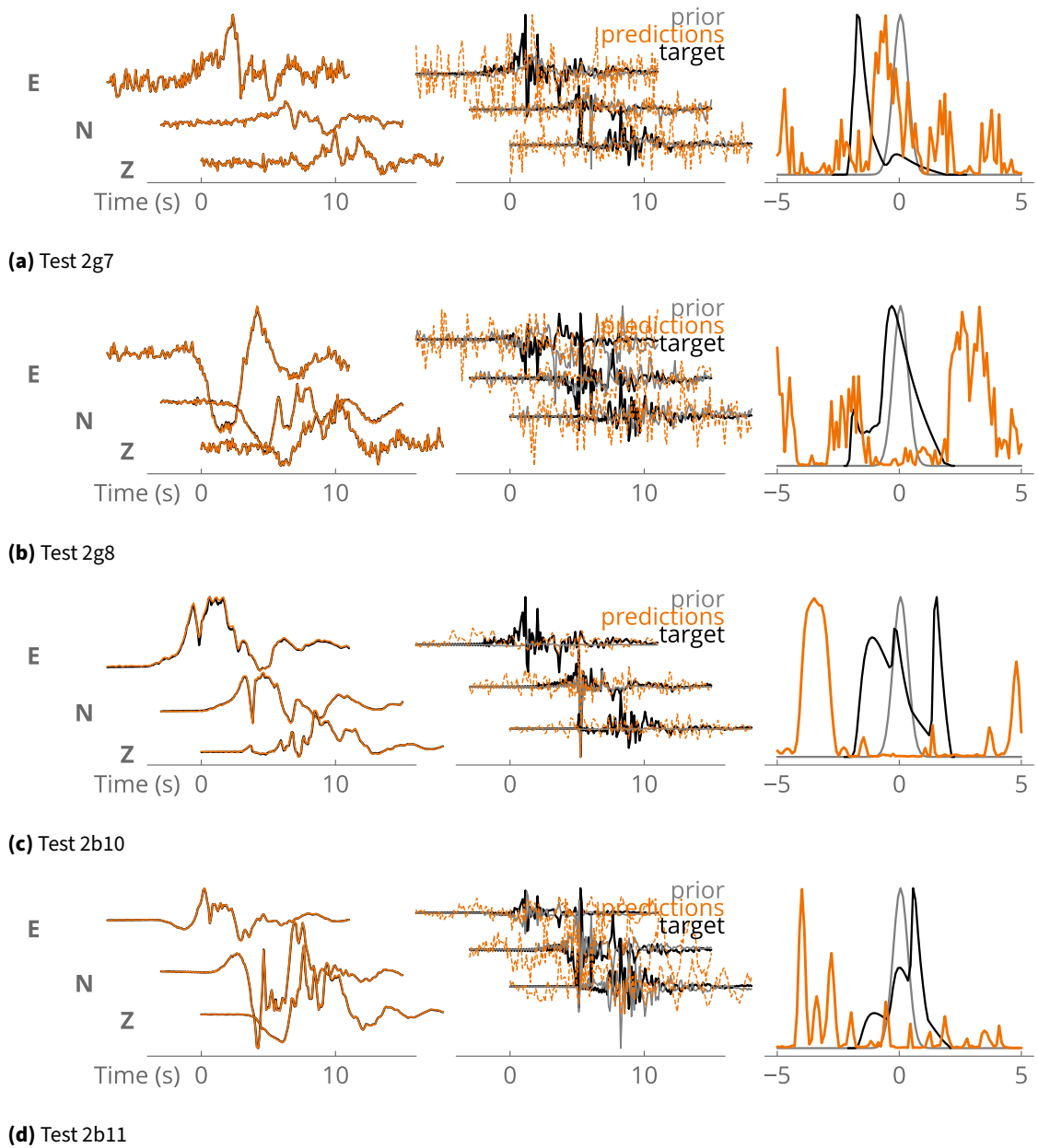


**Figure S17** Inferred (orange) and target (black) waveforms (left), EGF (middle) and STF (right) for synthetic tests **2g7** to **2b11**. Prior EGF is in gray.

## S3 Toy models with recorded waveforms: the 2016 Borrego Springs sequence, CA

### S3.1 Data

We use seismic data recorded by the regional network (CI), plate boundary observatory (PB), ANZA network (AZ) and UCSB (SB) networks in Southern California for a ML 3.37 event that occurred on 17 July 2014 (SCSN-ID:15527617; 17 July 2014 14:24:34). We select stations within 100 km of this event, and we use both broadband and accelerometer data. We only present here a subset of the stations.

### S3.2 Description of the forward model

We use the normalized waveforms of the ML 3.37 event as EGF, to which we add white noise (PSNR 3%, the noise is different for each component). To obtain the target waveforms of the main toy model event, we convolve this EGF with an STF whose characteristics are similar to the fully synthetic toy models. STFs either have  $N_{STF} = 3$ ,  $D_{STF} = 2s$  or  $N_{STF} = 10$ ,  $D_{STF} = 9s$ . We add again white noise, PSNR 3%, to each of the components of the waveforms for the main toy model event.

We either use the full waveforms (both P and S arrivals, tests in Fig. S18) or the P arrivals only (tests in Figs. S19 and S20). For the later case, we trim the waveforms to just before the S waves arrivals. We use Phasenet (Zhu and Beroza, 2019) to determine phase arrivals. To decrease the computation time, we decimate the toy model waveforms (for both the EGF and main event) to 20 Hz (for broadband) or 25 Hz (for accelerometers) when using the full waveforms. We decimate the data to 40 or 50 Hz when using the P arrivals only (tests in Fig. S18).

#### Prior assumptions for DeepGEM

We used the following non-default parameters for DeepGEM:

```
num_epochs = 100
EMFull = True
stf_dur = 9
Elr = 8e-3
Mlr = 5e-6
data_sigma = 5e-6
```

#### Prior assumptions for the Landweber approach

For some tests, we compare DeepGEM inferences with a frequency-domain deconvolution using the approach proposed by Bertero et al. (1997). We use the same downsampling as with DeepGEM. We first fix the duration of the STF and optimize its time shift with a least-square approach. We impose 500 iterations. We estimate apparent STFs for each component and each EGF, and then either visually select the best fitting STF.

### S3.3 Results

#### List of figures:

- Fig. S18: full waveforms,  $N_{STF} = 3$
- Fig. S19, P waves arrivals,  $N_{STF} = 10$
- Fig. S20, P waves arrivals,  $N_{STF} = 10$

The average run time for these toy models is of 8 minutes.

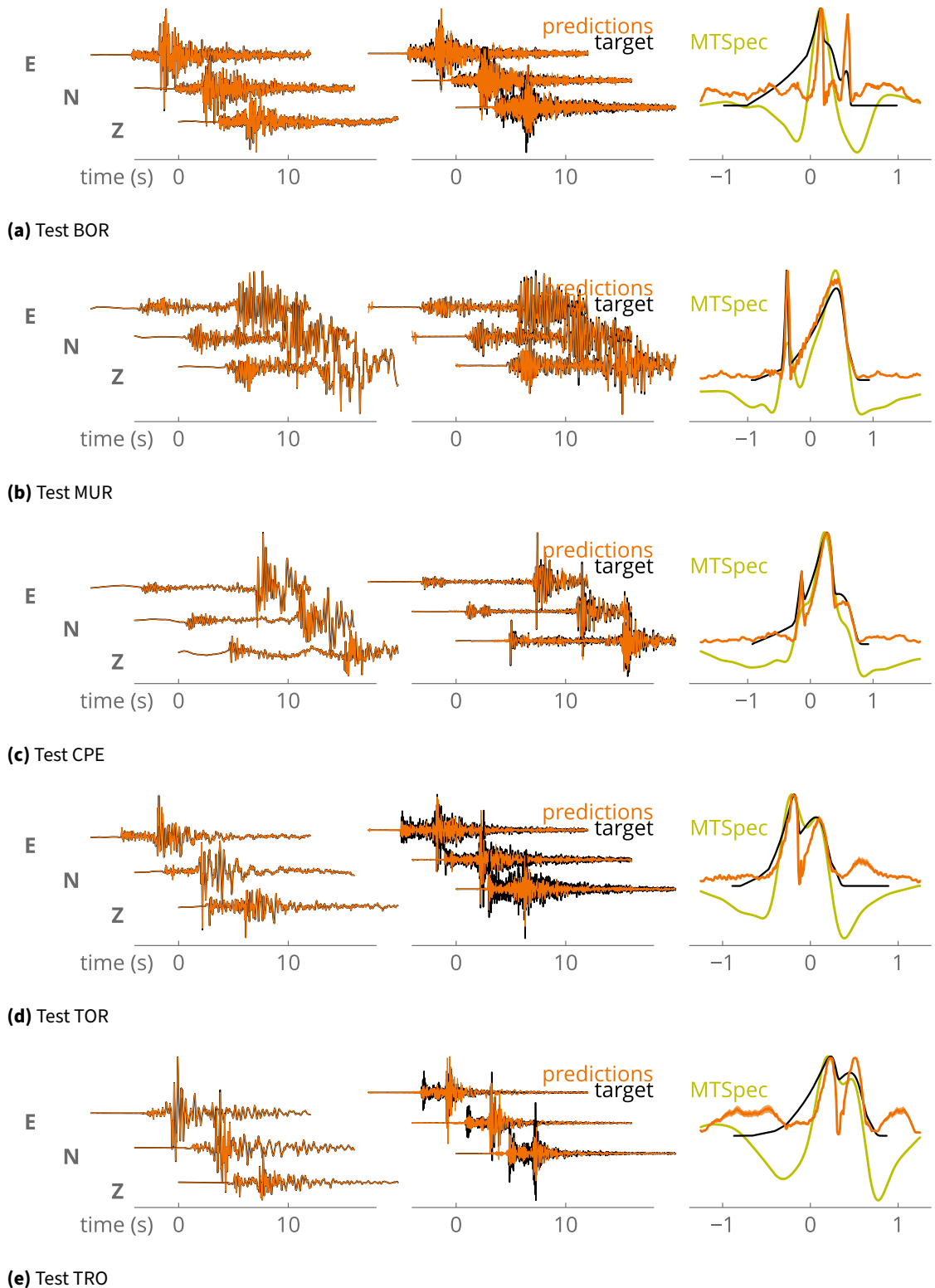


**Figure S18** Inferred (orange) and target (black) waveforms (left), EGF (middle) and STF (right) for toy models designed with full waveforms for a M 3.37 event that occurred in 2017 near Borrego Springs, CA.



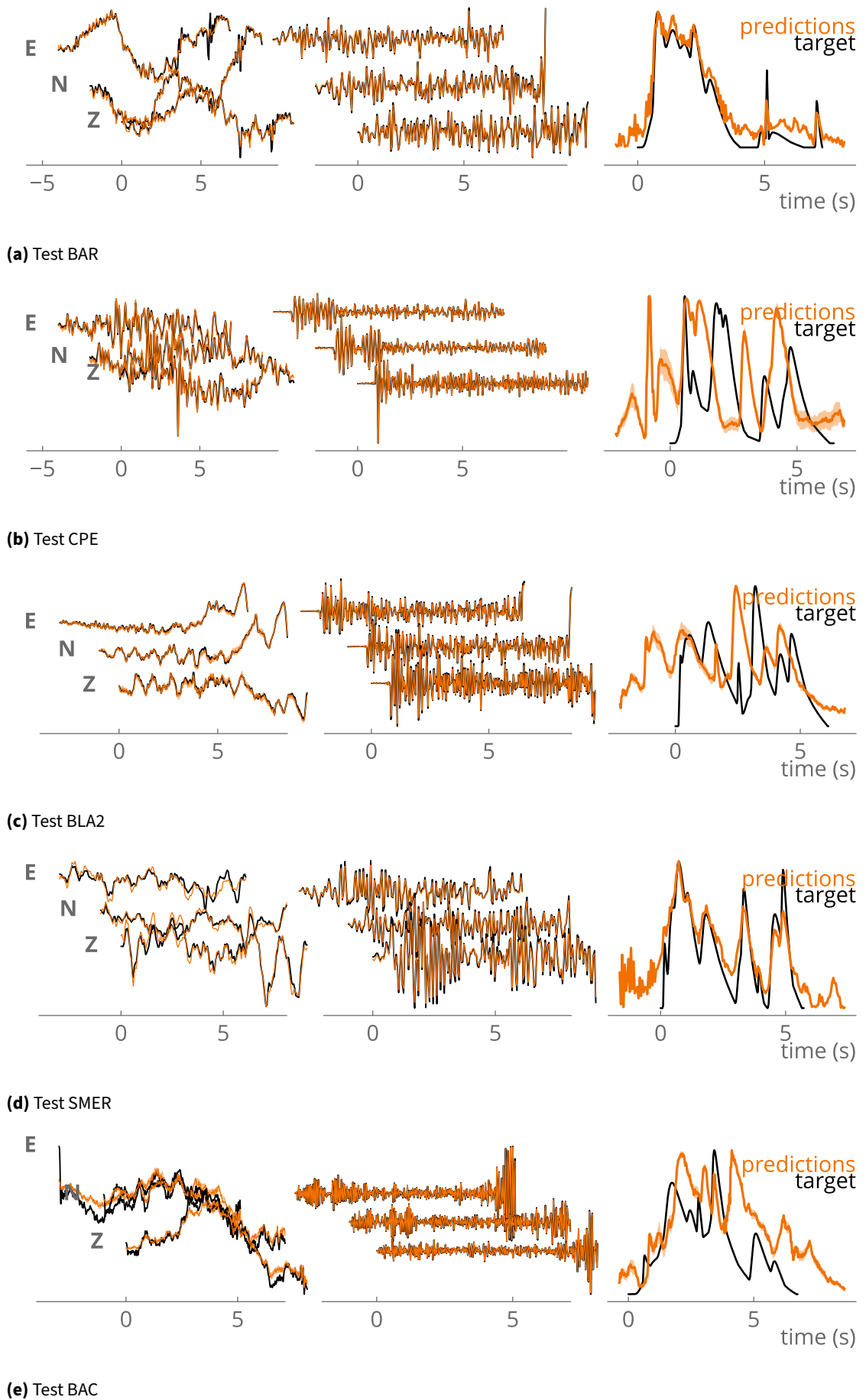


**Figure S19** Inferred (orange) and target (black) waveforms (left), EGF (middle) and STF (right) for toy models shown in Figure 2, designed with P arrivals for a M 3.37 event that occurred in 2017 near Borrego Springs, CA.

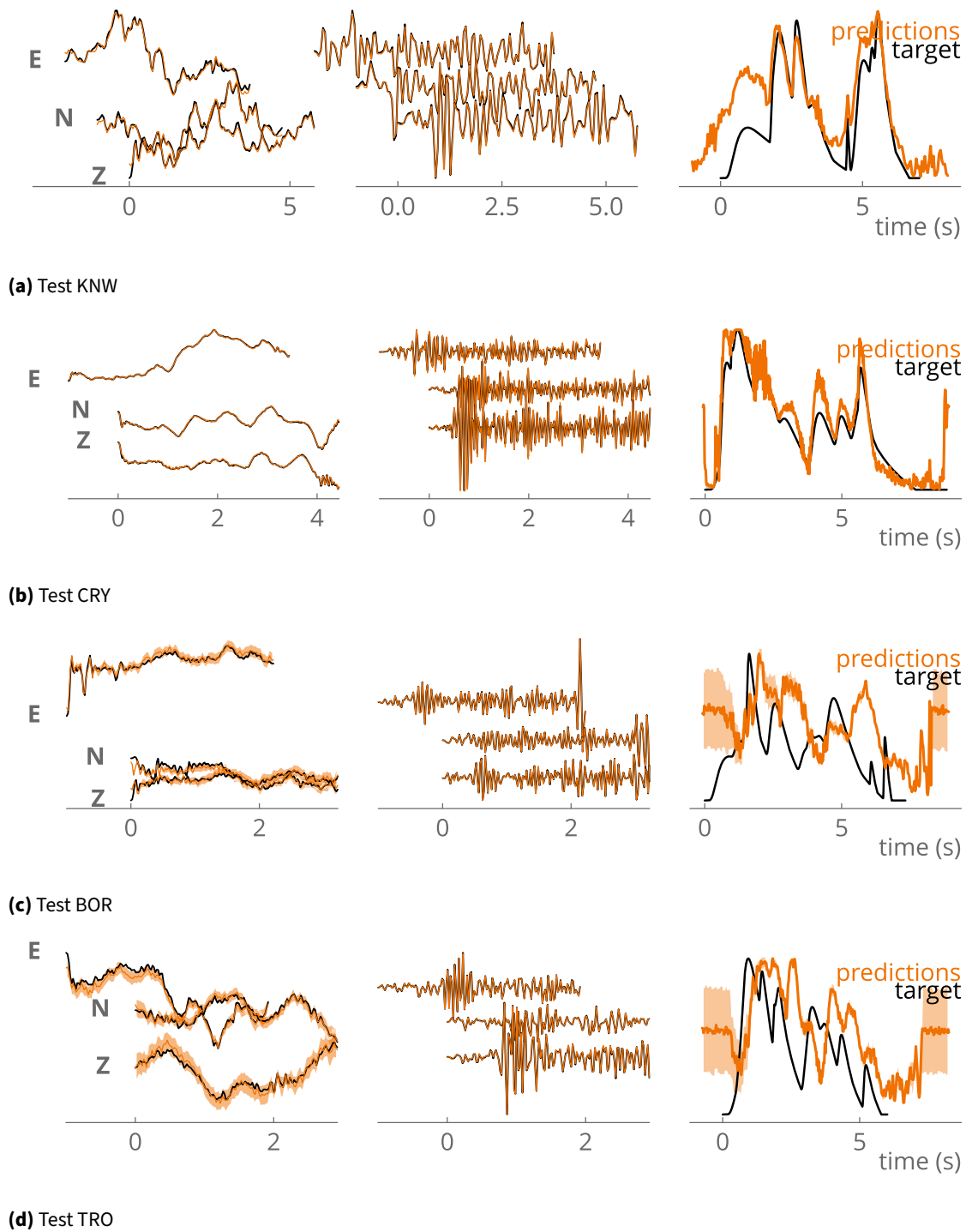


**Figure S20** Inferred (orange) and target (black) waveforms (left), EGF (middle) and STF (right) for toy models shown in Figure 2, designed with P arrivals for a M 3.37 event that occurred in 2017 near Borrego Springs, CA.

## S4 Case study: the 2019 Cahuilla swarm, CA

### S4.1 Data

We use broadband seismic data recorded by the regional network (CI), plate boundary observatory (PB), ANZA network (AZ) and UCSB (SB) networks in Southern California for the 2018 Mw 4.41 mainshock (SCSN-ID:38245496; August 15, 2018, 01:24:26) and several  $M \sim 2$ -2.5 events that occurred during the Cahuilla swarm (Ross et al., 2020). We use stations located within 100 km of the mainshock. Stations locations are shown in Figs 2 and 4 of the main text. We either use the full waveforms (both P and S arrivals), the P arrivals only, or the S arrivals. For the later cases, we trim the waveforms to just before the S waves arrivals. We use Phasenet (Zhu and Beroza, 2019) to determine phase arrivals. To decrease computation time, we decimate the waveforms to 20 Hz.

The selection of prior EGFs is described separately for the toy models and results.

**Table S9** Four potential EGFs selected for the Cahuilla case study.

event ID	date	Mw	Relocated distance to mainshock (km)
38050943	2018-09-07	2.44	0.306
38242792	2018-08-11	2.33	0.307
38245688	2018-08-15	2.11	0.347
38038871	2018-08-29	2.05	0.354

### S4.2 Toy models with recorded waveforms

#### Description of the forward model

We select prior EGFs, with a  $2 < Mw < 2.5$ , from their distance to the mainshock (Table S9), based on the relocated catalog from Ross et al. (2020). We only use stations which recorded the 4 (or 3) selected EGFs.

Target EGFs are calculated as a weighted sum of the normalized waveforms recorded for three or four of  $M \sim 2$  events, to which we add white noise with a PSNR of 3%. To obtain the target waveforms of the main toy model event, we convolve the target EGFs with a randomly calculated STF. The STF is a stack of  $N_{STF}$  (3 or 10) Gaussian STFs, each of the Gaussian STFs being characterized by a random risetime, a random amplitude, and a random padding, while the total duration  $D_{STF}$  ranges from 5 to 7 s. We add again white noise with a PSNR of 3% to each of the components of the waveforms for the main toy model event.

We design two series of tests. In the first one (Table S10), the target EGF consists in a sum of three  $M \sim 2$  events (event ID:37195604 discarded), while the STF has  $N_{STF} = 3$  and  $D_{STF} = 5$ s. The full waveforms are used. We also compute frequency-domain deconvolution for each prior EGF. Results are compiled in Fig. S21 and plotted below for each test.

In the second serie of tests (Table S11), whose results are displayed in the main text in Fig. 3, the target EGF consists of a sum of the four  $M \sim 2$  events, and the STF has  $N_{STF} = 10$  and  $D_{STF} = 7$ s. We only use the P-wave arrivals. Results are plotted below for each test. Additionally, we also perform two tests with 8 EGFs for station TOR. In one case, the additional four waveforms are weighted sums of the initial four prior EGFs (Figs. S38 and S40), and in another the additional four waveforms are the target ones with 10% of random weighted sum (Fig. S39).

#### Prior assumptions for DeepGEM

In this case, we use multiple prior EGFs. The prior EGFs are the ones used for calculation of the synthetic Green's functions. The waveforms are normalized and we only solve for the shape of the STF, not its amplitude.

We used the following non-default parameters for DeepGEM:

```
num_epochs = 150
EMFull = False
stf_dur = 9
Elr = 1e-3
Mlr = 1e-4
stf_init_weight = 1e0
data_sigma = 5e-6
```

**Table S10** Weights ( $\alpha$ ) used for toy models using a weighted sum of 3 EGFs. For those, the STF is characterized by  $N_{STF} = 3$  and  $D_{STF} = 5s$ .

name	station	$\alpha_1$ , ID:38194264	$\alpha_2$ , ID:37949151	$\alpha_3$ , ID:Z38242792
CSH	CSH	0.1	0.3	0.6
DGR	DGR	0.8	0.1	0.1
PALA	PALA	0.3	0.3	0.4
PLM	PLM	0.6	0.3	0.1
POB2	POB2	0.5	0.4	0.1
CSH_2_2	CSH	0.8	0.1	0.1
DGR_2_2	DGR	0.3	0.3	0.4
PALA_2	PALA	0.6	0.3	0.1
PLM_2	PLM	0.5	0.4	0.1
POB2_2_2	POB2	0.1	0.3	0.6
CSH_3	CSH	0.4	0.35	0.25
PLM_3	PLM	0.35	0.4	0.25

**Table S11** Weights ( $\alpha$ ) used for toy models using a weighted sum of 4 EGFs, shown in Fig. 3. For those, the STF is characterized by  $N_{STF} = 10$  and  $D_{STF} = 7s$ . We only use the P-wave arrivals.

name	station	$\alpha_0$ , ID:37195604	$\alpha_1$ , ID:38194264	$\alpha_2$ , ID:37949151	$\alpha_3$ , ID:38242792
CTW	CTW	0.37335196	0.33257028	0.1458018	0.14827596
TOR	TOR	0.77052845	0.05954214	0.08736548	0.08256393
PSD	PSD	0.50688547	0.05116649	0.29047711	0.15147093
LMH	LMH	0.45428515	0.26398319	0.04305582	0.23867585

## Results

### List of figures:

First set of tests (Table S10), STF with  $N_{STF} = 3$ :

- Fig. S22
- Fig. S23
- Fig. S24
- Fig. S25
- Fig. S26
- Fig. S27
- Fig. S28
- Fig. S29
- Fig. S30
- Fig. S31
- Fig. S32
- Fig. S33

Second set of tests (Table S11), STF with  $N_{STF} = 10$ :

- Fig. S34
- Fig. S35
- Fig. S36
- Fig. S37
- Fig. S38 station TOR, test A with 4 EGFs (to compare with tests B and C at same station)
- Fig. S40 station TOR, test B with 8 EGFs, 4 additional EGFs are random
- Fig. S39 station TOR, test C with 8 EGFs, 4 additional EGFs are close to target

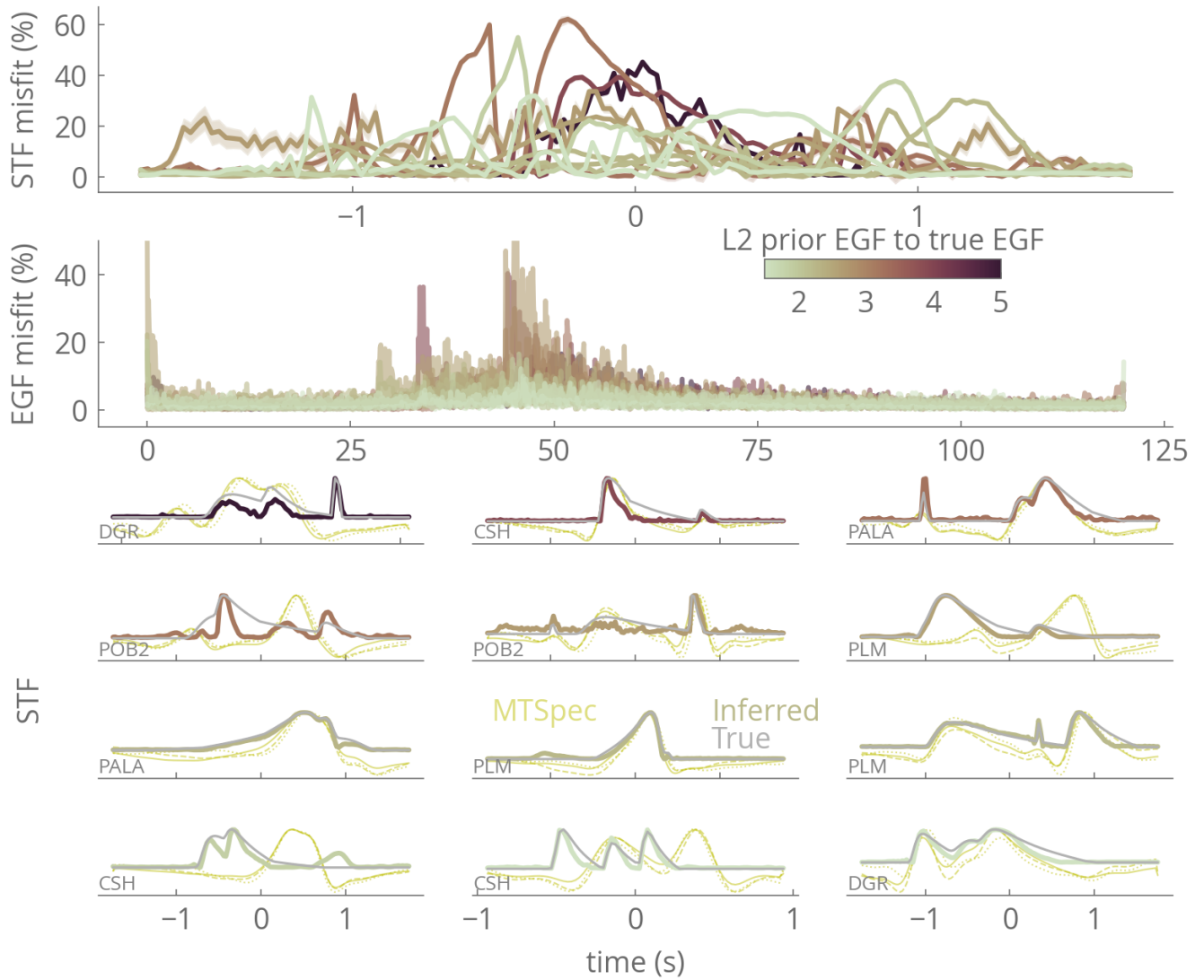


**Figure S21** Goodness of fit for the STFs and EGFs for synthetic tests designed for the Cahuilla case study. (first row) Misfit (in % of amplitude) against time (s) between the inferred STF and the true STF used for calculation of the waveforms of reference. The misfit is color-coded from the average distance between the prior EGF and the true Green's function used for calculation of the waveforms of reference. (second row) Misfit (in % of amplitude) against time (s) between the best inferred EGF and the true GF used for calculation of the waveforms of reference. (bottom) True (gray), inferred STF (color), and STFs inferred with MTSpec (green). The name of the station is shown in gray.

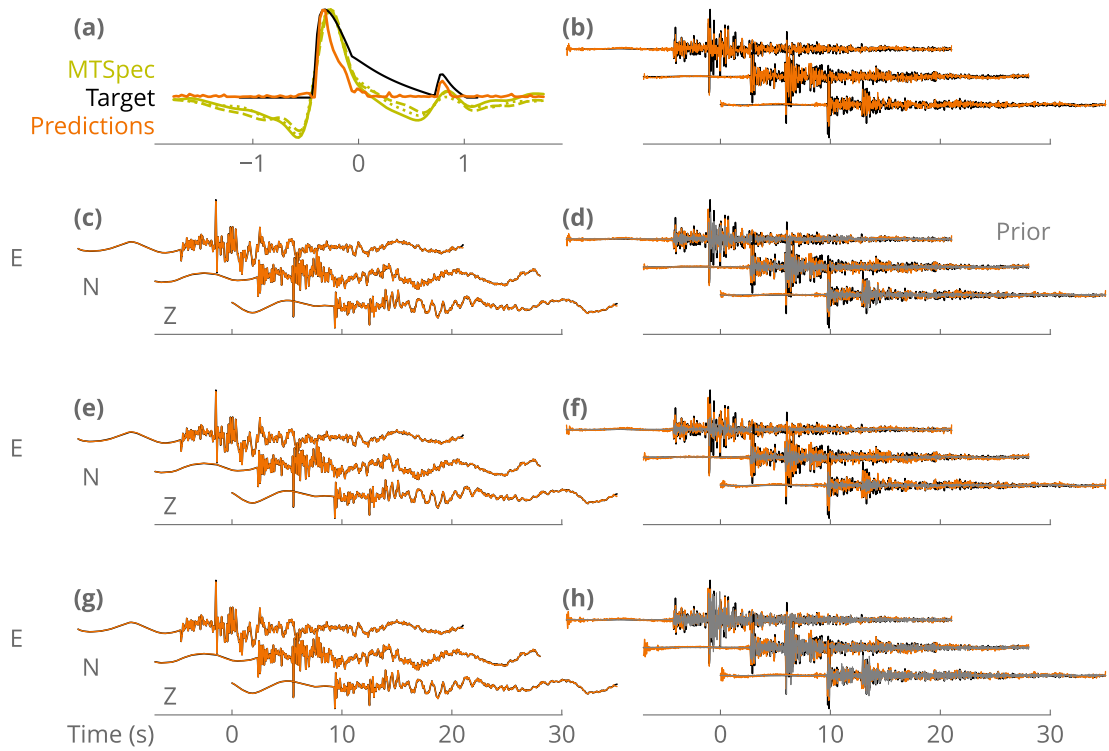


**Figure S22** Inferred (orange) and target (black) STFs (a) and best inferred EGF (b) for toy model **CSH** whose characteristics are summarized in Table S10. In (d,f,h) and (c,e,g) are shown the prior (gray), inferred and target EGFs and waveforms for the main toy model event. In (a) the STF estimated in the frequency-domain is shown in green.

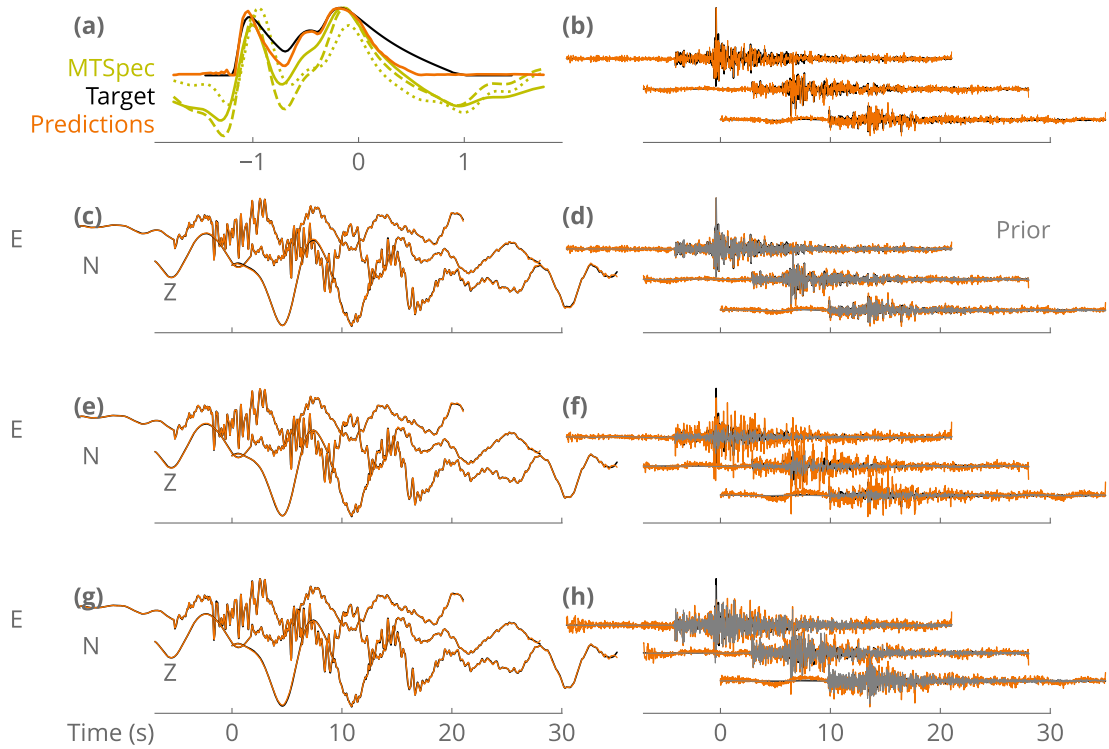


**Figure S23** Inferred (orange) and target (black) STFs (a) and best inferred EGF (b) for toy model **DGR** whose characteristics are summarized in Table S10. In (d,f,h) and (c,e,g) are shown the prior (gray), inferred and target EGFs and waveforms for the main toy model event. In (a) the STF estimated in the frequency-domain is shown in green.

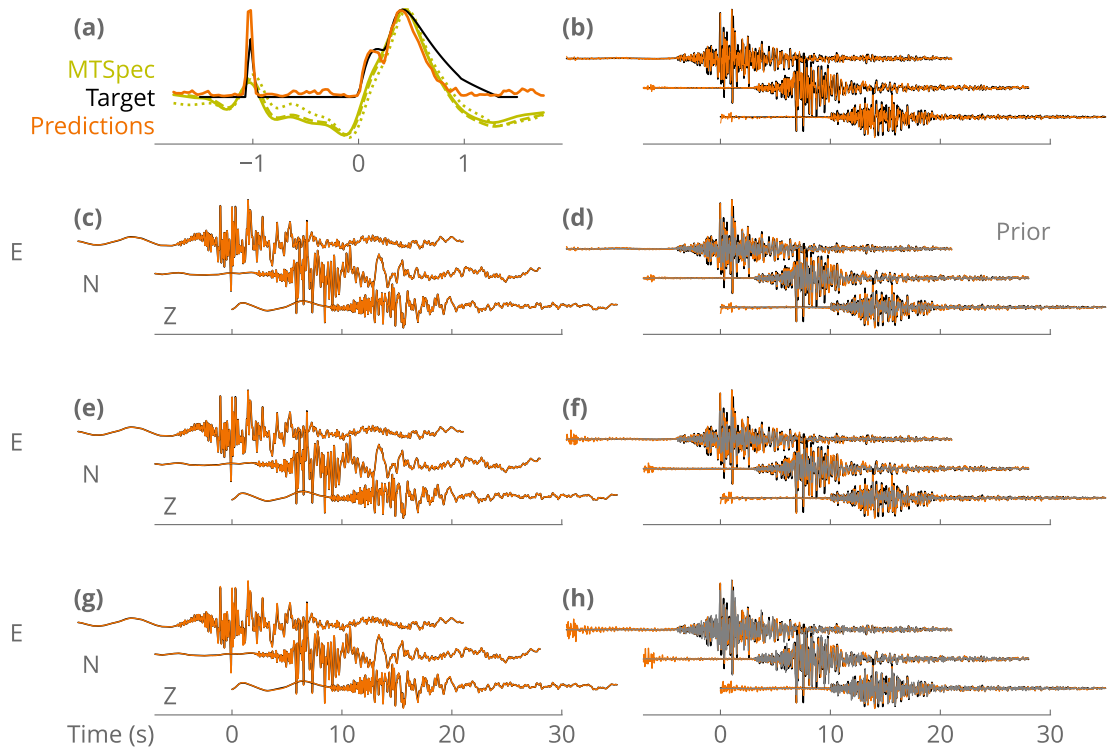


**Figure S24** Inferred (orange) and target (black) STFs (a) and best inferred EGF (b) for toy model **PALA** whose characteristics are summarized in Table S10. In (d,f,h) and (c,e,g) are shown the prior (gray), inferred and target EGFs and waveforms for the main toy model event. In (a) the STF estimated in the frequency-domain is shown in green.

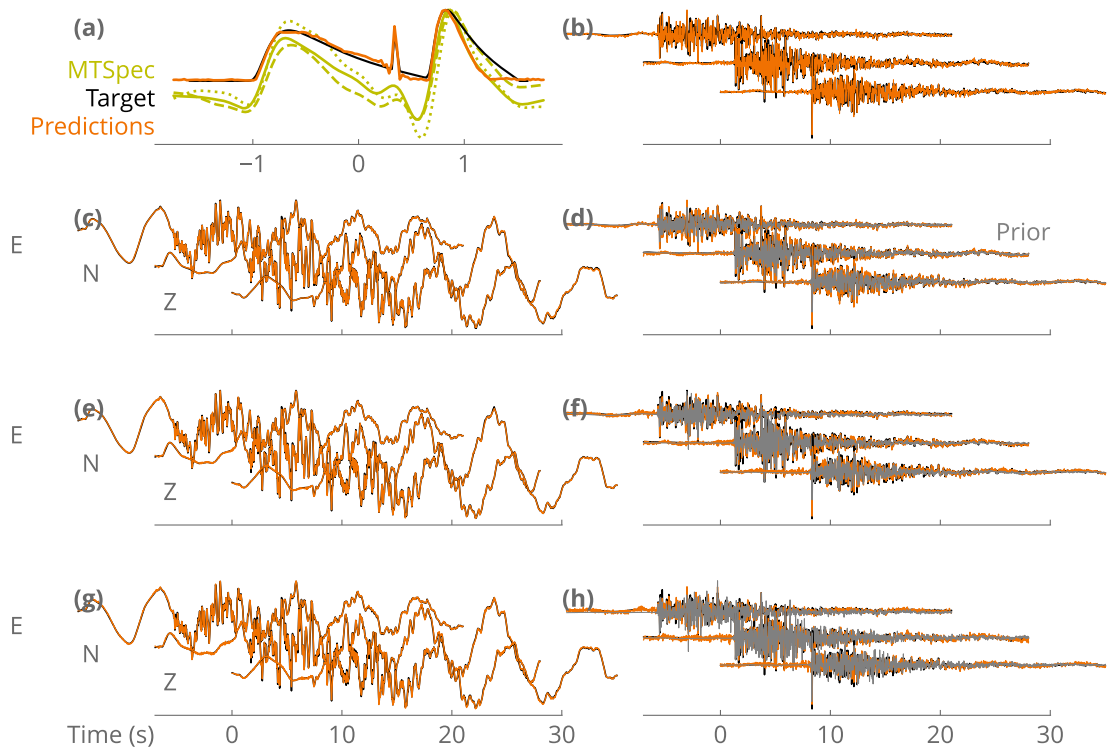


**Figure S25** Inferred (orange) and target (black) STFs (a) and best inferred EGF (b) for toy model **PLM** whose characteristics are summarized in Table S10. In (d,f,h) and (c,e,g) are shown the prior (gray), inferred and target EGFs and waveforms for the main toy model event. In (a) the STF estimated in the frequency-domain is shown in green.



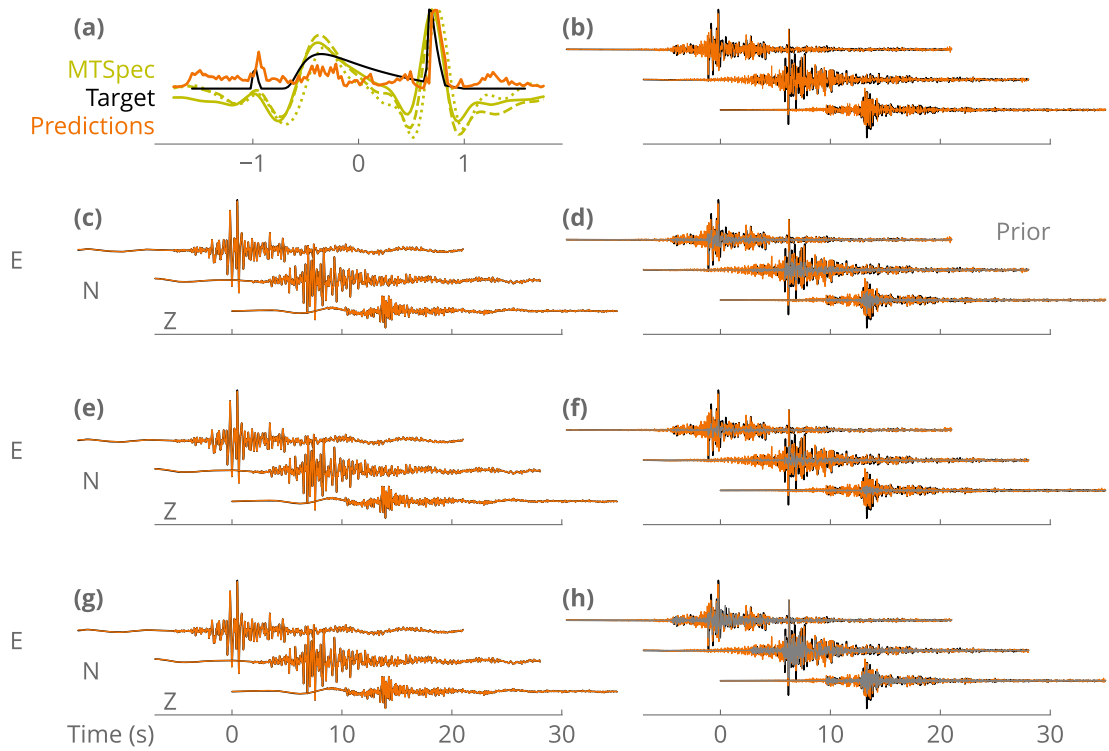


**Figure S26** Inferred (orange) and target (black) STFs (a) and best inferred EGF (b) for toy model **POB2** whose characteristics are summarized in Table S10. In (d,f,h) and (c,e,g) are shown the prior (gray), inferred and target EGFs and waveforms for the main toy model event. In (a) the STF estimated in the frequency-domain is shown in green.

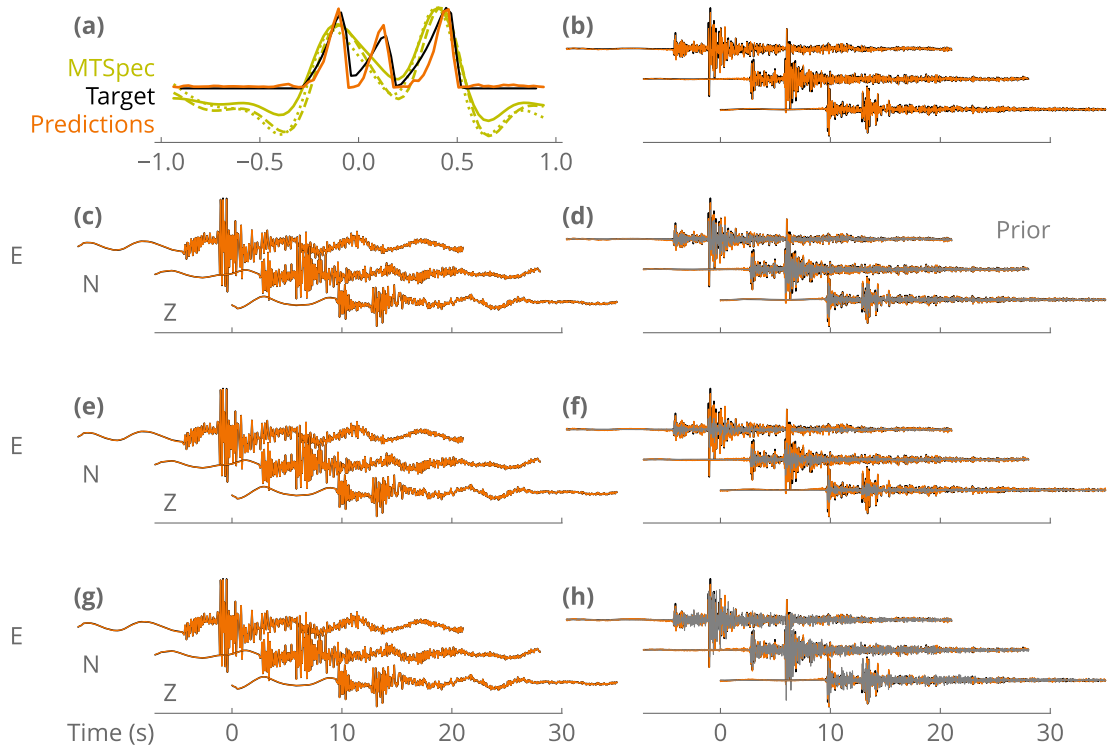


**Figure S27** Inferred (orange) and target (black) STFs (a) and best inferred EGF (b) for toy model **CSH\_2\_2** whose characteristics are summarized in Table S10. In (d,f,h) and (c,e,g) are shown the prior (gray), inferred and target EGFs and waveforms for the main toy model event. In (a) the STF estimated in the frequency-domain is shown in green.

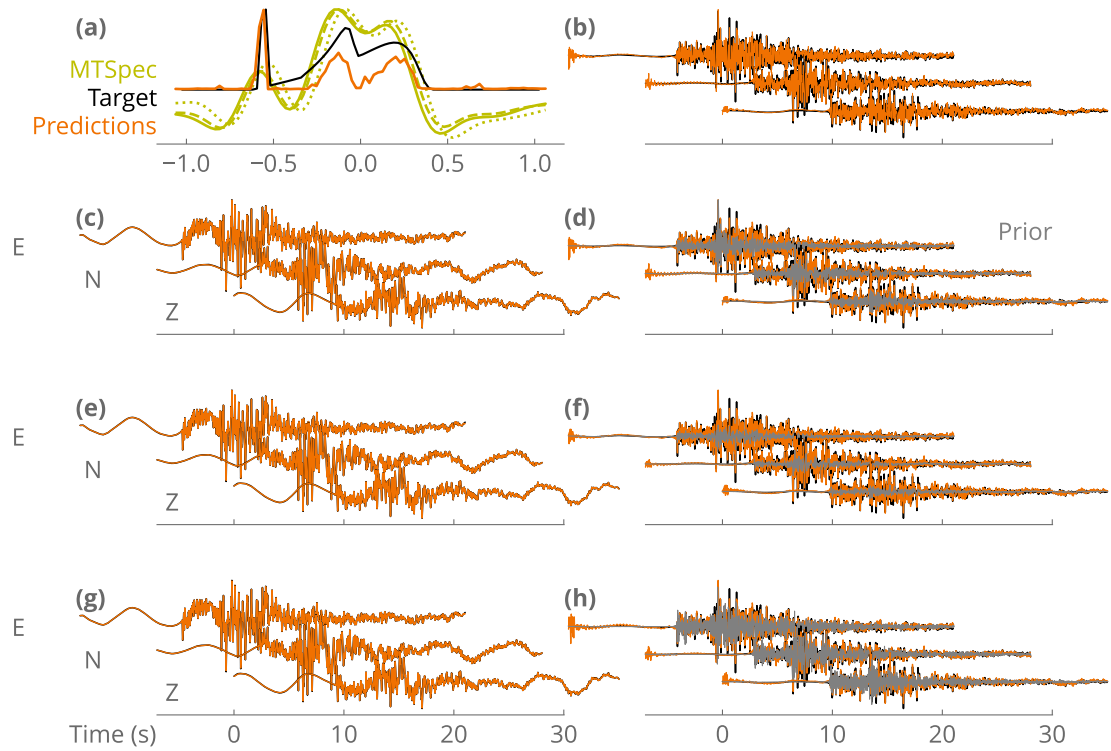


**Figure S28** Inferred (orange) and target (black) STFs (a) and best inferred EGF (b) for toy model **DGR\_2\_2** whose characteristics are summarized in Table S10. In (d,f,h) and (c,e,g) are shown the prior (gray), inferred and target EGFs and waveforms for the main toy model event. In (a) the STF estimated in the frequency-domain is shown in green.

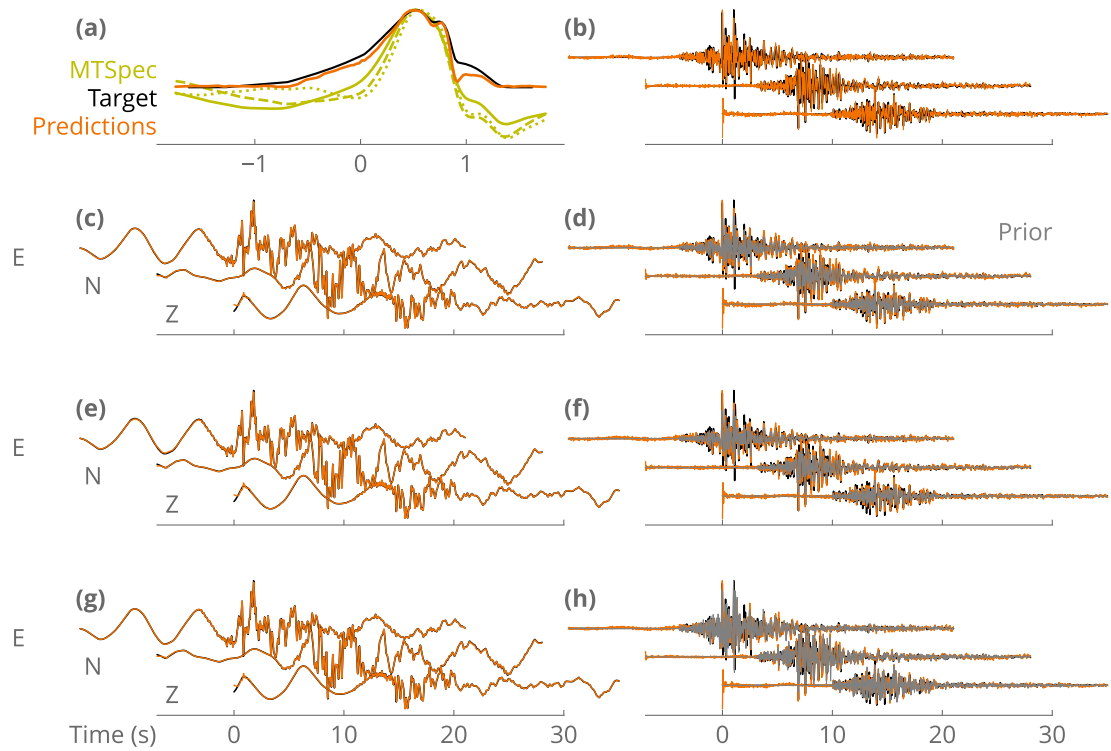


**Figure S29** Inferred (orange) and target (black) STFs (a) and best inferred EGF (b) for toy model **PALA\_2** whose characteristics are summarized in Table S10. In (d,f,h) and (c,e,g) are shown the prior (gray), inferred and target EGFs and waveforms for the main toy model event. In (a) the STF estimated in the frequency-domain is shown in green.

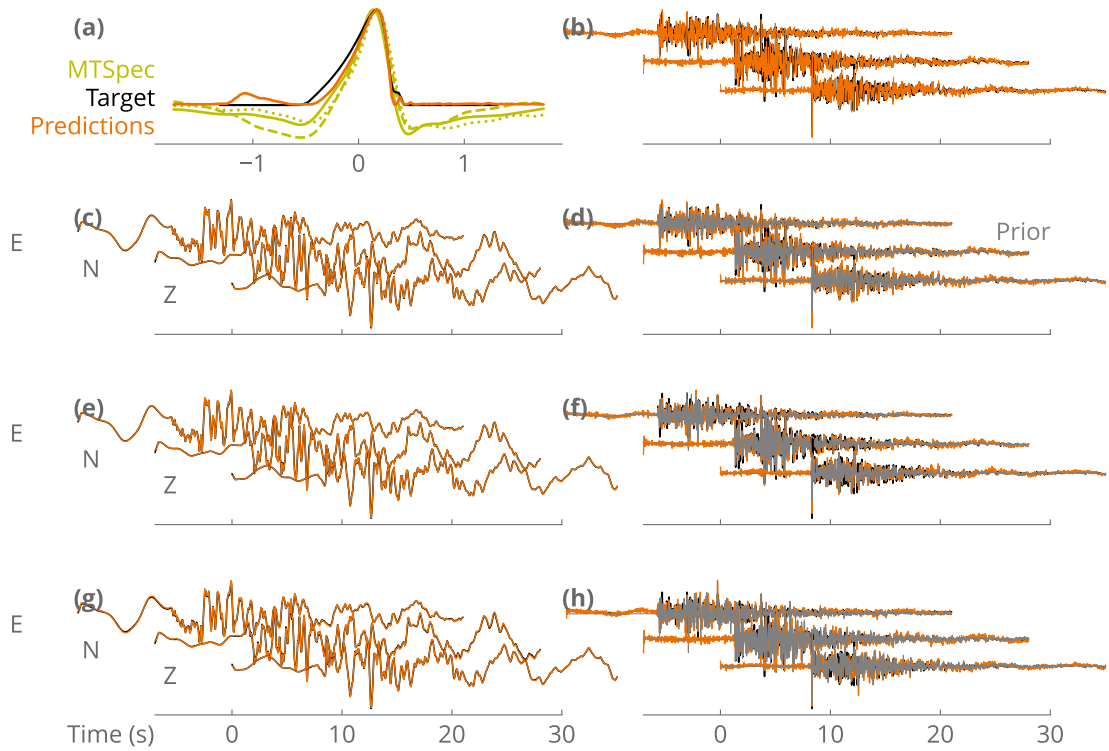


**Figure S30** Inferred (orange) and target (black) STFs (a) and best inferred EGF (b) for toy model **PLM\_2** whose characteristics are summarized in Table S10. In (d,f,h) and (c,e,g) are shown the prior (gray), inferred and target EGFs and waveforms for the main toy model event. In (a) the STF estimated in the frequency-domain is shown in green.

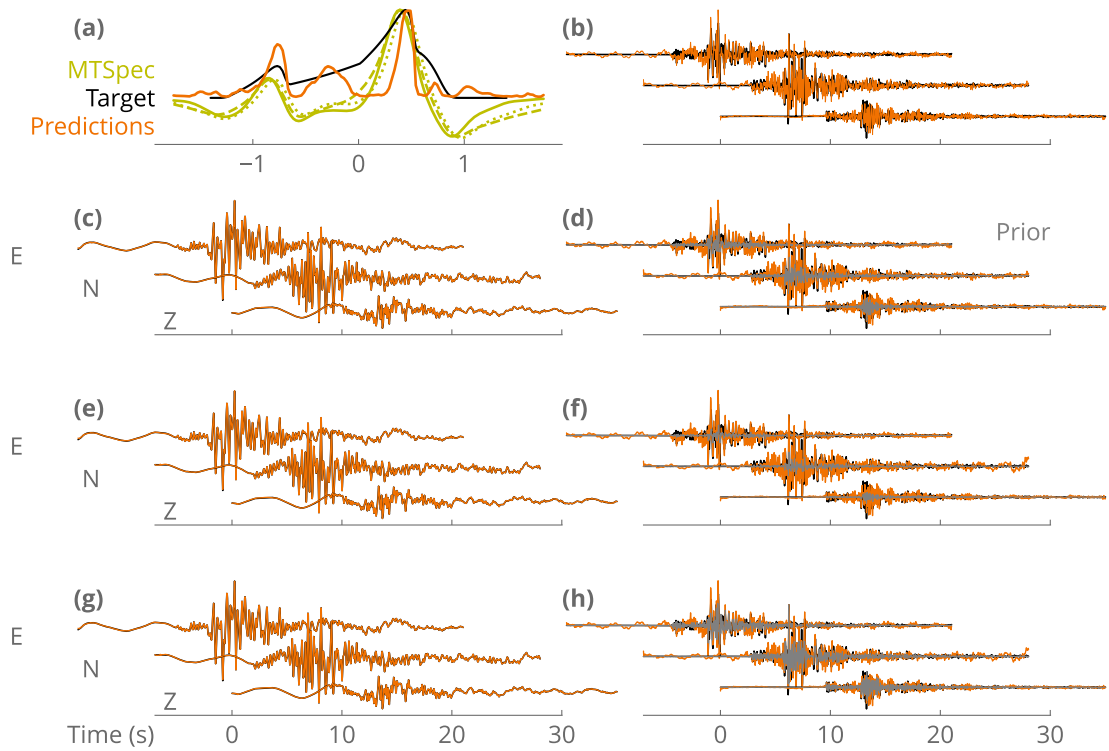


**Figure S31** Inferred (orange) and target (black) STFs (a) and best inferred EGF (b) for toy model **POB2\_2\_2** whose characteristics are summarized in Table S10. In (d,f,h) and (c,e,g) are shown the prior (gray), inferred and target EGFs and waveforms for the main toy model event. In (a) the STF estimated in the frequency-domain is shown in green.

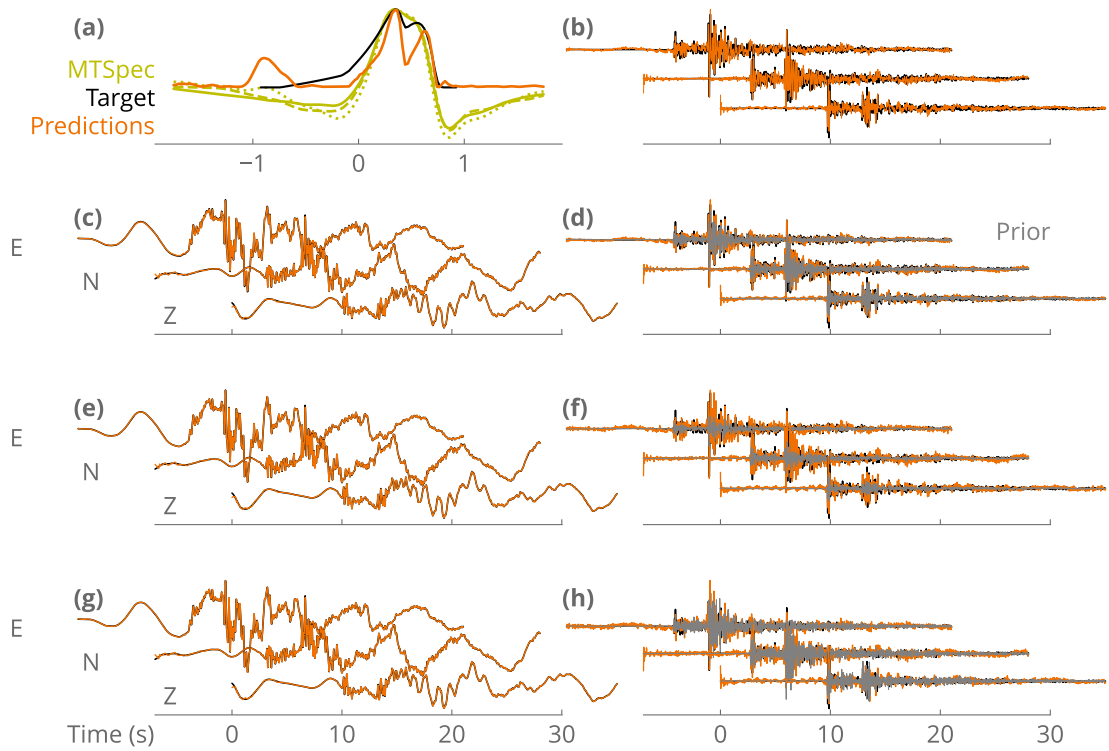


**Figure S32** Inferred (orange) and target (black) STFs (a) and best inferred EGF (b) for toy model **CSH\_3** whose characteristics are summarized in Table S10. In (d,f,h) and (c,e,g) are shown the prior (gray), inferred and target EGFs and waveforms for the main toy model event. In (a) the STF estimated in the frequency-domain is shown in green.

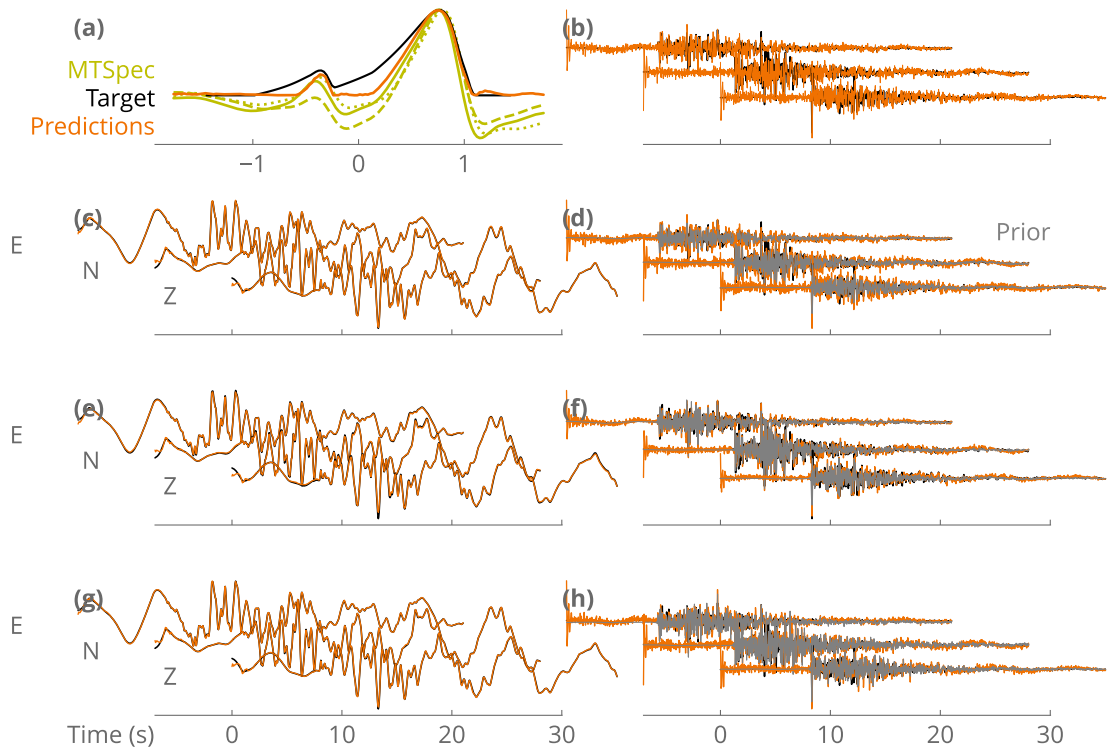


**Figure S33** Inferred (orange) and target (black) STFs (a) and best inferred EGF (b) for toy model **PLM\_3** whose characteristics are summarized in Table S10. In (d,f,h) and (c,e,g) are shown the prior (gray), inferred and target EGFs and waveforms for the main toy model event. In (a) the STF estimated in the frequency-domain is shown in green.

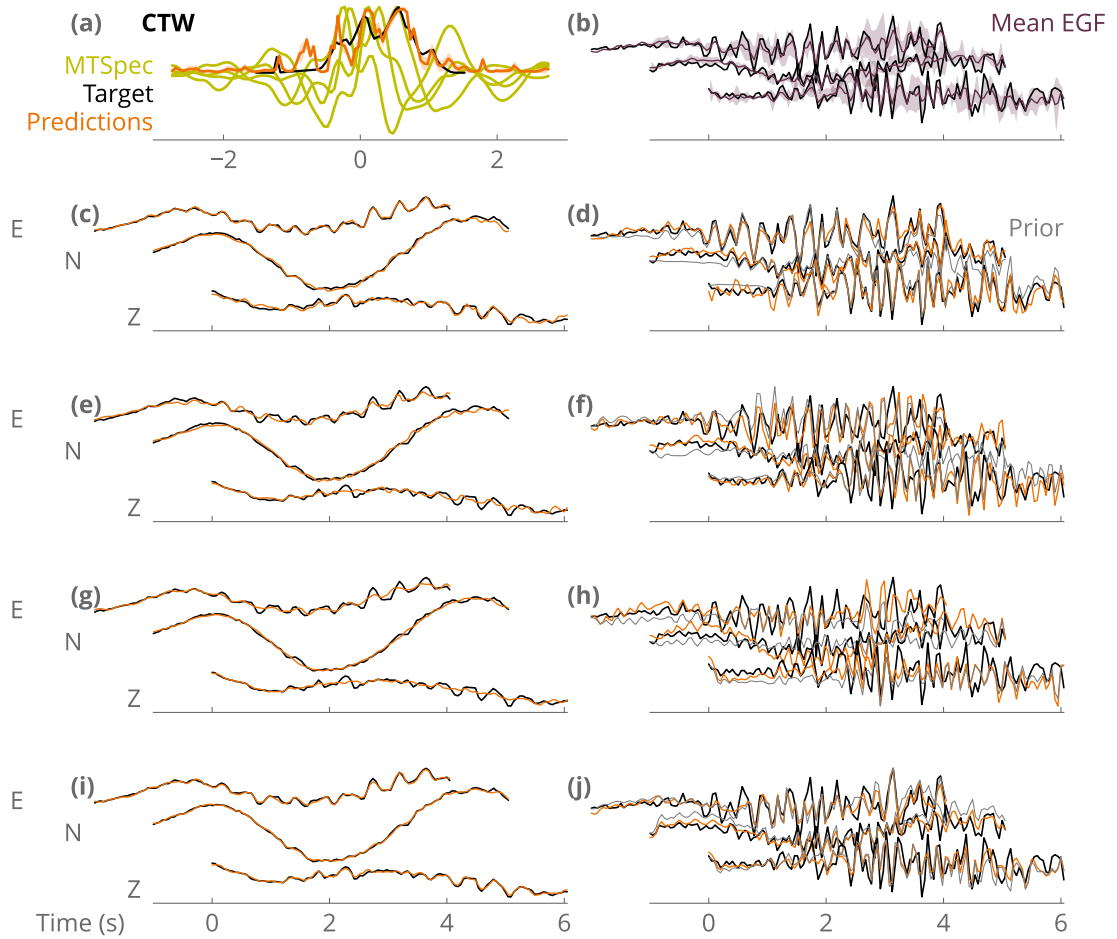


**Figure S34** Inferred (orange) and target (black) STFs (a), EGFs (b,d,f,h,j) and waveforms of the main event (c,e,g,i) for toy model **CTW** whose characteristics are summarized in Table S11. In (a) the STFs estimated in the frequency-domain, assuming each EGF separately, are shown in green. In (b) the mean EGF and its standard deviation are in purple. In (d,f,h,j) the prior EGF is in gray.

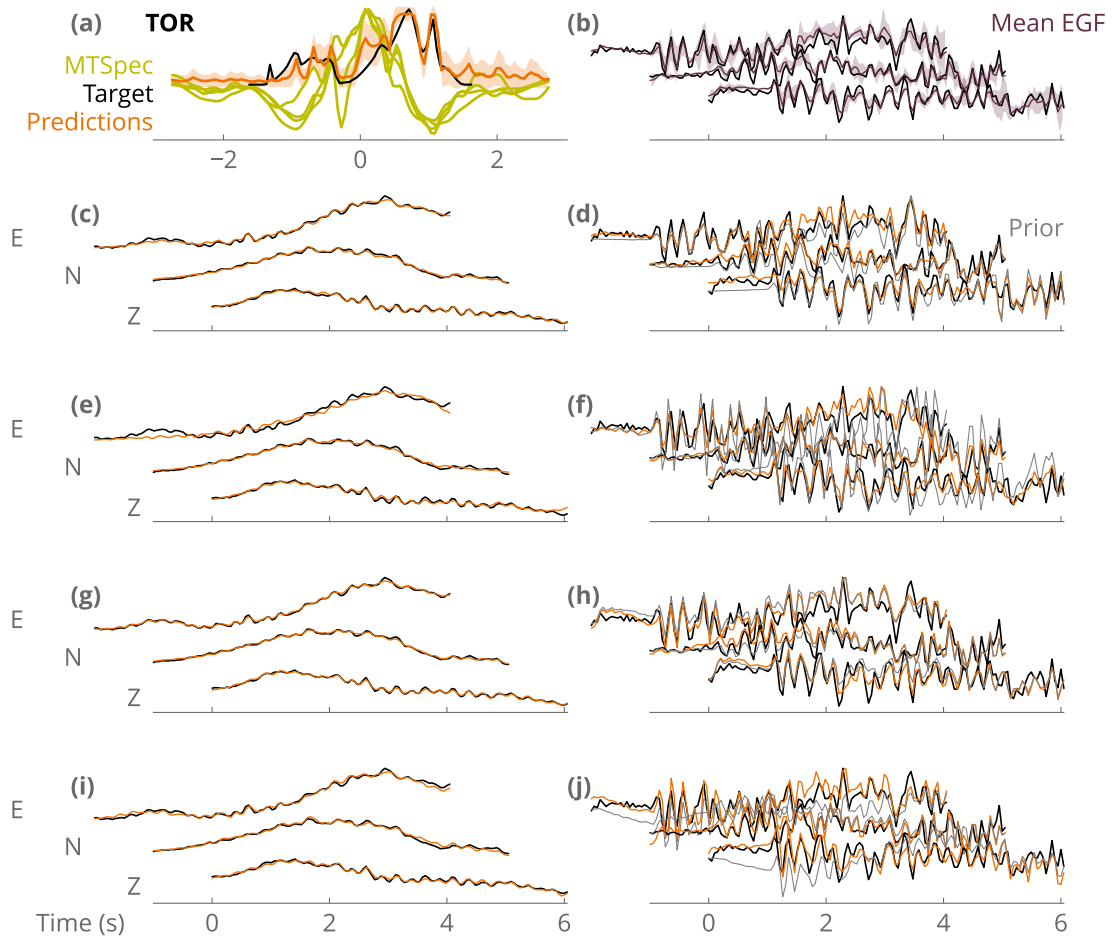


**Figure S35** Inferred (orange) and target (black) STFs (a), EGFs (b,d,f,h,j) and waveforms of the main event (c,e,g,i) for toy model **TOR** whose characteristics are summarized in Table S11. In (a) the STFs estimated in the frequency-domain, assuming each EGF separately, are shown in green. In (b) the mean EGF and its standard deviation are in purple. In (d,f,h,j) the prior EGF is in gray.

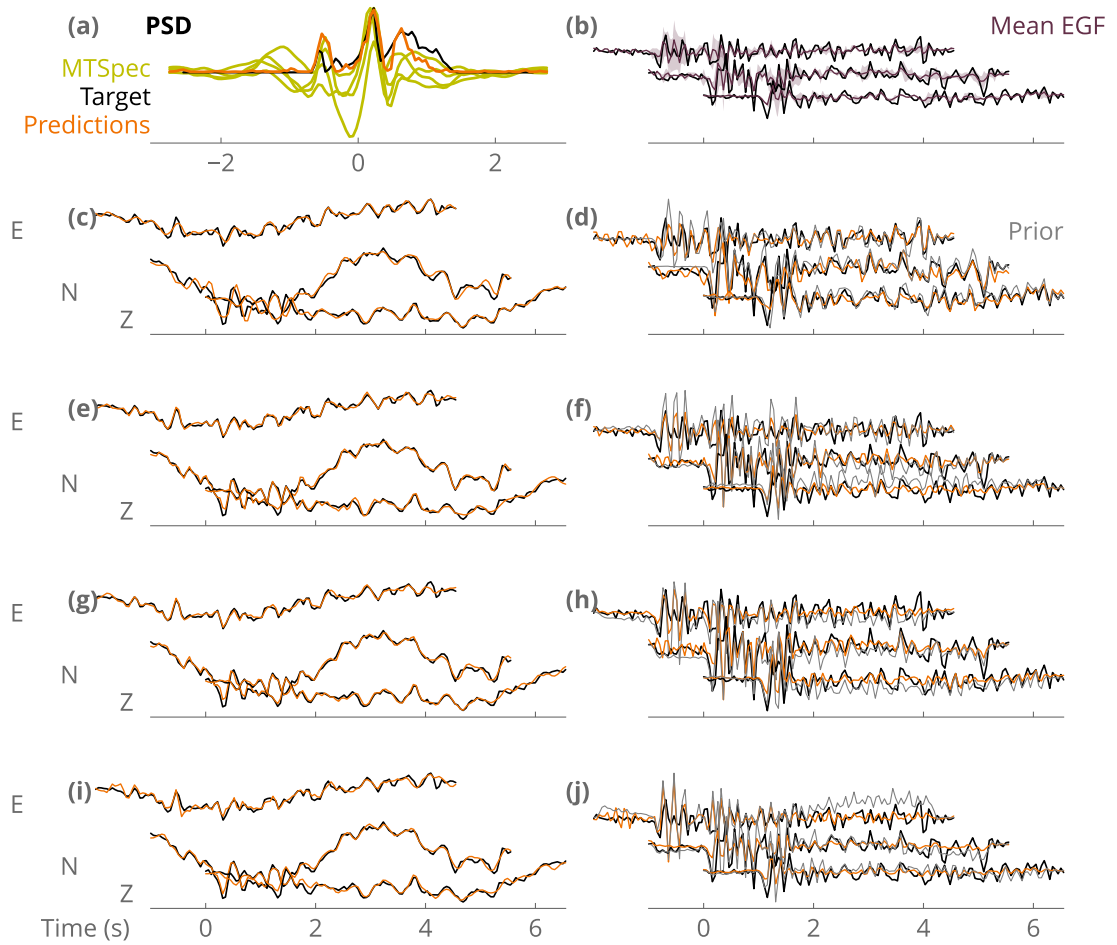


**Figure S36** Inferred (orange) and target (black) STFs (a), EGFs (b,d,f,h,j) and waveforms of the main event (c,e,g,i) for toy model **PSD** whose characteristics are summarized in Table S11. In (a) the STFs estimated in the frequency-domain, assuming each EGF separately, are shown in green. In (b) the mean EGF and its standard deviation are in purple. In (d,f,h,j) the prior EGF is in gray.



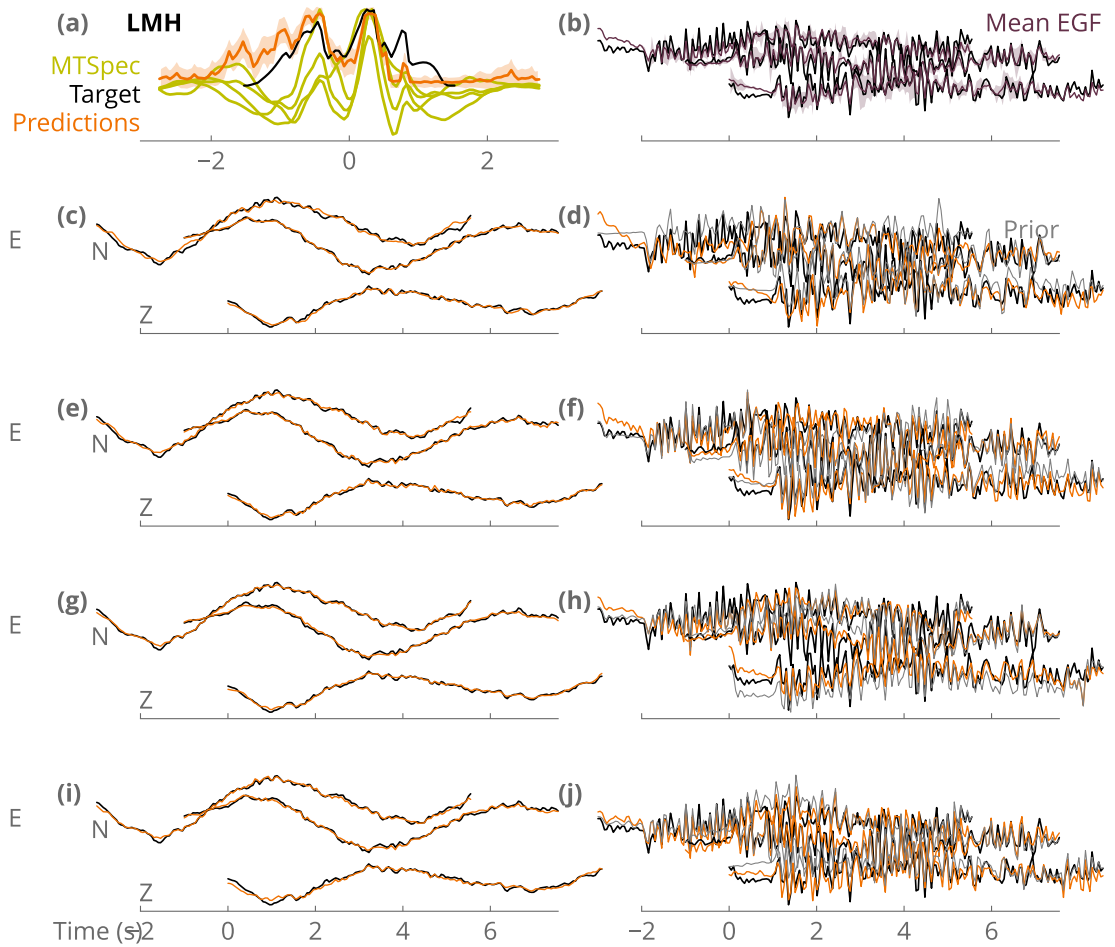


**Figure S37** Inferred (orange) and target (black) STFs (a), EGFs (b,d,f,h,j) and waveforms of the main event (c,e,g,i) for toy model **LMH** whose characteristics are summarized in Table S11. In (a) the STFs estimated in the frequency-domain, assuming each EGF separately, are shown in green. In (b) the mean EGF and its standard deviation are in purple. In (d,f,h,j) the prior EGF is in gray.



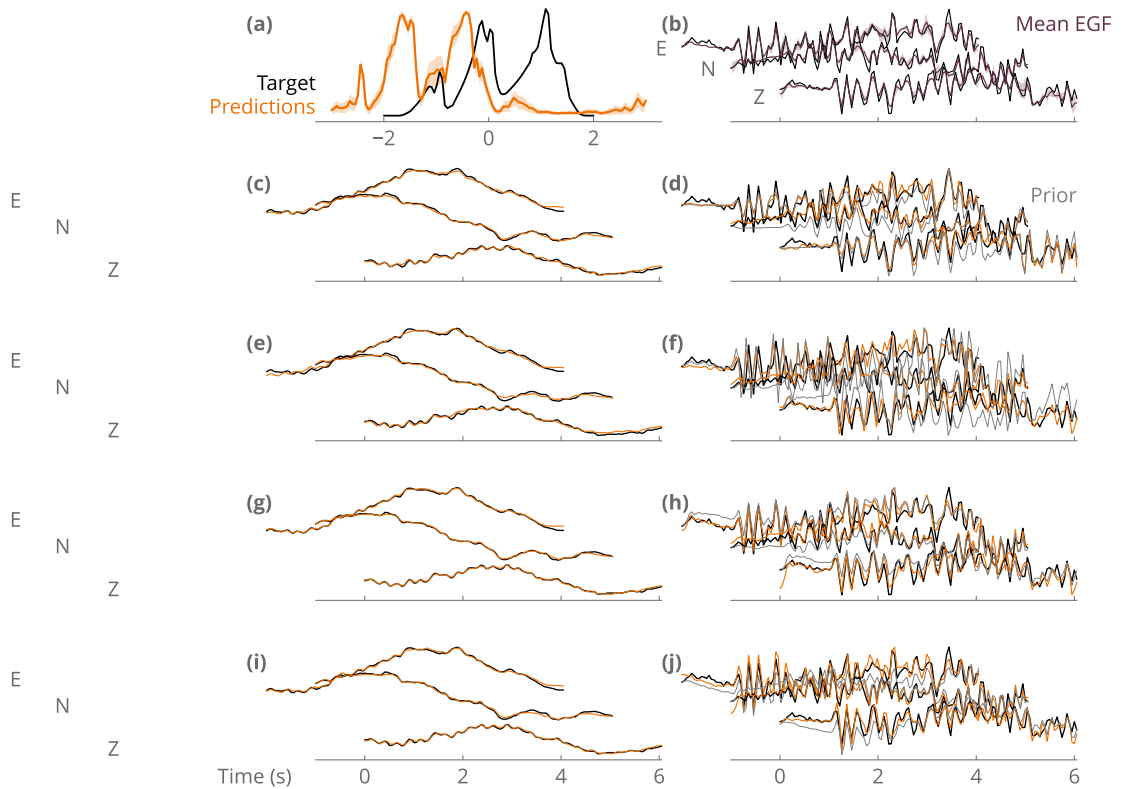


**Figure S38** Inferred (orange) and target (black) STFs (a), EGFs (right) and waveforms of the main event (left) for station TOR, test **A with 4 EGFs**. In (a) the STFs estimated in the frequency-domain, assuming each EGF separately, are shown in green. In (b) the mean EGF and its standard deviation are in purple. The prior EGF is in gray.

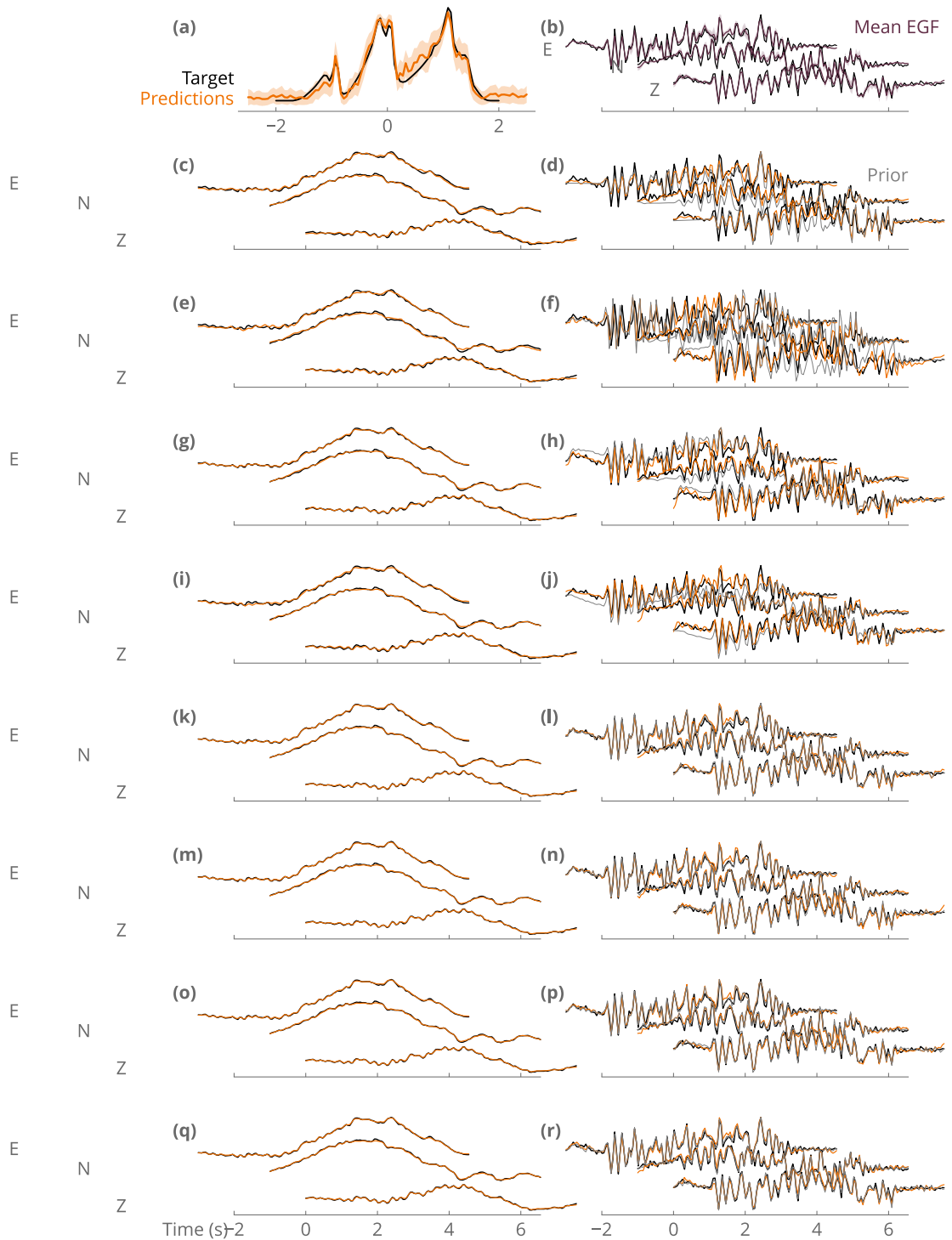


**Figure S39** Inferred (orange) and target (black) STFs (a), EGFs (right) and waveforms of the main event (left) for station TOR, test **B with 8 EGFs**. In (a) the STFs estimated in the frequency-domain, assuming each EGF separately, are shown in green. In (b) the mean EGF and its standard deviation are in purple. The prior EGF is in gray.

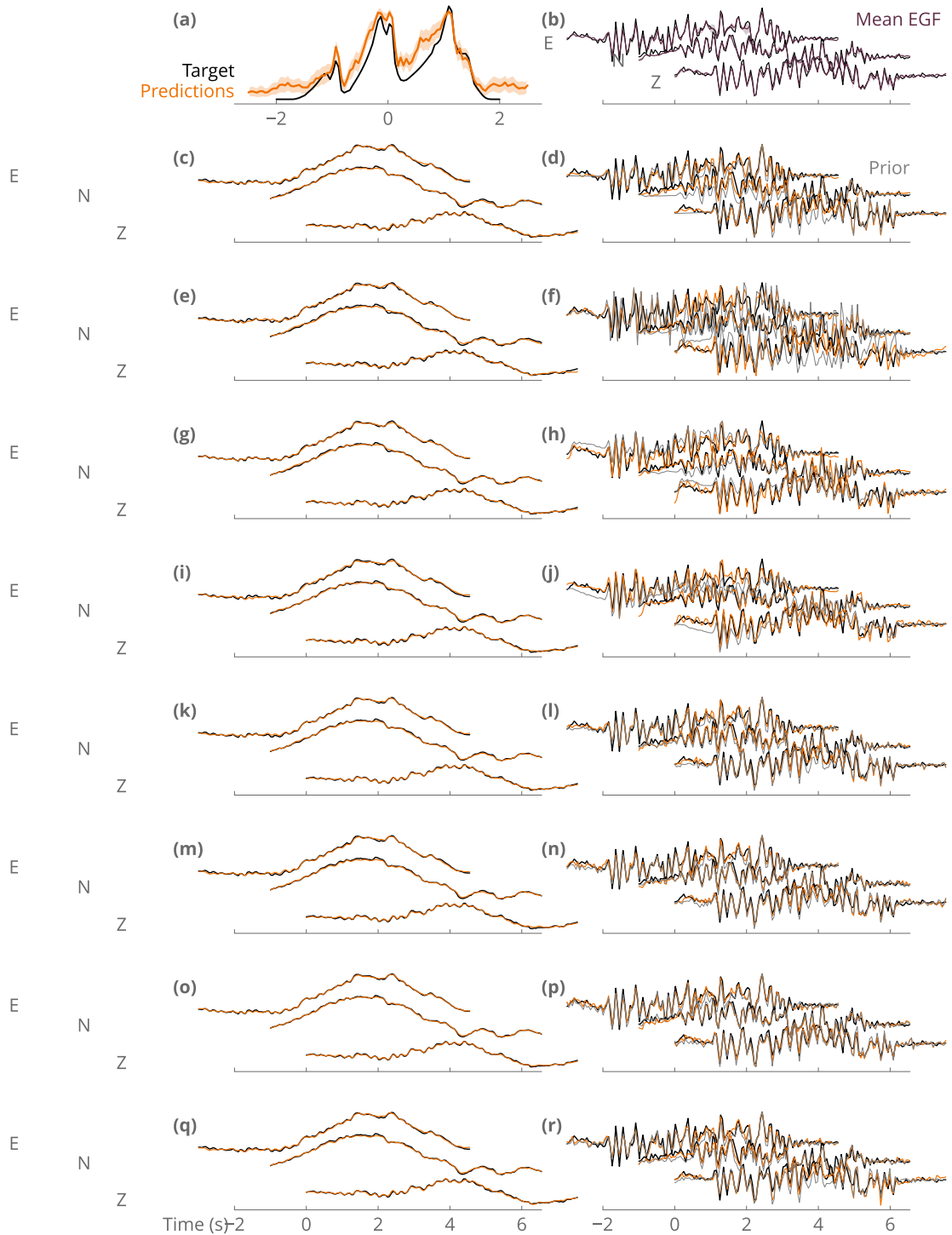


**Figure S40** Inferred (orange) and target (black) STFs (a), EGFs (right) and waveforms of the main event (left) for station TOR, test **C with 8 EGFs**. In (a) the STFs estimated in the frequency-domain, assuming each EGF separately, are shown in green. In (b) the mean EGF and its standard deviation are in purple. The prior EGF is in gray.

**Table S12** Four potential EGFs for the Cahuilla case study, selected based on their cross-correlation with the mainshock waveforms at station PLM.

event ID	date	Mw	Relocated distance to mainshock (km)	Cross-correlation
38049295	2018-09-06	2.35	0.909	0.563
38243232	2018-08-12	2.29	0.928	0.612
38245472	2018-08-15	2.03	0.924	0.641
37195604	2018-09-07	2.16	0.918	0.686

### S4.3 Description of the forward model

We assume three different sets of prior EGFs, with P arrivals only (3 sec.) or S arrivals only (13 sec.):

- **set A, P waves:** 4 EGFs, distance-based, similar to toy models, EGFs listed in Table S9.
- **set B, P waves:** 4 EGFs, based on their cross-correlation with the mainshock waveforms at station PLM, that are located at less than 1 km from the mainshock. Listed in Table S12. The choice of the station is based on the quality of the recordings.
- **set C, P waves:** We select 1 to 4 events for each station. The choice is based on the cross-correlation of their waveforms with the mainshock waveforms at each station (P or S arrivals waveforms only). EGFs are at a distance of less than 1 km from the mainshock. The number of assumed EGFs depends on their SNR that should be larger than 2. This amounts to a total of 69 single events.

### Prior assumptions for the Landweber approach

We compare DeepGEM inferences with the approach proposed by Bertero et al. (1997). We use the same downsampling as with DeepGEM. We first fix the duration of the STF and then optimize its time shift with a least-square approach. We impose 500 iterations. We estimate apparent STFs for each component and each EGF, and then derive mean and standard deviation from those multiple estimates.

### S4.4 Results

We only provide here a subset of the results for a few key stations to allow for comparison. STFs at all stations are plotted in Fig. 4 in the main text.

#### at station BOR:

- Fig. S41 : set A, P waves
- Fig. S42 : set B, P waves
- Fig. S43 : set C, P waves
- Fig. S44 : set C, S waves

#### at station BLA2:

- Fig. S45 : set A, P waves
- Fig. S46 : set B, P waves
- Fig. S47 : set C, P waves
- Fig. S48 : set C, S waves

#### at station PLS:

- Fig. S49 : set A, P waves
- Fig. S50 : set B, P waves
- Fig. S51 : set C, P waves
- Fig. S52 : set C, S waves

#### at station LMH:

- Fig. S53 : set A, P waves
- Fig. S54 : set B, P waves
- Fig. S55 : set C, P waves
- Fig. S56 : set C, S waves

#### at station PLM:

- Fig. S57 : set A, P waves
- Fig. S58 : set B, P waves
- Fig. S59 : set C, P waves

- Fig. S60 : set C, S waves

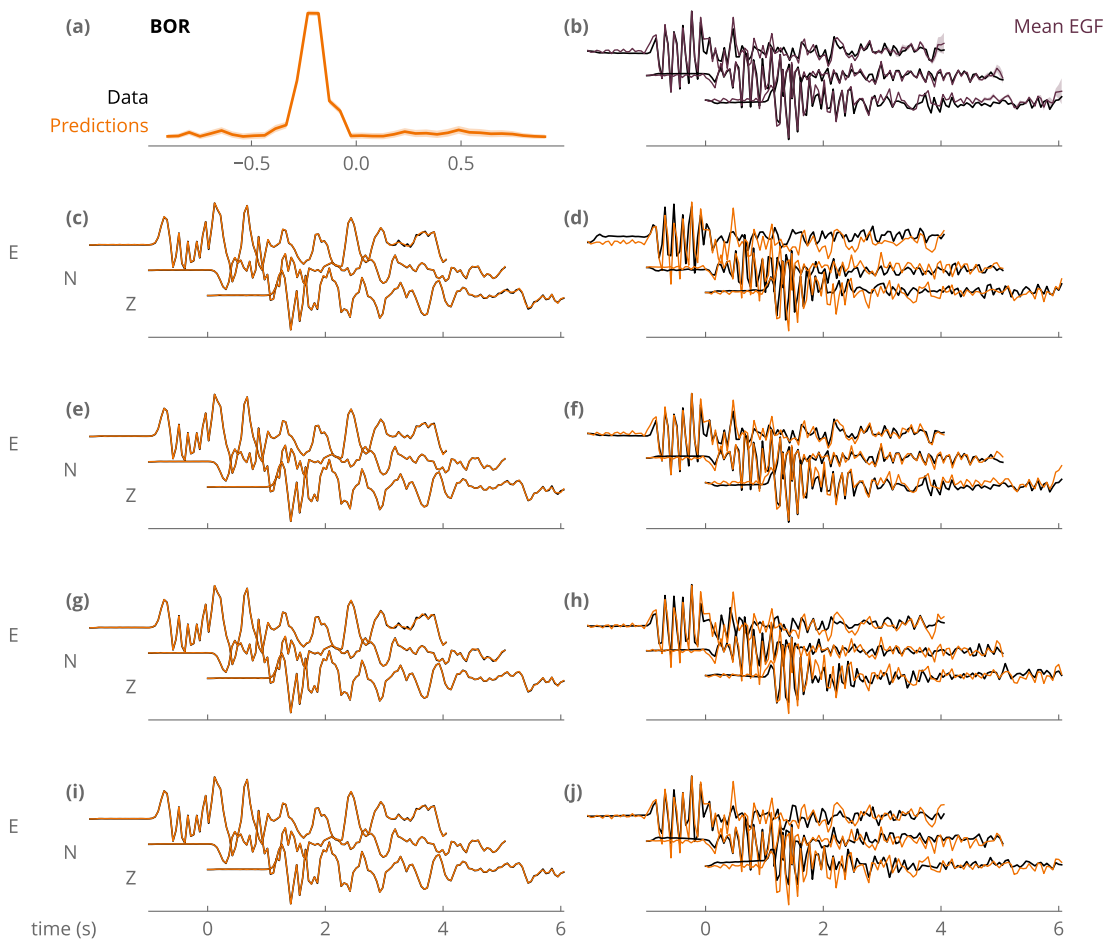


**Figure S41** Inferred mean STF (a, orange) and EGF (b, purple) and their standard deviation (lighter) at station **BOR** for the Cahuilla case study. Inferred (orange) and observed (black) waveforms for the mainshock and EGFs are plotted on the left or right, respectively. (right) Prior EGFs are from set **(A)**.

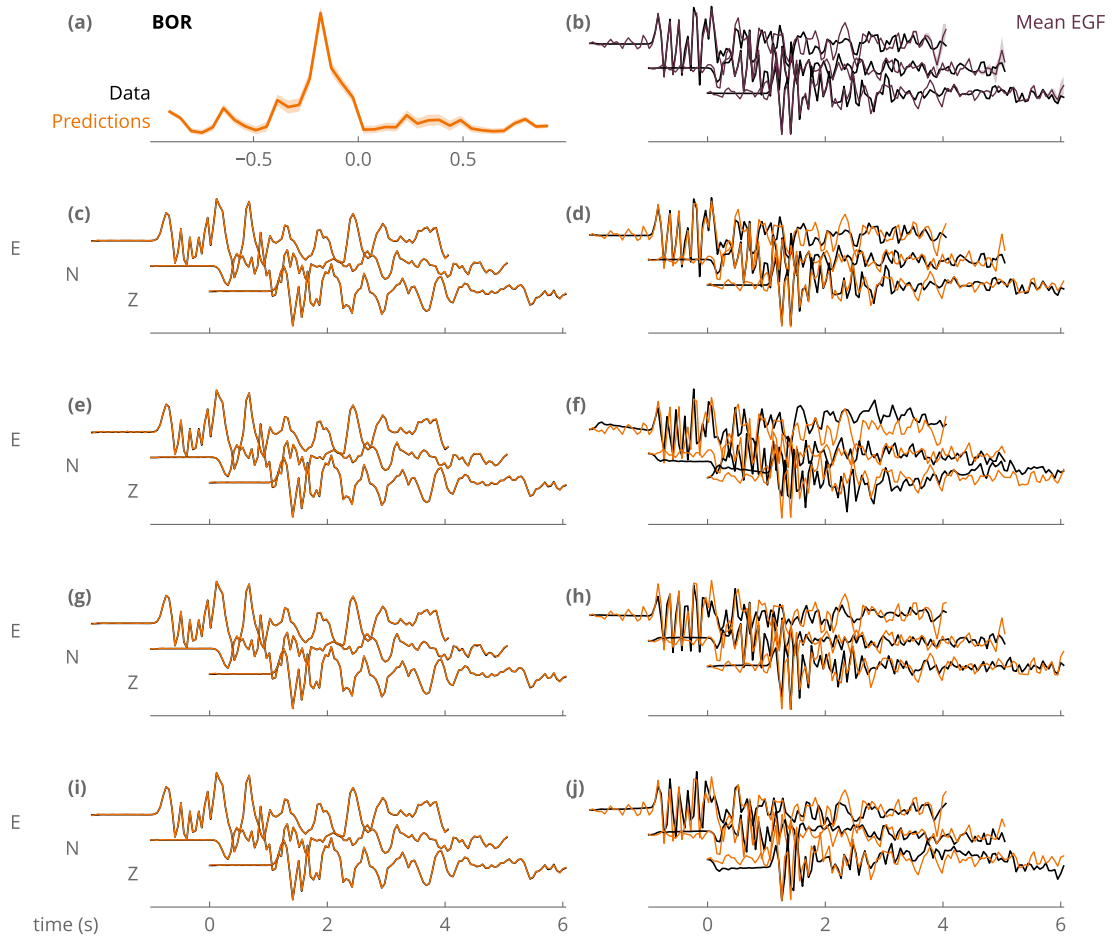


**Figure S42** Inferred mean STF (a, orange) and EGF (b, purple) and their standard deviation (lighter) at station **BOR** for the Cahuilla case study. Inferred (orange) and observed (black) waveforms for the mainshock and EGFs are plotted on the left or right, respectively. (right) Prior EGFs are from set **(B)**.

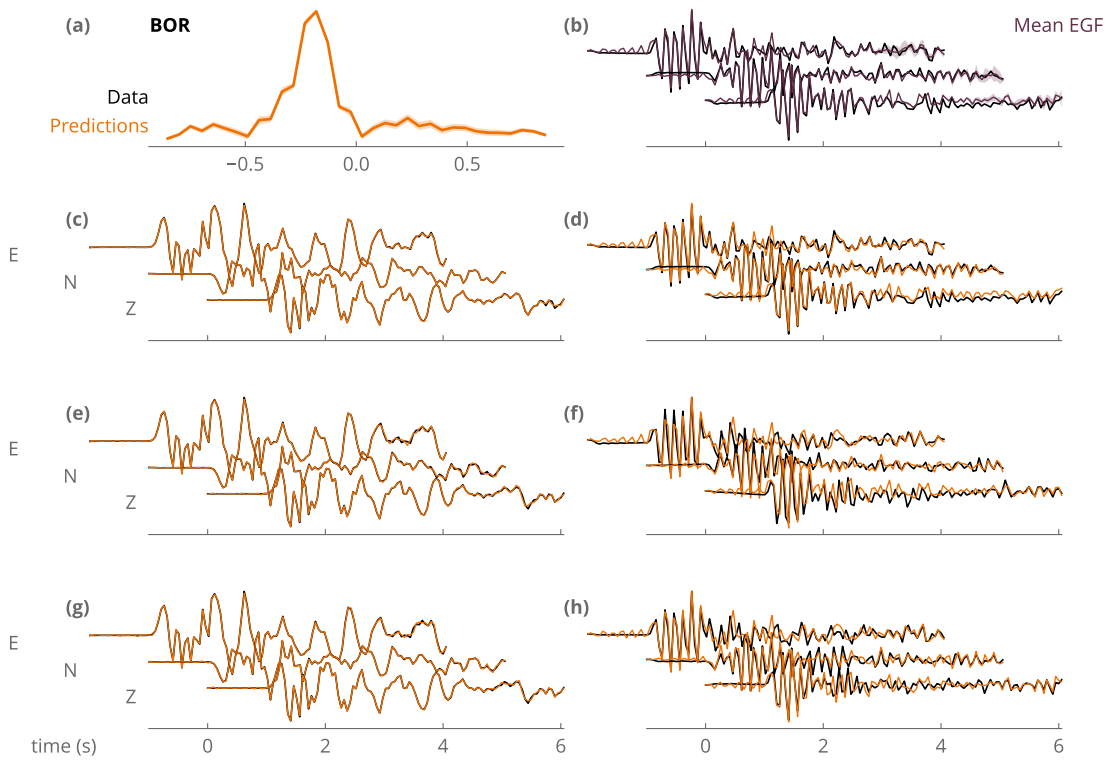


**Figure S43** Inferred mean STF (a, orange) and EGF (b, purple) and their standard deviation (lighter) at station **BOR** for the Cahuilla case study. Inferred (orange) and observed (black) waveforms for the mainshock and EGFs are plotted on the left or right, respectively. (right) Prior EGFs are from set **(C)**.

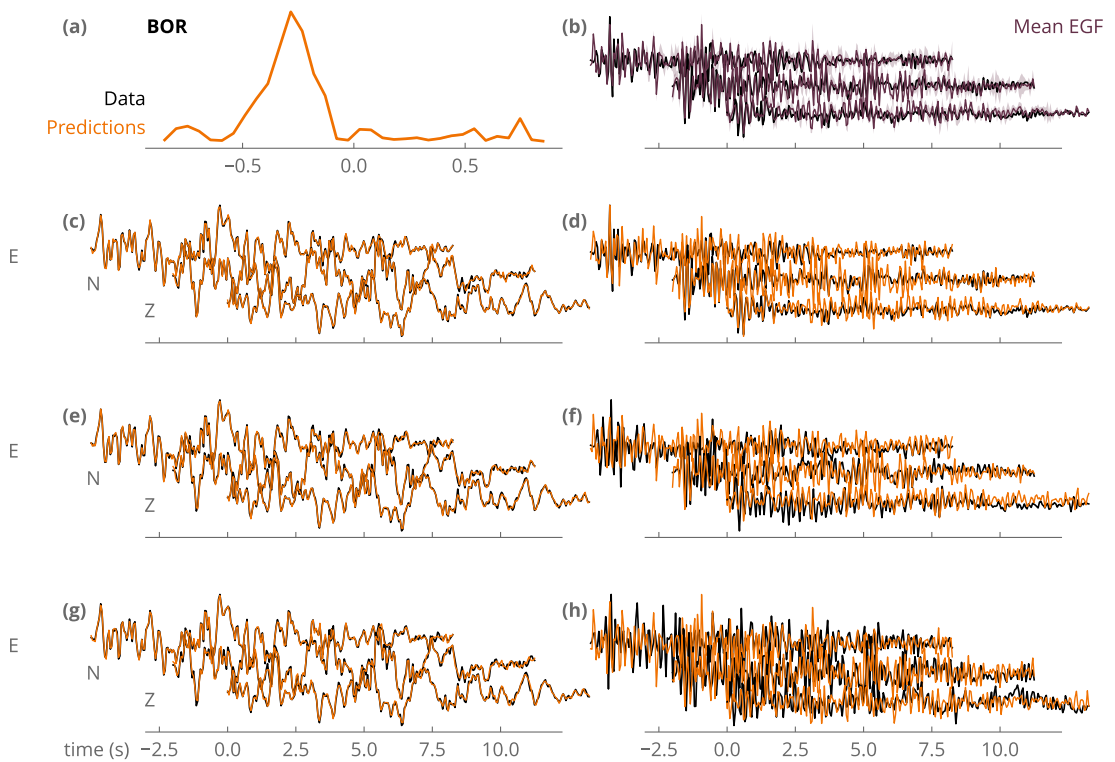


**Figure S44** Inferred mean STF (a, orange) and EGF (b, purple) and their standard deviation (lighter) at station **BOR** for the Cahuilla case study. Inferred (orange) and observed (black) waveforms for the mainshock and EGFs are plotted on the left or right, respectively. (right) Prior EGFs are from set **(S)**.



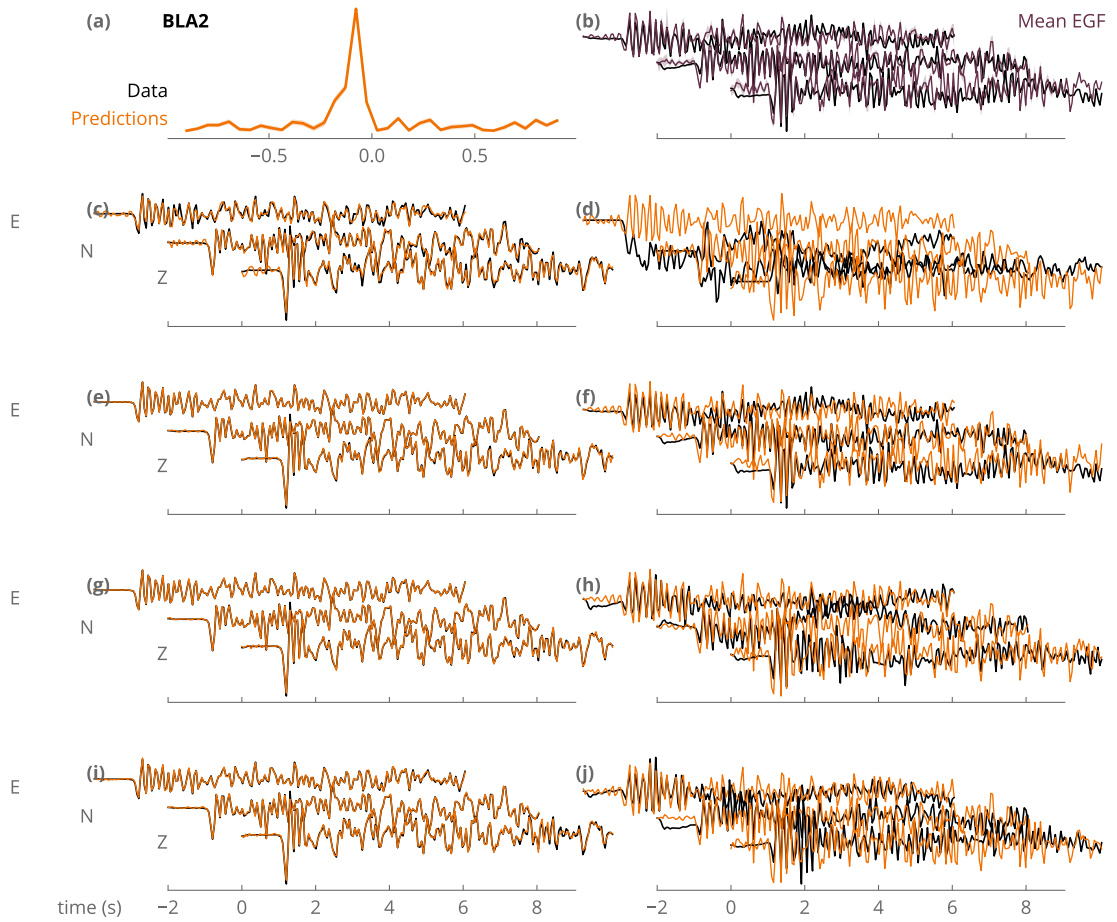


**Figure S45** Inferred mean STF (a, orange) and EGF (b, purple) and their standard deviation (lighter) at station **BLA2** for the Cahuilla case study. Inferred (orange) and observed (black) waveforms for the mainshock and EGFs are plotted on the left or right, respectively. (right) Prior EGFs are from set **(A)**.



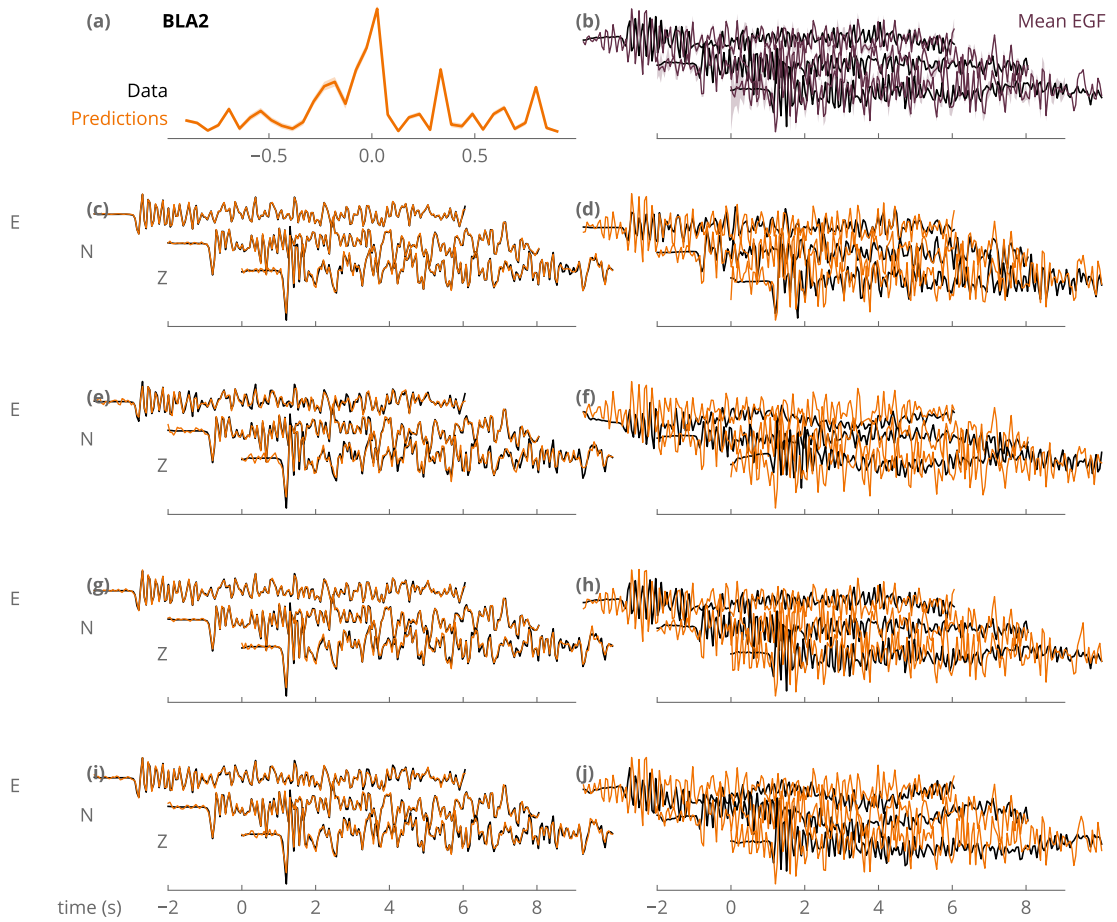


**Figure S46** Inferred mean STF (a, orange) and EGF (b, purple) and their standard deviation (lighter) at station **BLA2** for the Cahuilla case study. Inferred (orange) and observed (black) waveforms for the mainshock and EGFs are plotted on the left or right, respectively. (right) Prior EGFs are from set **(B)**.

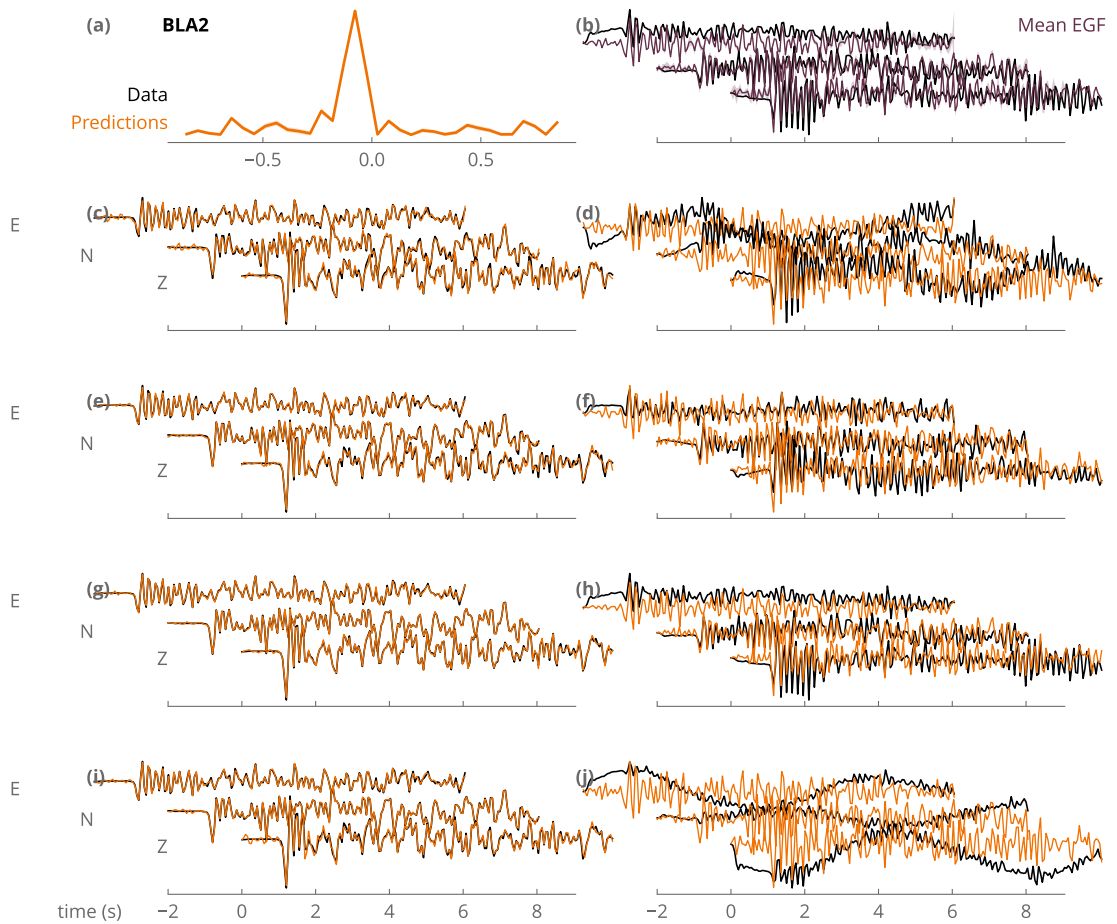


**Figure S47** Inferred mean STF (a, orange) and EGF (b, purple) and their standard deviation (lighter) at station **BLA2** for the Cahuilla case study. Inferred (orange) and observed (black) waveforms for the mainshock and EGFs are plotted on the left or right, respectively. (right) Prior EGFs are from set **(C)**.

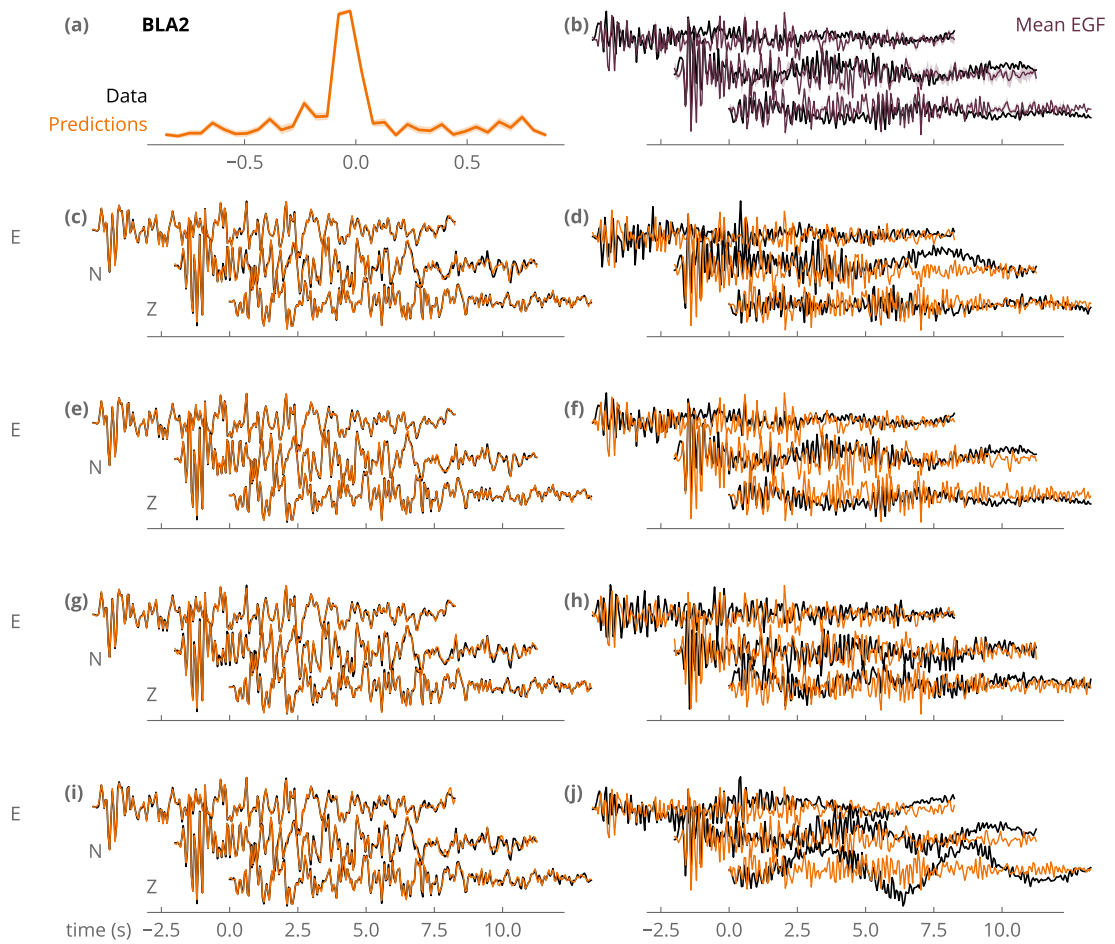


**Figure S48** Inferred mean STF (a, orange) and EGF (b, purple) and their standard deviation (lighter) at station **BLA2** for the Cahuilla case study. Inferred (orange) and observed (black) waveforms for the mainshock and EGFs are plotted on the left or right, respectively. (right) Prior EGFs are from set **(S)**.

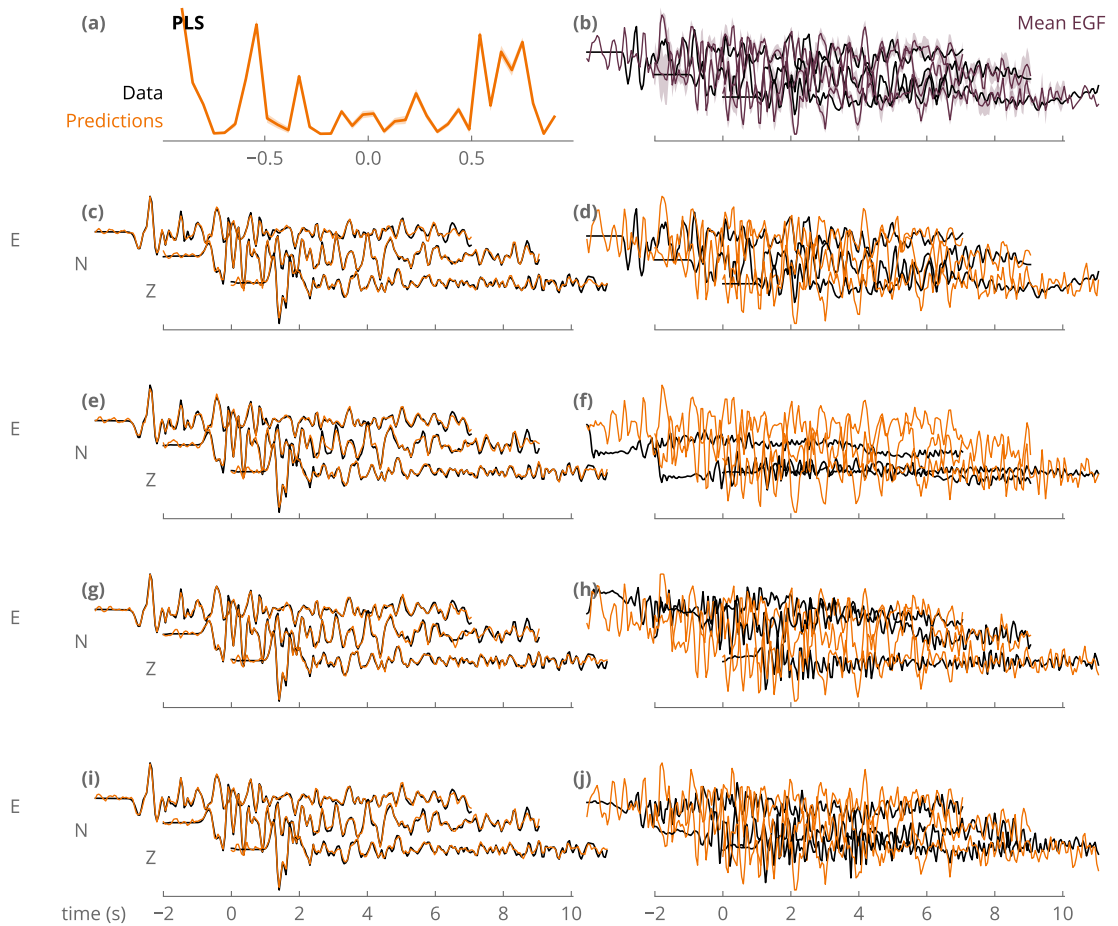


**Figure S49** Inferred mean STF (a, orange) and EGF (b, purple) and their standard deviation (lighter) at station **PLS** for the Cahuilla case study. Inferred (orange) and observed (black) waveforms for the mainshock and EGFs are plotted on the left or right, respectively. (right) Prior EGFs are from set **(A)**.

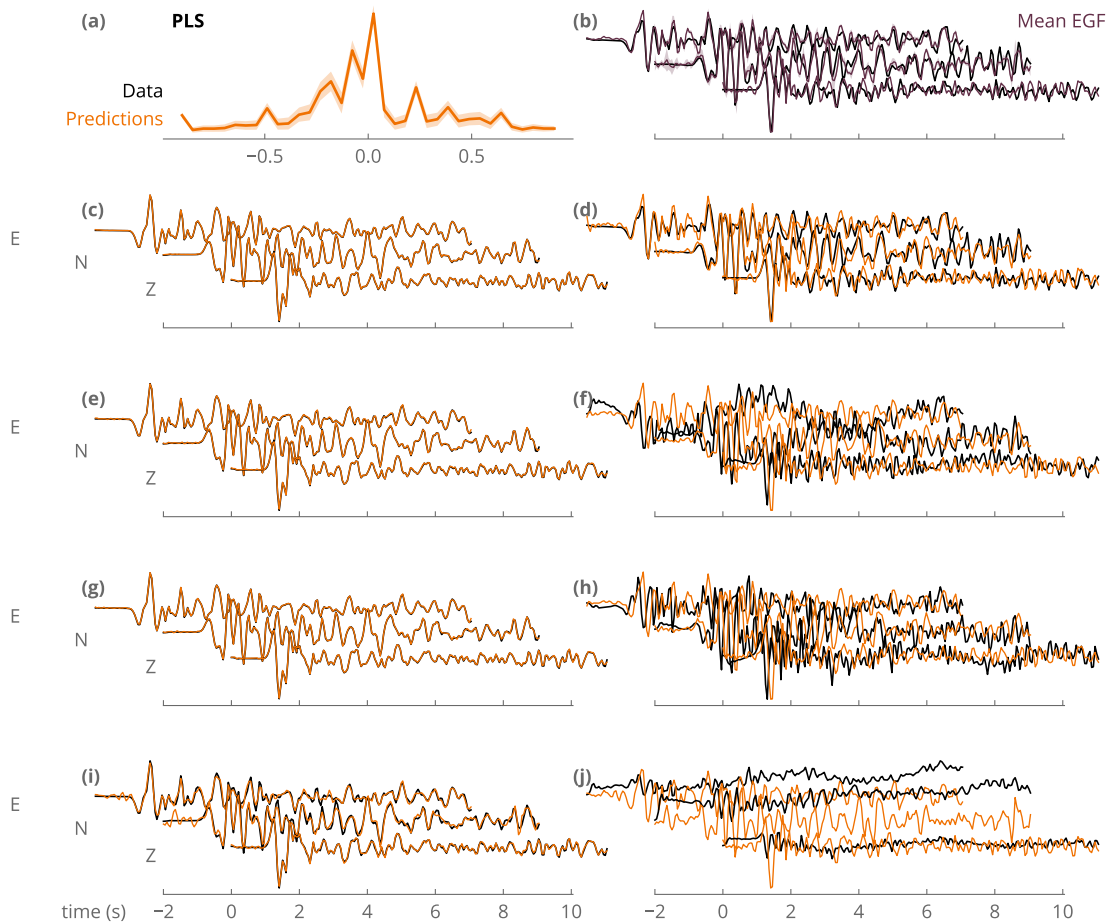


**Figure S50** Inferred mean STF (a, orange) and EGF (b, purple) and their standard deviation (lighter) at station **PLS** for the Cahuilla case study. Inferred (orange) and observed (black) waveforms for the mainshock and EGFs are plotted on the left or right, respectively. (right) Prior EGFs are from set **(B)**.

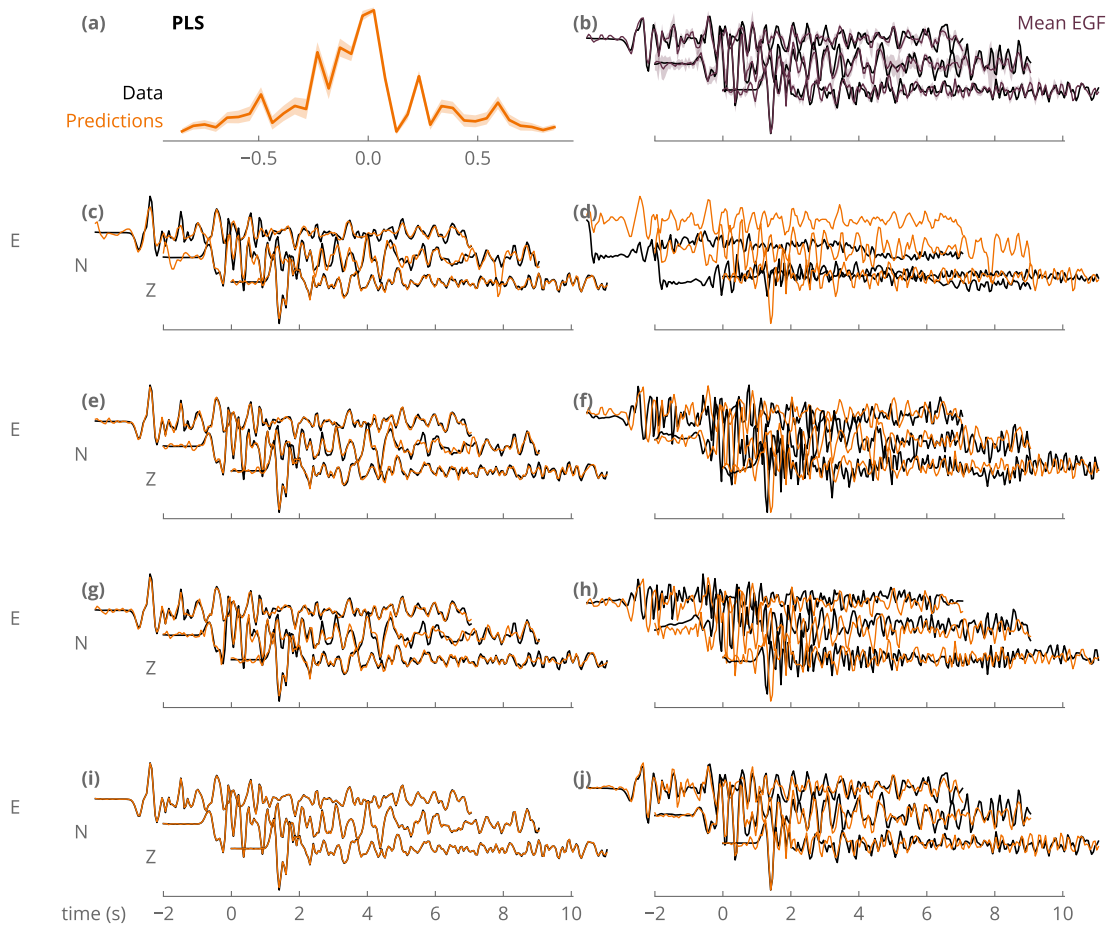


**Figure S51** Inferred mean STF (a, orange) and EGF (b, purple) and their standard deviation (lighter) at station **PLS** for the Cahuilla case study. Inferred (orange) and observed (black) waveforms for the mainshock and EGFs are plotted on the left or right, respectively. (right) Prior EGFs are from set **(C)**.

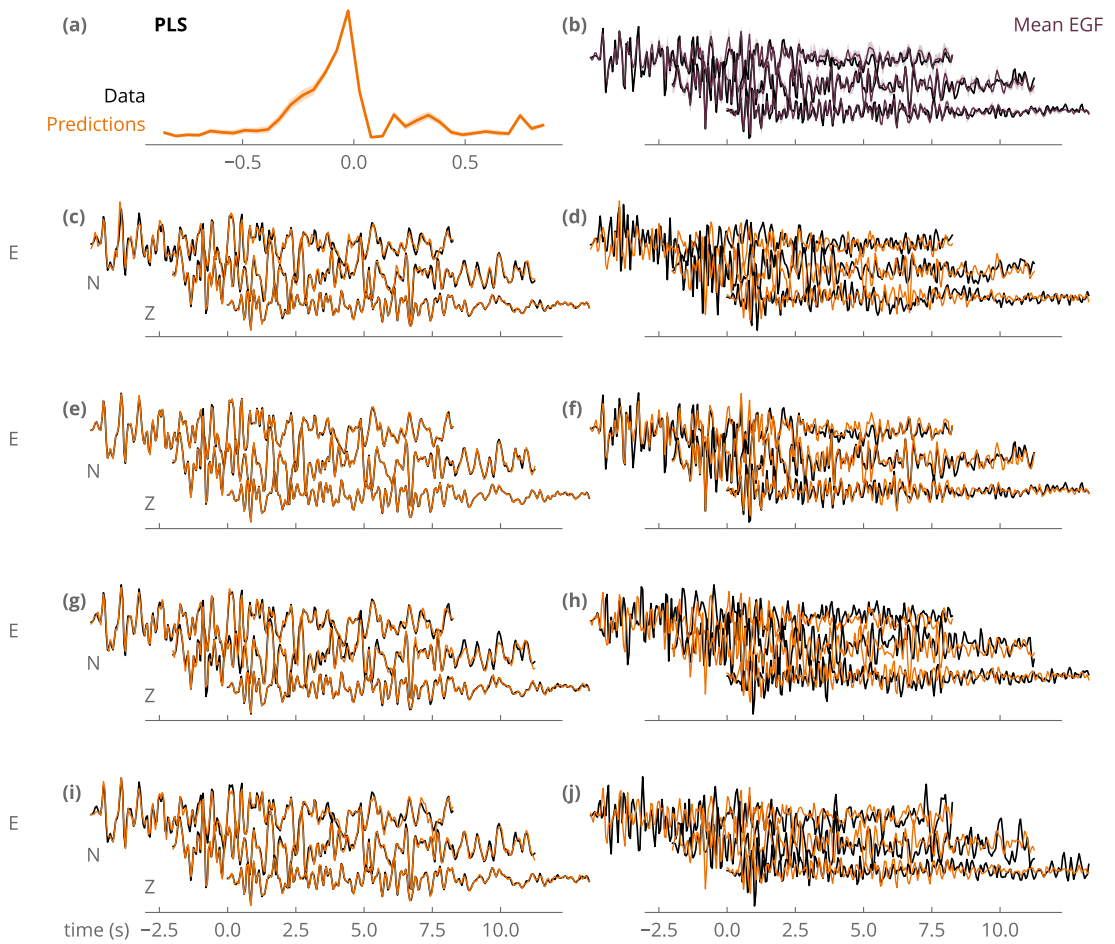


**Figure S52** Inferred mean STF (a, orange) and EGF (b, purple) and their standard deviation (lighter) at station **PLS** for the Cahuilla case study. Inferred (orange) and observed (black) waveforms for the mainshock and EGFs are plotted on the left or right, respectively. (right) Prior EGFs are from set **(S)**.



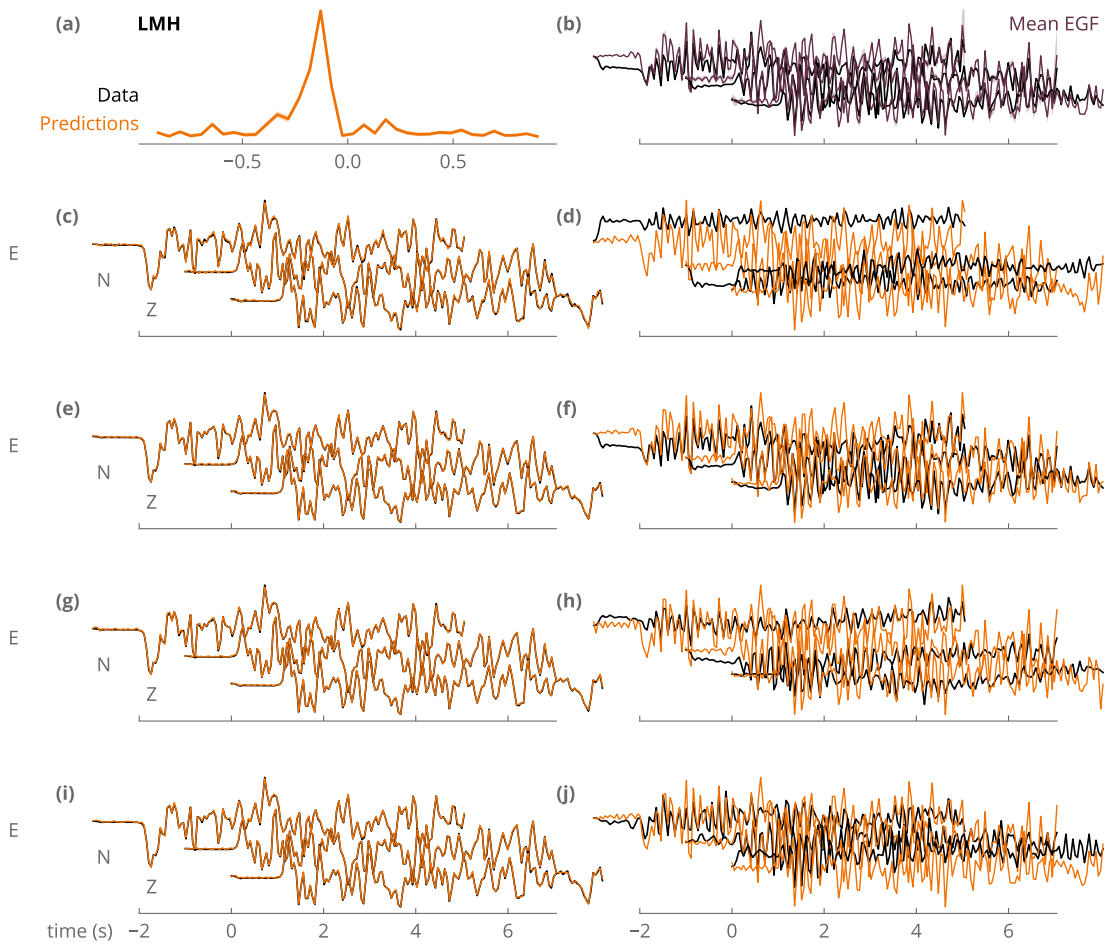


**Figure S53** Inferred mean STF (a, orange) and EGF (b, purple) and their standard deviation (lighter) at station **LMH** for the Cahuilla case study. Inferred (orange) and observed (black) waveforms for the mainshock and EGFs are plotted on the left or right, respectively. (right) Prior EGFs are from set **(A)**.



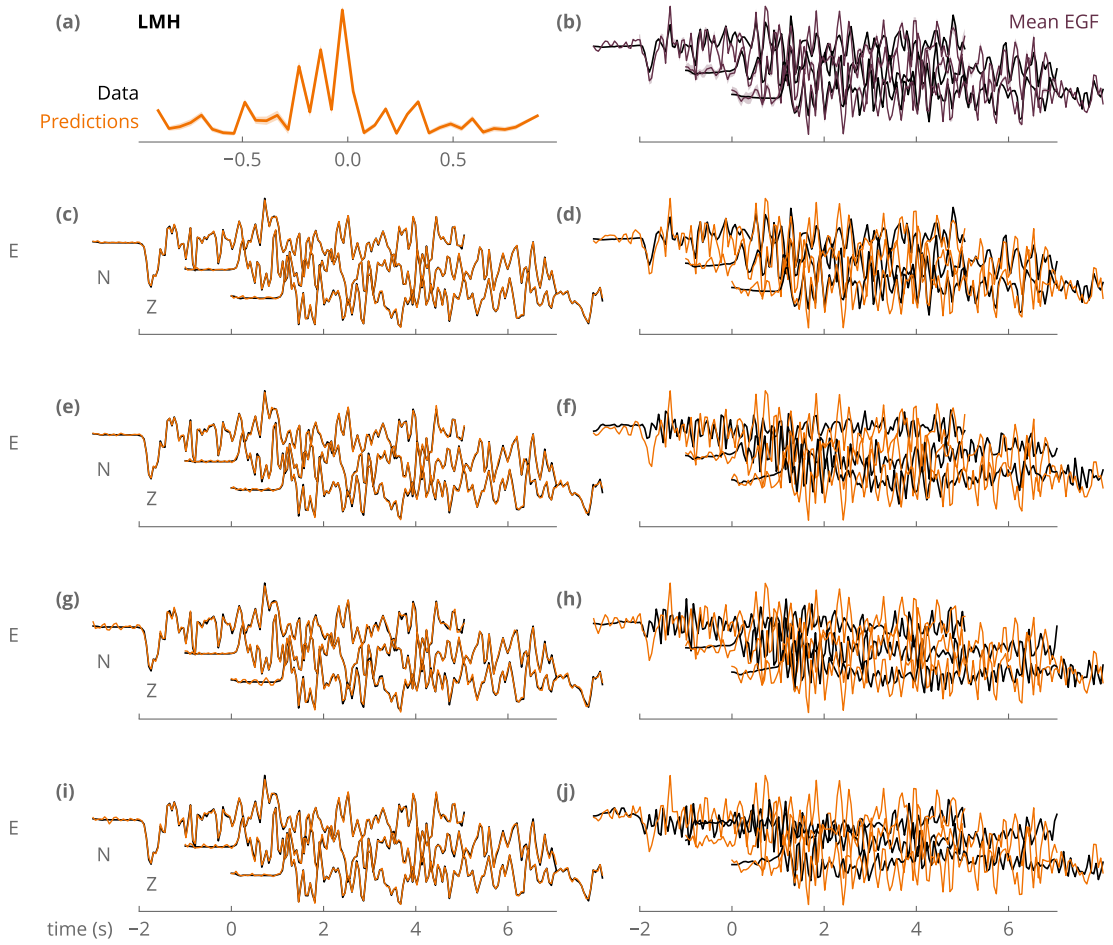


**Figure S54** Inferred mean STF (a, orange) and EGF (b, purple) and their standard deviation (lighter) at station **LMH** for the Cahuilla case study. Inferred (orange) and observed (black) waveforms for the mainshock and EGFs are plotted on the left or right, respectively. (right) Prior EGFs are from set **(B)**.

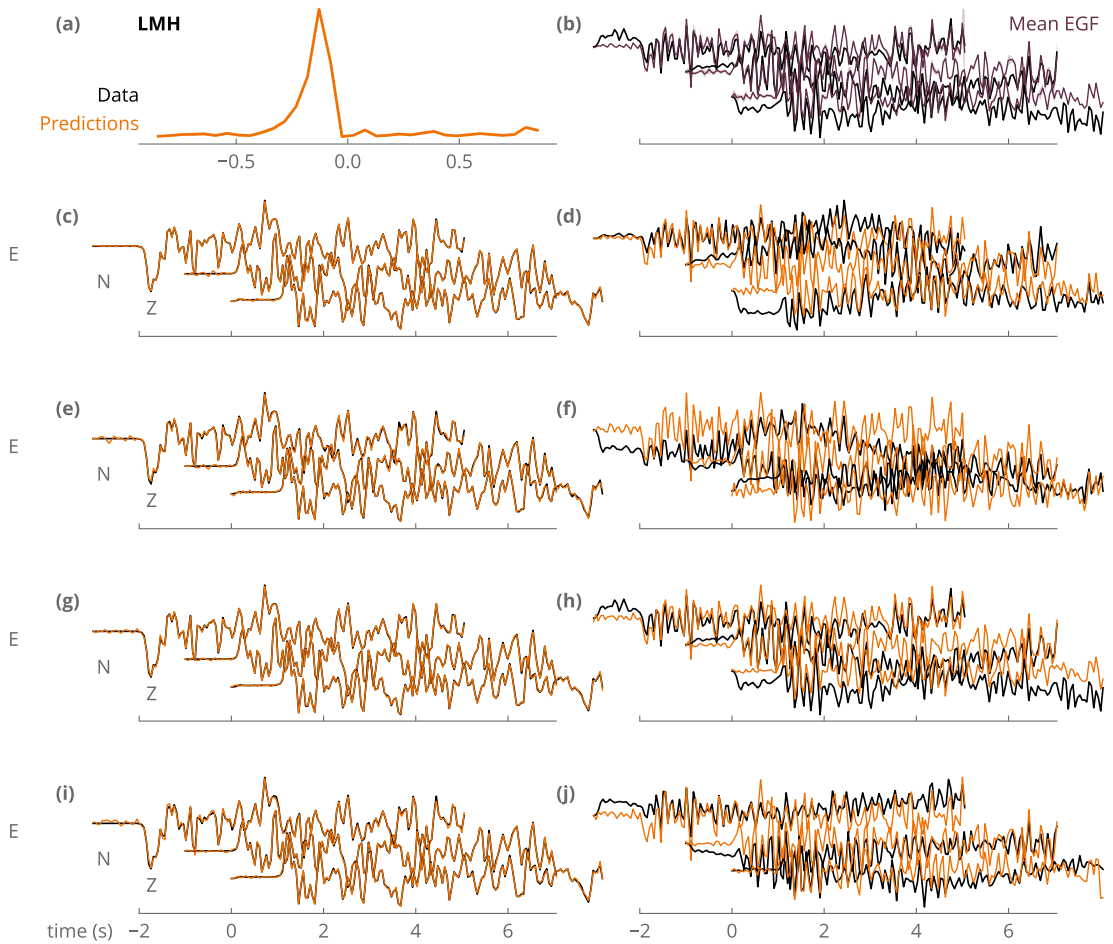


**Figure S55** Inferred mean STF (a, orange) and EGF (b, purple) and their standard deviation (lighter) at station **LMH** for the Cahuilla case study. Inferred (orange) and observed (black) waveforms for the mainshock and EGFs are plotted on the left or right, respectively. (right) Prior EGFs are from set **(C)**.

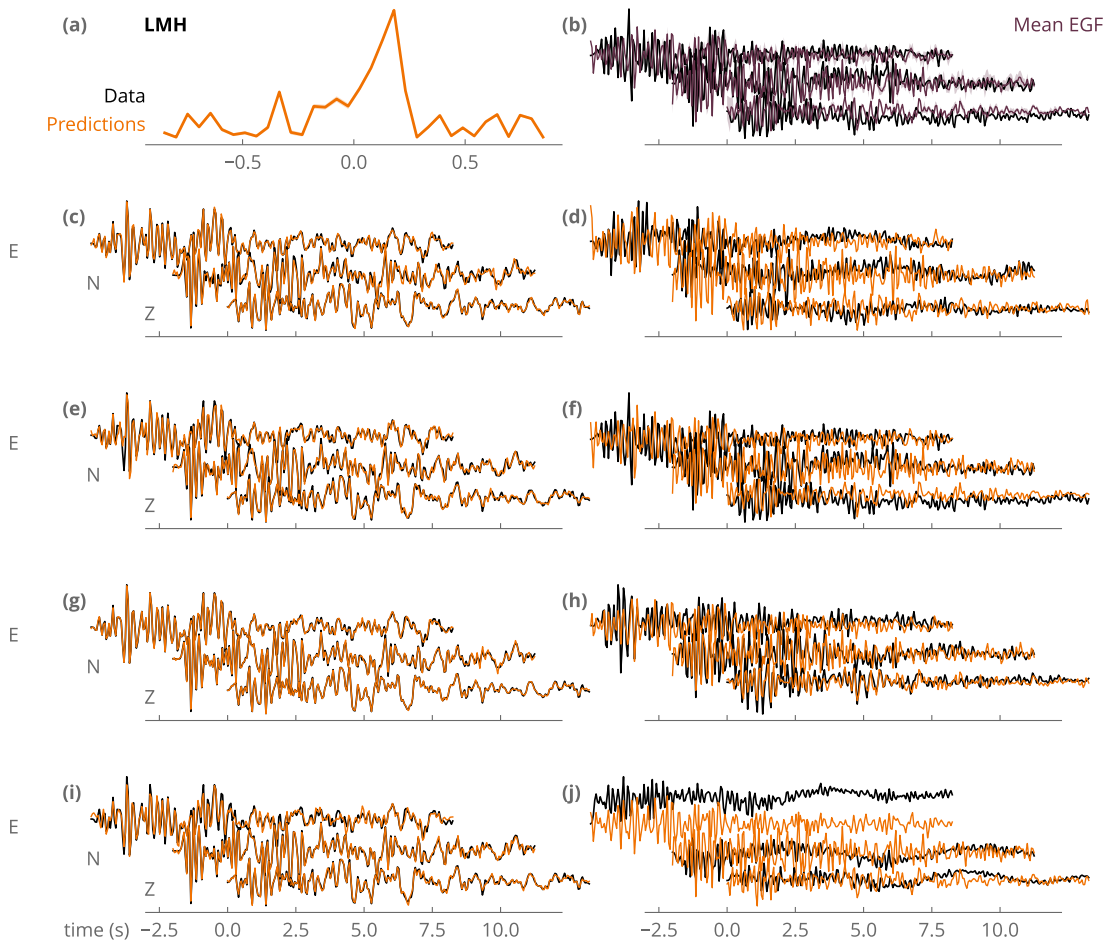


**Figure S56** Inferred mean STF (a, orange) and EGF (b, purple) and their standard deviation (lighter) at station **LMH** for the Cahuilla case study. Inferred (orange) and observed (black) waveforms for the mainshock and EGFs are plotted on the left or right, respectively. (right) Prior EGFs are from set **(S)**.

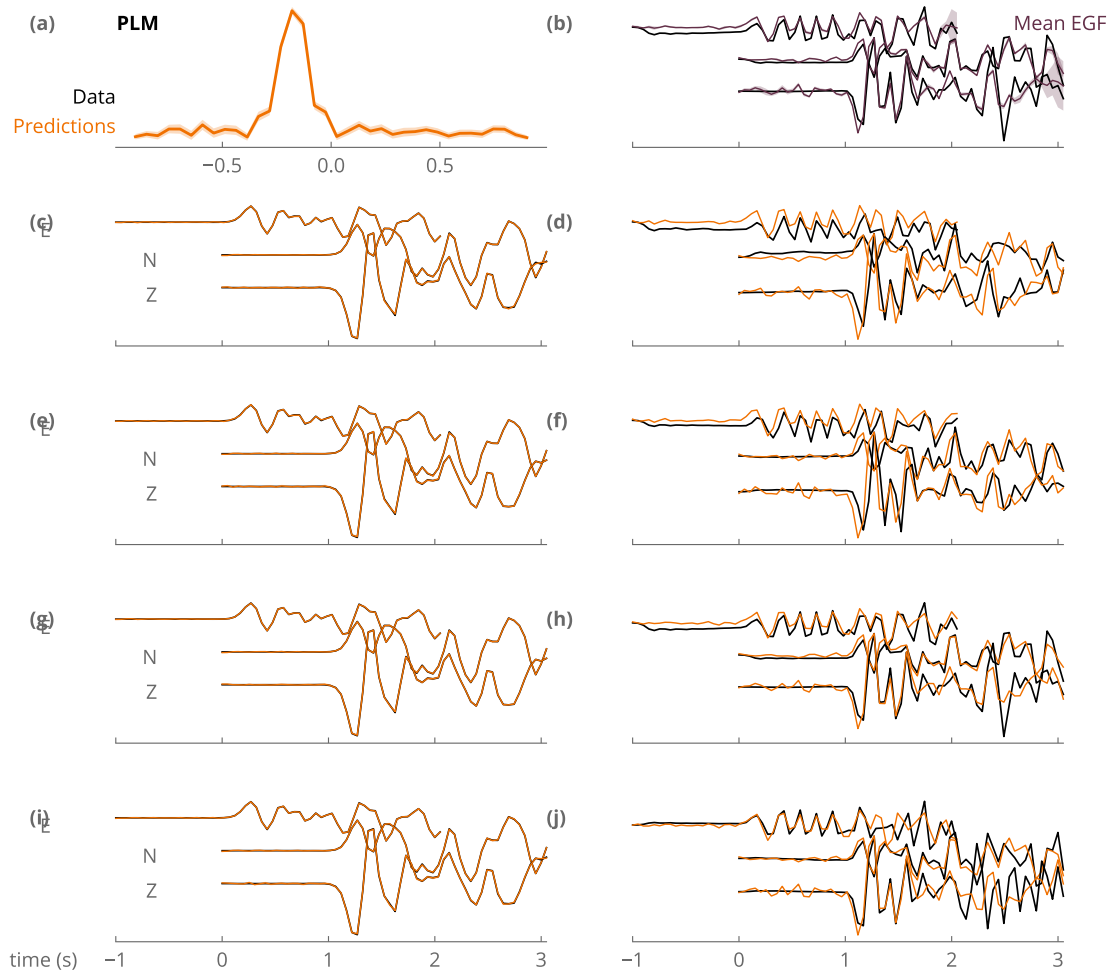


**Figure S57** Inferred mean STF (a, orange) and EGF (b, purple) and their standard deviation (lighter) at station **PLM** for the Cahuilla case study. Inferred (orange) and observed (black) waveforms for the mainshock and EGFs are plotted on the left or right, respectively. (right) Prior EGFs are from set **(A)**.

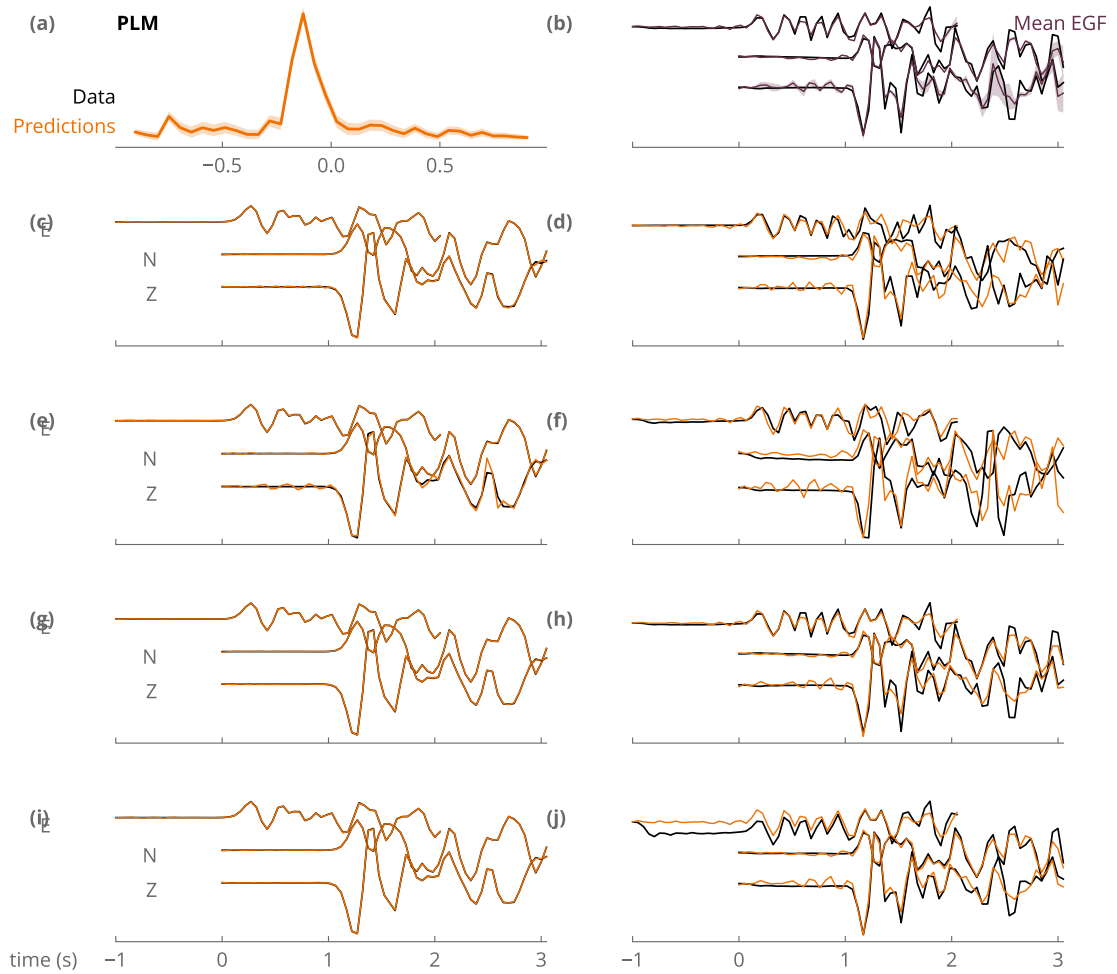


**Figure S58** Inferred mean STF (a, orange) and EGF (b, purple) and their standard deviation (lighter) at station **PLM** for the Cahuilla case study. Inferred (orange) and observed (black) waveforms for the mainshock and EGFs are plotted on the left or right, respectively. (right) Prior EGFs are from set **(B)**.

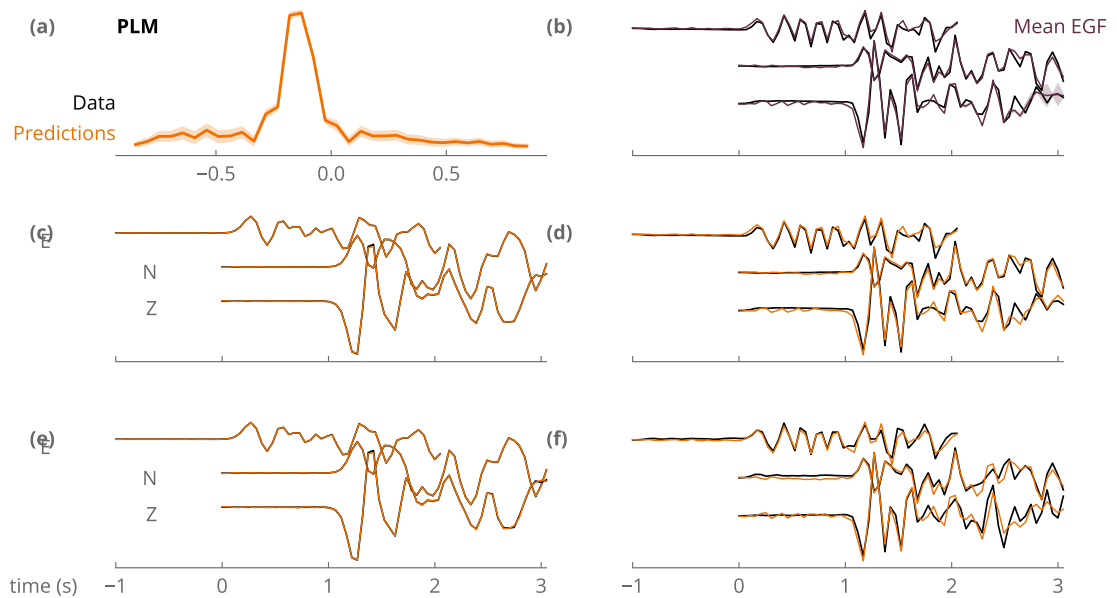


**Figure S59** Inferred mean STF (a, orange) and EGF (b, purple) and their standard deviation (lighter) at station **PLM** for the Cahuilla case study. Inferred (orange) and observed (black) waveforms for the mainshock and EGFs are plotted on the left or right, respectively. (right) Prior EGFs are from set **(C)**.

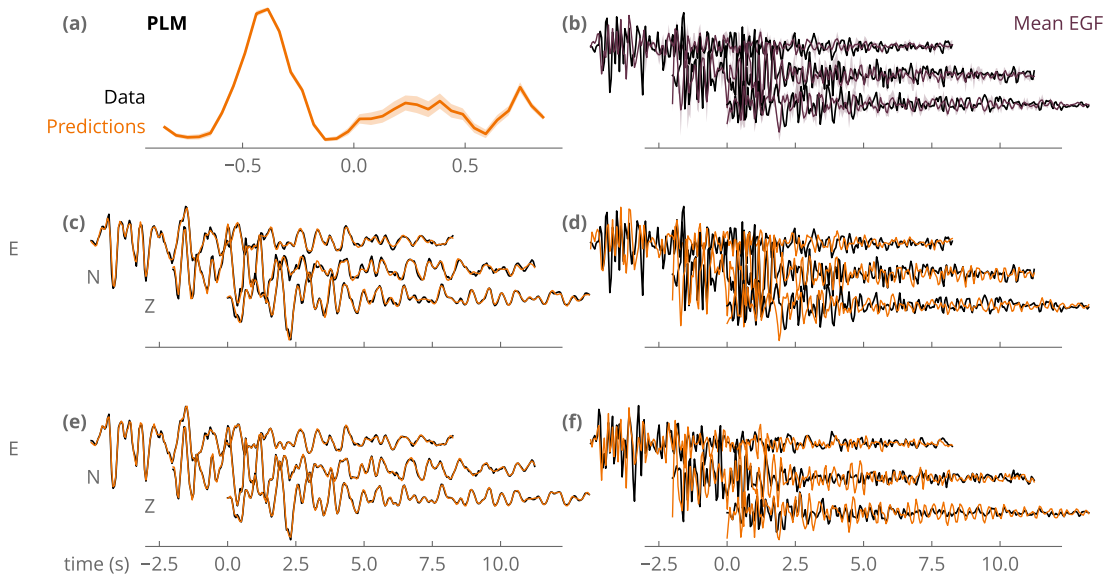


**Figure S60** Inferred mean STF (a, orange) and EGF (b, purple) and their standard deviation (lighter) at station **PLM** for the Cahuilla case study. Inferred (orange) and observed (black) waveforms for the mainshock and EGFs are plotted on the left or right, respectively. (right) Prior EGFs are from set (**S**).

## References

- Bertero, M., Bindi, D., Boccacci, P., Cattaneo, M., Eva, C., and Lanza, V. (1997). Application of the projected Landweber method to the estimation of the source time function in seismology. *Inverse Problems*, 13(2):465. [27](#), [48](#)
- Heimann, S., Steinberg, A., Sudhaus, H., Vasyura-Bathke, H., Dahm, T., and Isken, M. (2017). Pyrocko: A Versatile Software Framework for Seismology. [4](#)
- Ross, Z. E., Cochran, E. S., Trugman, D. T., and Smith, J. D. (2020). 3D fault architecture controls the dynamism of earthquake swarms. *Science*, 368(6497):1357–1361. [31](#)
- Zhu, W. and Beroza, G. C. (2019). PhaseNet: A deep-neural-network-based seismic arrival-time picking method. *Geophysical Journal International*, 216(1):261–273. [27](#), [31](#)